



HAL
open science

Modelling and control of systems of conservation laws with a moving interface: an application to an extrusion process

Mamadou Lamine Diagne

► **To cite this version:**

Mamadou Lamine Diagne. Modelling and control of systems of conservation laws with a moving interface: an application to an extrusion process. Automatic Control Engineering. Université Claude Bernard - Lyon I, 2013. English. NNT : 2013LYO10098 . tel-01813636

HAL Id: tel-01813636

<https://theses.hal.science/tel-01813636>

Submitted on 12 Jun 2018

HAL is a multi-disciplinary open access archive for the deposit and dissemination of scientific research documents, whether they are published or not. The documents may come from teaching and research institutions in France or abroad, or from public or private research centers.

L'archive ouverte pluridisciplinaire **HAL**, est destinée au dépôt et à la diffusion de documents scientifiques de niveau recherche, publiés ou non, émanant des établissements d'enseignement et de recherche français ou étrangers, des laboratoires publics ou privés.

N° d'ordre: 98-2013

Année 2013

THESE DE L'UNIVERSITE DE LYON

délivrée par

ECOLE DOCTORALE ED EEA 160 DE LYON

DIPLOME DE DOCTORAT

(arrêté du 7 août 2006 / arrêté du 6 janvier 2005)

soutenue publiquement le 26 Juin 2013

par

M. Mamadou Lamine Diagne

Modelling and control of systems of conservation laws with a moving interface: an application to an extrusion process

Directeurs de thèse: M. Bernhard Maschke et M. Françoise Couenne

JURY

M. Yann Le Gorrec	ENSMM de Besançon
M. Didier Georges	Institut Polytechnique de Grenoble
M. Nicolas Petit	Ecole des Mines ParisTech
M. Hans Zwart	University of Twente
M. Jean-Michel Coron	Université Pierre et Marie Curie
M. Michaël Di Loreto	INSA Lyon
M. Bernhard Maschke	Université Claude Bernard Lyon 1
Mme. Françoise Couenne	Centre National de la Recherche Scientifique

UNIVERSITE CLAUDE BERNARD - LYON 1

Président de l'Université	M. François-Noël GILLY
Vice-président du Conseil d'Administration	M. le Professeur Hamda BEN HADID
Vice-président du Conseil des Etudes et de la Vie Universitaire	M. le Professeur Philippe LALLE
Vice-président du Conseil Scientifique	M. le Professeur Germain GILLET
Directeur Général des Services	M. Alain HELLEU

COMPOSANTES SANTE

Faculté de Médecine Lyon Est - Claude Bernard	Directeur: M. le Professeur J. Etienne
Faculté de Médecine et de Maieutique Lyon Sud - Charles Mérieux	Directeur: Mme la Professeure C. BURILLON
UFR d'Odontologie	Directeur: M. le Professeur D. Bourgeois
Institut des Sciences Pharmaceutiques et Biologiques	Directeur: Mme la Professeure C. VINCIGUERRA
Institut des Sciences et Techniques de la Réadaptation	Directeur: M. le Professeur Y. Matillon
Département de formation et Centre de Recherche en Biologie Humaine	Directeur: M. le Professeur P. Farge

COMPOSANTES ET DEPARTEMENTS DE SCIENCES ET TECHNOLOGIE

Faculté des Sciences et Technologies	Directeur: M. le Professeur F. DE MARCHI
Département Biologie	Directeur: M. le Professeur F. Fleury
Département Chimie Biochimie	Directeur: Mme le Professeur H. Parrot
Département GEP	Directeur: M. N. Siauve
Département Informatique	Directeur: M. le Professeur S. Akkouche
Département Mathématiques	Directeur: M. le Professeur A. Goldman
Département Mécanique	Directeur: M. le Professeur H. Ben Hadid
Département Physique	Directeur: Mme S. Fleck
Département Sciences de la Terre	Directeur: Mme le Professeur I. Daniel
UFR Sciences et Techniques des Activités Physiques et Sportives	Directeur: M. C. Collignon
Observatoire des Sciences de l'Univers de Lyon	Directeur: M. B. Guiderdoni
Ecole Polytechnique Universitaire de Lyon 1	Directeur: M. P. Fournier
Ecole Supérieure de Chimie Physique Electron- ique	Directeur: M. G. Pignault
Institut Universitaire de Technologie de Lyon 1	Directeur: M. le Professeur C. Coulet
Institut de Science Financière et d'Assurances	Directeur: M. le Professeur J-C. Augros
Institut Universitaire de Formation des Maitres	Directeur: M. R. Bernard

To my mother, Fatoumata Sylla

Acknowledgements

I would like to express my deepest appreciation to all those who provided me the possibility to complete this report. I am grateful to my thesis directors Professor Bernhard Maschke and Doctor Françoise Couenne. Without their encouragement and guidance this thesis would not have materialized.

I would like to thank my committee members, Professor Jean-Michel Coron, Doctor Michael Di Loreto, Professor Didier Georges, Professor Yann Le Gorrec, Professor Nicolas Petit and Professor Hans Zwart for their detailed revision of the thesis manuscript. Their comments help me to improve significantly the final version of the manuscript. Professor Jean-Michel Coron has encouraged my collaboration with Peipei Shang and Zhiqiang Wang and gave me the opportunity to learn advanced technics in mathematical analysis. Along this years, I had very interesting discussions with Professor Hans Zwart on Hamiltonian formulation of moving interface problems and his advices gave me large perspectives in this subject.

I acknowledge the director of the Laboratoire d'Automatique et de Génie des Procédés (LAGEP), Professor Hatem Fessi for receiving me in his lab these last four years. I have only great thoughts towards the group **Dynamique des procédés et commande à base de lois de conservation** in which I had the pleasure to work in LAGEP. I would like to thank each and every person of the group, specially Professor Christian Jallut for interesting discussions in extrusion processes modelling. I am very thankful to the personnel of LAGEP, in particular Nadia Chapel, Jean Pierre Valour and Olivier Garrigues.

I would like to thank the French Ministry of Higher Education and Research for the grant supporting my Ph.D. work and the French National Research Agency sponsored project HAMECMOPSYS (ANR-11- BS03-0002) for its partial financial support.

Also, I like to thank Weijun, Yongxin, Goma, Sofiane, Naveed, Mariem, Kun, Lamice, Hoang, Redha with whom I shared very good time.

I am grateful to my friends Amadou Bah, Silcarneyni Gueye, Abdou Ndiaye and Samba Cor Thiandoum who encouraged me during these years.

Finally, I would like to express my deepest appreciation to my parents ABdou Diagne and Fatoumata Sylla, my brother Papa Ibrahima Diagne and my nephew Souleymane Sy Savané for their love and constant support.

Contents

Table of contents	ix
1 Résumé en français	1
1.1 Modélisation d'un procédé d'extrusion pour la commande	2
1.1.1 Modèle bi-zone d'une extrudeuse	4
1.1.1.1 Bilans de matière et d'énergie dans les deux zones	5
1.1.1.2 Modèle de la zone partiellement remplie ou <i>PFZ</i>	5
1.1.1.3 Modèle de la zone entièrement remplie ou <i>FFZ</i>	6
1.1.2 Dynamique de l'interface mobile $\mathbf{l}(\mathbf{t})$ et relations d'interface	6
1.1.2.1 Relations d'interface	6
1.1.2.2 Bilan de masse et dynamique de l'interface	8
1.1.3 Conditions frontières et conditions initiales	8
1.1.3.1 Frontière en $x = 0$	8
1.1.3.2 Conditions initiales	8
1.2 Etude du problème de Cauchy associé au modèle de l'extrudeuse	9
1.2.1 Modèle adimensionnel à domaine fixe $(0, 1)$	9
1.2.2 Principaux résultats	10
1.3 Stabilisation de l'interface par une approche de commande prédictive	12
1.3.1 Les équations de conservation de masse dans une extrudeuse	12
1.3.2 Résolution de l'équation de transport	13
1.3.3 Système à retard sur l'entrée dépendant de l'état	14
1.4 Systèmes Hamiltoniens à ports couplés par une interface mobile	15
1.4.1 Définition d'un système Hamiltonien à ports pour deux lois de conservation	15
1.4.2 Interconnexion de deux systèmes Hamiltoniens à ports à travers une interface fixe	16
1.4.3 Interconnexion de deux systèmes Hamiltoniens à ports à travers une interface mobile	17

2	Introduction	21
2.1	Motivation and previous work	21
2.2	Organization and contribution of the thesis	24
2.3	Publications	25
3	Extrusion processes modelling for control	27
3.1	Introduction	27
3.1.1	Organization of the chapter	29
3.1.2	Contributions	30
3.2	Bi-zone model of an extruder	31
3.2.1	Zones defined by the pressure gradient	31
3.2.2	Modelling assumptions and definition of the variables	32
3.2.2.1	Modelling assumptions	32
3.2.2.2	Definition of the variables	33
3.3	Model of the Partially Filled Zone	34
3.3.1	Mass balance in the Partially Filled Zone	34
3.3.2	Moisture balance in the Partially Filled Zone	36
3.3.3	Energy balance in the Partially Filled Zone	36
3.4	Model of the Fully Filled Zone	38
3.4.1	The momentum balance of the Fully Filled Zone	38
3.4.2	Moisture balance in the Fully Filled Zone	40
3.4.3	Energy balance in the Fully Filled Zone	41
3.5	Description of the interface	41
3.5.1	Dynamics of the moving interface	41
3.5.2	Interface relations	43
3.5.2.1	Coupling relations for moisture content and temperature evolutions	43
3.5.2.2	Coupling relations for total mass balance equation	44
3.5.2.2.1	Continuity of pressure at the interface	44
3.5.2.2.2	Continuity of the flux of momentum flux	44
3.6	Control problem associated to the extrusion process model	45
3.7	Open loop simulations of mass and energy balance equations	47
3.7.1	Description of the simulated extrusion process model	47
3.7.2	Numerical computation by finite volume method	48
3.7.3	Simulations results	50
3.8	Conclusion	53
4	Well-posedness of the extrusion process model	55
4.1	Introduction	55

4.1.1	Organization of the chapter	58
4.1.2	Contributions	58
4.2	Model expressed in fixed spatial domain	59
4.3	Main Results	61
4.4	Proof of Theorem 1	63
4.4.1	Local solution to Cauchy problem (4.2.9)-(4.2.10)	63
4.4.2	Semi-global solution to Cauchy problem (4.2.9)-(4.2.10)	69
4.4.3	Solving the moisture equation (4.2.11) for PFZ zone and FFZ zone	70
4.4.4	Solving the temperature equation (4.2.12) for PFZ zone and FFZ zone	74
4.5	Proof of Theorem 2	75
4.6	Conclusion	76
4.7	Acknowledgements	77
5	Control of mass transport as an input delay system	79
5.1	Introduction	79
5.1.1	Organization of the chapter	80
5.1.2	Contribution	80
5.2	From transport equation to delay system for the extrusion process	81
5.2.1	Mass conservation equations in an extrusion process	81
5.2.2	Recalling the formulation of coupling relations at $l(t)$	82
5.2.3	Transport equation solution	83
5.2.4	State dependent input delay system for the extruder model	84
5.3	Generality on predictor-based controllers	85
5.3.1	Predictor-based controllers for constant input delay systems	85
5.3.2	Predictor design for time-varying delay	87
5.3.3	Predictor design for state-dependent input delay system	88
5.4	Stabilization of the position of the interface	91
5.4.1	Static models associated with the interface relations	92
5.4.2	Feedback stabilization of the position of the interface	94
5.4.2.1	Feedback stabilization of the nonlinear without delay	94
5.4.2.2	Control of the system with input delay	96
5.5	Simulation results	96
5.6	Conclusion	98
6	Port Hamiltonian formulation-PDEs- Moving interface	101
6.1	Introduction	101
6.1.1	Organization of the chapter	102
6.1.2	Contributions	103
6.2	Two port Hamiltonian systems coupled by an interface	103

6.2.1	Port Hamiltonian system of two conservation laws	103
6.2.2	Interconnection of port Hamiltonian systems through an interface . . .	105
6.2.3	Augmenting the port Hamiltonian systems with color functions	107
6.2.3.1	Prolongation of the variables on the domain $[a, b]$	107
6.2.3.2	Conservation laws and interface relations as a single system of balance equations	108
6.2.3.3	Hamiltonian system extended with color functions	110
6.2.3.4	Extension to a Boundary Port Hamiltonian system arising from a skew-adjoint operator	111
6.3	Port Hamiltonian systems coupled through a moving interface	115
6.3.1	Balance equations with moving interface	116
6.3.2	Port Hamiltonian Formulation	117
6.3.3	Model of the interface's displacement	122
6.4	Conclusion	124
7	Conclusion	125
7.1	General conclusion	125
7.2	Future research	127
8	Nomenclature	129
	Bibliography	131

Chapter 1

Résumé en français

L'étude de la commande des systèmes de lois de conservation couplés par une interface mobile reste très peu développée dans la littérature. Ces problèmes d'interface apparaissent dans la modélisation d'un grand nombre de systèmes physiques donnant lieu à des phénomènes de changement de phases, de croissance de cristaux, d'évolution biologique (modèle d'évolution de tumeur) etc. Dans cette thèse, nous nous intéressons aux systèmes hyperboliques couplés à travers une interface mobile. Cette étude est développée autour d'un modèle bi-zone d'un procédé d'extrusion. D'autre part nous proposons une analyse des structures d'interface en utilisant le formalisme Hamiltonien à port. Les contributions de cette thèse sont évoquées ci dessous :

- le *Chapitre 3* est dédié à la modélisation des procédés d'extrusion. Le modèle est basée sur la description des phénomènes de transport de masse et de chaleur dans une extrudeuse. Nous obtenons par les bilans de matière et d'énergie des équations de transport couplées à travers une interface mobile. Deux relations de couplage à l'interface sont étudiées : l'une repose sur l'hypothèse de continuité de pression et l'autre sur la continuité du flux de quantité de mouvement. Des simulations numériques sont proposées pour illustrer la cohérence du modèle.
- le *Chapitre 4* traite de l'analyse mathématique des équations de transport définies sur des domaines temps-variants complémentaires. Nous utilisons le théorème du point fixe de Banach pour prouver l'existence et l'unicité de la solution pour le modèle de l'extrudeuse. La méthode de résolution repose sur un changement de coordonnées qui permet de définir le système sur un domaine fixe. Cette normalisation fait apparaître des termes de convection fictifs dans les coefficients multiplicatifs de l'opérateur différentiel de transport. Nous obtenons finalement l'existence, l'unicité et la régularité de la solution faible du problème de Cauchy.
- le *Chapitre 5* concerne l'étude d'un système hyperbolique couplé à une interface mobile. Il s'agit des équations issues du bilan de masse dans une extrudeuse sous certaines

hypothèses simplificatrices. Nous représentons les équations aux dérivées partielles et ordinaires couplées par un système à retards particulier : le retard est sur l'entrée et dépend de l'état. Cette représentation est obtenue en résolvant l'équation de transport de masse par la méthode des caractéristiques. La stabilisation de l'interface autour d'une position d'équilibre s'effectue au moyen d'un prédicteur.

- le **Chapitre 6** est une extension de l'analyse des problèmes d'interface à une classe particulière de systèmes. Nous considérons deux systèmes de deux lois de conservation décrites sous le formalisme Hamiltonien à port et définis sur des domaines complémentaires variant dans le temps. Nous proposons une formulation basée sur l'utilisation de la fonction couleur ou fonction caractéristique du domaine pour étendre les variables sur l'ensemble du domaine et définissons un système Hamiltonien augmenté des fonctions couleur. Dans un deuxième temps nous considérons un système à interface mobile et nous montrons que le système augmenté d'une entrée définie comme étant la vitesse de l'interface avec une sortie conjuguée reste un système Hamiltonien à port.

1.1 Modélisation d'un procédé d'extrusion pour la commande

Les procédés d'extrusion sont destinés à la fabrication de produits finis ou semi-finis par utilisation de vis sans fin en rotation dans un fourreau cylindrique disposant d'un système de chauffage comme le montre le schéma de la figure 4.4.1.

La matière tout au long de son parcours subit certaines transformations (réaction chimique, cuisson, homogénéisation...). Elle est ainsi transportée vers le dispositif de mise en forme, la filière, par lequel la matière est expulsée par des petits orifices sous l'action de fortes pressions.

D'un point de vue industriel, on cherche à obtenir à la sortie de la machine un débit régulier, avec un matériau homogène ayant les propriétés d'usage désirées, à température contrôlée, et des conditions de production satisfaisantes (débit maximal, consommation énergétique limitée). Dans ce chapitre nous élaborons un modèle dynamique qui pourra être utilisé pour la commande.

Ces procédés sont complexes et composés de phénomènes hydrodynamiques, thermiques et physico-chimiques fortement couplés. Une littérature importante existe sur la modélisation en régime *stationnaire* des écoulements de la matière dans une extrudeuse [140, 57, 91]. Des modèles dynamiques ont aussi été développés. On trouve des modèles issus de l'identification paramétrique [85, 68, 145, 144] développés pour la commande PID ou prédictive.

Des modèles *dynamiques* en dimension finie [37] et infinie [86, 80, 81, 75, 76] ont été développés. Citons le modèle de dimension finie d'extrusion réactive proposé par [37] prédisant le régime dynamique sous différentes conditions opératoires (débit d'alimentation, concentration à l'entrée des différentes espèces, puissance de chauffe des fourreaux) et basé sur une représentation par une cascade de *RCPA* (réacteurs continus parfaitement agités) avec

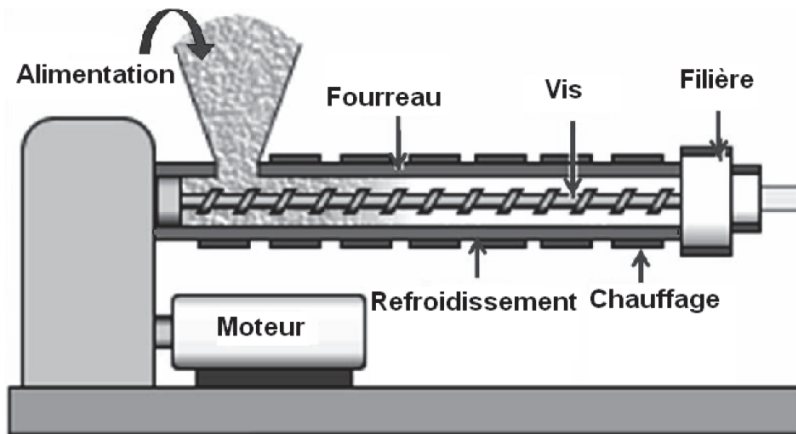


Figure 1.1.1: Description schématique d'une extrudeuse

reflux. En dimension infinie, les modèles 1D proposés dans [86] et [89] mettent en évidence les couplages des phénomènes de transport de la matière et d'échange de chaleur.

Ces modèles de connaissance, en dimension infinie, restent toujours inexploités pour des objectifs de commande. La difficulté pour la commande de ces procédés à partir de ces modèles résulte de l'existence d'une interface mobile entre deux zones aux propriétés d'écoulement différentes.

Il existe une littérature très fournie concernant la modélisation et la simulation de systèmes avec interface mobile. Un problème très souvent traité et référencé, comme le problème de Stefan, étudie le déplacement de l'interface entre deux zones spatiales ayant des dynamiques différentes sous l'influence de phénomènes diffusifs et/ou convectifs. Il concerne un vaste champ d'applications [66] comme par exemple, le gonflement de nanocapsules [26], la lyophilisation [138], la cuisson [119].

La commande de systèmes à frontière mobile a aussi été étudiée dans [14] pour un modèle parabolique semi-linéaire et dans [47] pour un modèle parabolique non linéaire. Dans cette seconde publication, le problème de commande est étudié à partir d'un modèle linéarisé de dimension finie. Une discussion concernant les problèmes de commande d'écoulements réactifs à frontière mobile est aussi proposée dans [116].

Dans ce chapitre nous proposons un modèle bi-zone d'extrudeuse composé de deux systèmes d'équations d'évolution de type hyperbolique couplés par une interface mobile dont la dynamique est donnée par une EDO. Le modèle 1D bi-zone est déduit des bilans de matière et d'énergie exprimées en termes de taux de remplissage et d'un taux d'humidité ainsi que de la température, les variables de commande étant la vitesse de rotation des vis, la température du fourreau et le débit d'alimentation. Les relations d'interface sont déduites des hypothèses de continuité de flux de quantité de mouvement ou de pression l'interface et permettent de calculer la pression en amont de la filière.

1.1.1 Modèle bi-zone d'une extrudeuse

Nous présentons ici un modèle idéalisé des phénomènes de transfert de matière et de chaleur dans une extrudeuse corotative bi-vis dont le profil de vis est supposé uniforme. De plus nous supposons l'existence de deux zones (représentées sur la figure 4.4.5), une zone de convoyage et une zone de pompage suivant que la matière remplit complètement ou non le volume efficace de l'extrudeuse [86] ; [89].

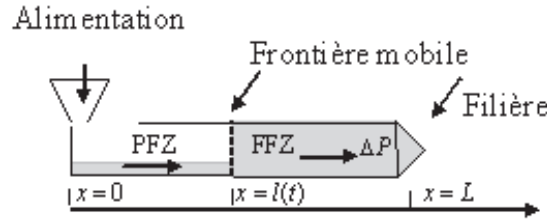


Figure 1.1.2: Schéma des deux zones de convoyage et pompage

La zone partiellement remplie, notée PFZ, est une zone de transport avec une grande surface libre permettant l'introduction aisée de réactifs : la matière est chauffée et transportée vers la zone de fusion. Cette région est caractérisée par des débits de reflux nuls (la matière est transportée en aval sous l'effet de la rotation de la vis), une pression constante égale à la pression atmosphérique et de faibles échanges thermiques entre la matière et le fourreau.

Dans la zone entièrement remplie, notée FFZ, la matière est chauffée, mélangée, mise sous pression et convectée vers la filière avec des échanges thermiques importants entre le fourreau et la matière. Un gradient de pression se crée à partir de la filière provoquant la circulation d'un débit de reflux. De forts auto-échauffements par dissipation visqueuse sont aussi présents.

Ces deux zones sont couplées à travers une interface mobile notée $l(t)$ qui sépare la zone où l'extrudeuse est complètement remplie (taux de remplissage égal à 1) de celle où elle est partiellement remplie (taux de remplissage < 1). Cet interface caractérise donc la discontinuité du taux de remplissage.

Nous considérons que l'extrudat est un mélange contenant de l'eau, ce qui est le cas par exemple de l'extrusion alimentaire qui donne lieu à l'élaboration de produits complexes associant céréales et matières grasses et pour laquelle la teneur en eau est un facteur important. De plus nous faisons les hypothèses suivantes :

- l'écoulement est uni-dimensionnel ; c'est l'écoulement longitudinal qui détermine le débit de l'extrudeuse,
- la capacité calorifique C , la viscosité η et la masse volumique ρ_0 sont supposées constantes et les pertes de chaleur sont négligeables sur l'axe des vis.

1.1.1.1 Bilans de matière et d'énergie dans les deux zones

Le modèle repose sur l'écriture des bilans de masse totale, de l'eau et du bilan d'énergie pour chaque zone. Le bilan de quantité de mouvement est écrit et réduit à un modèle unidimensionnel stationnaire [25]. Les phénomènes de transfert de chaleur et de matière sont décrits selon les zones (*PFZ* ou *FFZ*) par les variables suivantes :

- le taux de remplissage $f(x, t)$: il est défini comme le rapport entre la densité linéique de volume occupé par la matière et la densité linéique de volume disponible ou efficace (dans la direction de l'écoulement de coordonnée x) ;
- le taux d'humidité $M(x, t)$: c'est le rapport de densité linéique de volume d'eau présente dans la matière sur la densité de volume disponible ;
- la température $T(x, t)$;
- la pression $P(x, t)$.

$x \in [0, L]$ est la variable spatiale et $t \in \mathbb{R}_+$ la variable temporelle.

1.1.1.2 Modèle de la zone partiellement remplie ou *PFZ*

Dans cette zone le taux de remplissage $f_p(x, t)$ varie dans l'intervalle $[0, 1]$. L'expression des bilans de matière et d'énergie aboutit aux équations d'évolution suivantes sur le taux de remplissage $f_p(x, t)$, le taux d'humidité $M_p(x, t)$ et la température $T_p(x, t)$:

$$\frac{\partial}{\partial t} \begin{pmatrix} f_p(x, t) \\ M_p(x, t) \\ T_p(x, t) \end{pmatrix} = -\xi N(t) I_3 \frac{\partial}{\partial x} \begin{pmatrix} f_p(x, t) \\ M_p(x, t) \\ T_p(x, t) \end{pmatrix} + \begin{pmatrix} 0 \\ 0 \\ \Omega_p(f_p, N, T_p, T_{F_p}) \end{pmatrix} \quad (1.1.1)$$

I_3 est la matrice identité de dimension 3. Le premier terme de ces équations d'évolution consiste simplement en trois équations de transport à la vitesse $v(t) = \xi N(t)$ uniforme et proportionnelle à la vitesse de rotation des vis $N(t)$ et au pas de vis ξ . Le terme source Ω intervient dans le bilan d'énergie uniquement et est défini par la fonction:

$$\Omega_p(f, N, T, T_F) = \frac{\mu \eta N^2(t)}{f_p(x, t) \rho_0 V_{eff} C} + \frac{S_{ech} \alpha}{\rho_0 V_{eff} C} (T_F - T_p) \quad (1.1.2)$$

Son premier terme correspond à la dissipation visqueuse due à la rotation et est proportionnelle au carré de la vitesse de rotation des vis $N(t)$ et le second terme représente les échanges de chaleur entre le fourreau et la matière et est proportionnel à la différence de température ($T_{F_p} - T_p$) entre le fourreau et la matière dans l'extrudeuse. Les paramètres sont la capacité calorifique C [$J \text{ kg}^{-1} \text{ K}^{-1}$], la masse volumique ρ_0 [kg m^{-3}], η [Pa s^{-1}] le coefficient de viscosité, μ [$J \text{ kg}^{-1} \text{ K}^{-1}$] le facteur de dissipation visqueuse de la matière, $V_{eff} = S_{eff} \xi$ est le volume efficace de l'extrudeuse (où S_{eff} est la section efficace de l'extrudeuse et ξ son

pas de vis) et S_{ech} [m^2] est la surface d'échange, α [$Jm^{-2}s^{-1}K^{-1}$] le coefficient d'échange thermique entre la matière et fourreau. Rappelons finalement que l'on suppose l'équilibre de pression avec la pression atmosphérique: $P(x, t) = P_0$.

1.1.1.3 Modèle de la zone entièrement remplie ou FFZ

Par définition de la zone entièrement remplie, le taux de remplissage atteint sa borne supérieure et vérifie: $f_f(x, t) = 1$. C'est donc la variable conjuguée, la pression qui varie dans cette zone. De l'hypothèse de la stationnarité de l'écoulement, on déduit l'expression du gradient de pression :

$$\frac{\partial P(x, t)}{\partial x} = \eta \frac{V_{eff}N(t)\rho_0 - F_d}{B\rho_0} \quad (1.1.3)$$

qui est proportionnel à la différence entre la capacité maximale de pompage ($V_{eff}N(t)\rho_0$) et le débit net en sortie de filière F_d :

$$F_d = \frac{K_d}{\eta} \Delta P \text{ avec } \Delta P = (P(L, t) - P_0) \quad (1.1.4)$$

où K_d caractérise la géométrie de la filière et dépendant aussi des caractéristiques géométriques de la vis B .

Les bilans de matière et d'énergie impliquent les équations d'évolution suivantes sur le taux d'humidité $M_f(x, t)$ et la température $T_f(x, t)$ dans la zone entièrement remplie :

$$\frac{\partial}{\partial t} \begin{pmatrix} M_f(x, t) \\ T_f(x, t) \end{pmatrix} = -\frac{F_d\xi}{\rho_0 V_{eff}} I_2 \frac{\partial}{\partial x} \begin{pmatrix} M_f(x, t) \\ T_f(x, t) \end{pmatrix} + \begin{pmatrix} 0 \\ \Omega_f(N, T_f, T_{F_f}) \end{pmatrix} \quad (1.1.5)$$

De nouveau le premier terme de ces équations d'évolution consiste simplement en deux équations de transport à la vitesse $v(t) = \frac{F_d\xi}{\rho_0 V_{eff}}$ et le second Ω_2 représente la source d'énergie thermique due à dissipation visqueuse et aux échanges de chaleur entre le fourreau et la matière.

$$\Omega_f(N, T, T_F) = \frac{\mu\eta N^2(t)}{\rho_0 V_{eff}C} + \frac{S_{ech}\alpha}{\rho_0 V_{eff}C} (T_F - T_f) \quad (1.1.6)$$

1.1.2 Dynamique de l'interface mobile $l(t)$ et relations d'interface

1.1.2.1 Relations d'interface

Nous faisons dans la suite l'hypothèse que la température et le taux d'humidité sont continus à l'interface :

$$\begin{aligned} T_p(l^-, t) &= T_f(l^+, t) \\ M_p(l^-, t) &= M_f(l^+, t) \\ \text{où } l^\pm(t) &= \lim_{\varepsilon \rightarrow 0} l(t) \pm \varepsilon \end{aligned}$$

La troisième relation d'interface est basée sur deux hypothèses qui permettent de résoudre l'équation 1.1.3 et de calculer la pression dans la zone entièrement remplie.

Cas 1 : la continuité du flux de quantité de mouvement

$$F(l^-, t)v(l^-, t) + P(l^-, t)f_p(l^-, t)S_{eff} = F(l^+, t)v(l^+, t) + P(l^+, t)S_{eff} \quad (1.1.7)$$

avec :

- $F(l^-, t) = \rho_0 N(t) V_{eff} f_p(l^-, t)$
- $F(l^+, t) = F_d(t)$
- $v(l^-, t) = \xi N(t)$
- $v(l^+, t) = \frac{\xi F_d(t)}{\rho_0 V_{eff}}$
- $P(l^-, t) = P_0$

L' intégration de l'équation 1.1.3 donne :

$$P(l^+, t) = P(L, t) + \eta \frac{V_{eff} N \rho_0 - F_d}{B \rho_0} (l^+ - L) \quad (1.1.8)$$

Des équations 1.1.4, 1.1.7 et 1.1.8 nous déduisons la pression à l'interface :

$$P(L, t) = P_0 + \frac{-[1 + \frac{K_d}{B \rho_0} (L - l^+)] + \sqrt{\Delta}}{\frac{2K_d^2}{\eta^2 \rho_0 S_{eff}^2}} \quad (1.1.9)$$

avec

$$\Delta = \left[1 + \frac{K_d}{B \rho_0} (L - l^+)\right]^2 + \Omega (f_p(l^-, t), N(t), l^+) \quad (1.1.10)$$

et

$$\Omega = \left(\frac{2K_d}{\eta S_{eff}}\right)^2 \left(\frac{\eta V_{eff} N(t)}{B \rho_0} (L - l^+)\right) + \xi^2 N^2(t) f_p(l^-, t) - (1 - f_p(l^-, t)) \frac{P_0}{\rho_0} \quad (1.1.11)$$

Le modèle suppose l'existence de deux zones *PFZ* et *FFZ*, ce qui n'est vrai que si $\Delta P = P(L, t) - P_0$ est positif. De ce fait Ω doit être strictement positif. Cette contrainte sur la fonction $\Omega (f_p(l^-, t), N(t), l^+)$ permet de déduire pour une vitesse de rotation donnée, la valeur minimum du taux de remplissage à la frontière pour que l'hypothèse sur l'existence des zones *PFZ* et *FFZ* soit satisfaite.

Cas 2 : la continuité de pression

$$\begin{cases} P(L, t) = P_0 + \frac{\eta V_{eff} N(t) \rho_0 (L - l(t))}{(B \rho_0 + K_d (L - l(t)))} \\ F_d(t) = \frac{K_d V_{eff} N(t) \rho_0 (L - l(t))}{(B \rho_0 + K_d (L - l(t)))} \end{cases} \quad (1.1.12)$$

Dans ce cas de figure le débit en sortie de filière est positif si $(L - l(t)) > 0$ ce qui est nécessairement vrai. Cette relation d'interface n'exige aucune contrainte sur le taux de remplissage à la frontière.

1.1.2.2 Bilan de masse et dynamique de l'interface

La *PFZ* et la *FFZ* sont séparées par une interface mobile $l(t)$. L'équation de la frontière s'obtient par un bilan de matière totale sur la zone entièrement remplie :

$$\frac{dl(t)}{dt} = \frac{F_d - F(l(t))}{\rho_0 S_{eff}(1 - f_p(l^-, t))} \quad (1.1.13)$$

$F(l(t))$ représente le débit entrant dans la zone entièrement remplie et F_d est le débit en sortie de filière. Le terme $\rho_0 S_{eff}(1 - f_p(l^-, t))$ montre que l'évolution de la frontière dépend du remplissage du volume non occupé par la matière ou volume disponible. Nous rappelons que ce modèle n'est valable que pour $f_p(l^-) < 1$.

1.1.3 Conditions frontières et conditions initiales

Les conditions limites en $x = 0$ et en $x = L$ sont établies sous l'hypothèse de la continuité du débit de matière, de la température et du flux de quantité de mouvement.

1.1.3.1 Frontière en $x = 0$

Le débit, la température et le taux d'humidité sont supposés continus :

- le débit est égal au débit d'alimentation en matière $F_{in}(t)$,
- la température $T_p(0, t)$ et le taux d'humidité $M_p(0, t)$ sont égaux à ceux de la matière mise dans le circuit d'alimentation soit $T_{in}(t)$ et $M_{in}(t)$:

$$f_p(0, t) = \frac{F_{in}(t)}{\rho_0 N V_{eff}} \quad (1.1.14)$$

$$T_p(0, t) = T_{in}(t) \quad (1.1.15)$$

$$M_p(0, t) = M_{in}(t) \quad (1.1.16)$$

1.1.3.2 Conditions initiales

À $t = 0$ nous supposons l'existence des deux zones d'où les conditions initiales suivantes :

- pour la *PFZ* :

$$f_p(x, 0) = f_{p0} \quad (1.1.17)$$

$$M_p(x, 0) = M_{p0} \quad (1.1.18)$$

$$T_p(x, 0) = T_{p0} \quad (1.1.19)$$

- pour la *FFZ* :

$$M_f(x, 0) = M_{f0} \quad (1.1.20)$$

$$T_f(x, 0) = T_{f0} \quad (1.1.21)$$

1.2 Étude du problème de Cauchy associé au modèle de l'extrudeuse

Le problème d'existence de solution pour les modèles de système à frontières mobiles est largement étudié dans le cas de modèles paraboliques [106] et des modèles hyperboliques [120] ; [43] où des EDPs sont définies sur la première zone spatiale, une EDO sur l'interface et un modèle algébrique sur la seconde zone spatiale. Le modèle d'extrudeuse considéré ici se distingue par le fait qu'il est composé de deux systèmes d'équations d'évolution de type hyperbolique couplés par une interface mobile. Nous proposons d'étudier le modèle associé au procédé d'extrusion par le *théorème du point fixe de Banach*. Dans un premier temps nous représentons le système dans le domaine $(0, 1)$ en utilisant les changements de coordonnées appropriés pour chaque zone. L'argument du point fixe permet ensuite de définir les conditions d'existence de solution pour ce problème.

1.2.1 Modèle adimensionnel à domaine fixe $(0, 1)$

Dans cette section nous présentons deux changements de variables qui permettent d'écrire les équations d'évolution sur le domaine fixe $(0, 1)$. Le domaine total $(0, L)$ est transformé en l'intervalle $(0, 1)$ et la position de l'interface mobile est ramenée à la valeur fixe 1. Un terme de convection fictive fonction de $l(t)$ apparaît alors dans les équations d'évolution.

Le modèle normalisé est constitué:

- d'une équation aux dérivées ordinaires décrivant la dynamique de l'interface

$$\begin{cases} \dot{l}(t) = F(l(t), N(t), f_p(t, 1)), & t \in (0, T) \\ l(0) = l^0, \end{cases} \quad (1.2.1)$$

- d'une équation de transport de masse:

$$\begin{cases} \partial_t f_p(t, x) + \alpha_p(t, x) \partial_x f_p(t, x) = 0, & (t, x) \in (0, T) \times (0, 1) \\ f_p(0, x) = f_p^0(x), & x \in (0, 1) \\ f_p(t, 0) = \frac{F_{in}(t)}{\theta(N(t))}, & t \in (0, T) \end{cases} \quad (1.2.2)$$

- de deux équations de transport du taux d'humidité:

$$\begin{cases} \partial_t M_p(t, x) + \alpha_p(t, x) \partial_x M_p(t, x) = 0, & (t, x) \in (0, T) \times (0, 1) \\ \partial_t M_f(t, x) + \alpha_f(t, x) \partial_x M_f(t, x) = 0, & (t, x) \in (0, T) \times (0, 1) \\ M_p(0, x) = M_p^0(x), & M_f(0, x) = M_f^0(x), & x \in (0, 1) \\ M_p(t, 0) = M_{in}(t), & M_f(t, 0) = M_p(t, 1), & t \in (0, T) \end{cases} \quad (1.2.3)$$

- et de deux équations de transport de la température

$$\begin{cases} \partial_t T_p(t, x) + \alpha_p(t, x) \partial_x T_p(t, x) = \Omega_p, & (t, x) \in (0, T) \times (0, 1) \\ \partial_t T_f(t, x) + \alpha_f(t, x) \partial_x T_f(t, x) = \Omega_f, & (t, x) \in (0, T) \times (0, 1) \\ T_p(0, x) = T_p^0(x), \quad T_f(0, x) = T_f^0(x), & x \in (0, 1) \\ T_p(t, 0) = T_{in}(t), \quad T_f(t, 0) = T_p(t, 1), & t \in (0, T) \end{cases} \quad (1.2.4)$$

1.2.2 Principaux résultats

Nous rappelons [40, Section 2.1], la définition de la solution faible du problème de Cauchy: (??)-(1.2.4).

Définition 1. . Soit $T > 0$, une solution faible du problème de Cauchy (1.2.1)-(1.2.4) est un vecteur $(l, f_p, M_p, M_f, T_p, T_f) \in W^{1,\infty}(0, T) \times W^{1,\infty}(Q) \times (C^0([0, T]; L^2(0, 1)))^4$, tel que pour tout $\tau \in [0, T]$, toute fonction test $\varphi_1, \varphi_2 = (\varphi_{21}, \varphi_{22}), \varphi_3 = (\varphi_{31}, \varphi_{32}) \in C^1([0, T] \times [0, 1])$ tel que

$$\varphi_i(\tau, x) = 0, \quad \forall x \in [0, 1], \quad i = 1, 2, 3, \quad (1.2.5)$$

$$\varphi_i(t, 1) = 0, \quad \forall t \in [0, T], \quad i = 1, 2, 3, \quad (1.2.6)$$

nous avons

$$l(t) = l^0 + \int_0^t F(l(s), N(s), f_p(s, 1)) ds, \quad t \in (0, \tau), \quad (1.2.7)$$

$$\begin{aligned} \int_0^\tau \int_0^1 f_p(\partial_t \varphi_1 + \partial_x(\alpha_p \varphi_1)) dx dt + \int_0^1 f_p^0(x) \varphi_1(0, x) dx \\ + \int_0^\tau \frac{F_{in}(t)}{\theta(N(t))} \alpha_p(t, 0) \varphi_1(t, 0) dt = 0, \end{aligned} \quad (1.2.8)$$

$$\begin{aligned} \int_0^\tau \int_0^1 M_p(\partial_t \varphi_{21} + \partial_x(\alpha_p \varphi_{21})) dx dt + \int_0^\tau \int_0^1 M_f(\partial_t \varphi_{22} + \partial_x(\alpha_f \varphi_{22})) dx dt \\ + \int_0^\tau \alpha_p(t, 0) M_{in}(t) \varphi_{21}(t, 0) dt + \int_0^\tau \alpha_f(t, 0) M_p(t, 1) \varphi_{22}(t, 0) dt \\ + \int_0^1 M_p^0(x) \varphi_{21}(0, x) dx + \int_0^1 M_f^0(x) \varphi_{22}(0, x) dx = 0, \end{aligned} \quad (1.2.9)$$

$$\begin{aligned} \int_0^\tau \int_0^1 T_p(\partial_t \varphi_{31} + \partial_x(\alpha_p \varphi_{31})) dx dt + \int_0^\tau \int_0^1 T_f(\partial_t \varphi_{32} + \partial_x(\alpha_f \varphi_{32})) dx dt \\ + \int_0^\tau \int_0^1 \Omega_p \varphi_{31} dx dt + \int_0^\tau \int_0^1 \Omega_f \varphi_{32} dx dt \\ + \int_0^\tau \alpha_p(t, 0) T_{in}(t) \varphi_{31}(t, 0) dt + \int_0^\tau \alpha_f(t, 0) T_p(t, 1) \varphi_{32}(t, 0) dt \\ + \int_0^1 T_p^0(x) \varphi_{31}(0, x) dx + \int_0^1 T_f^0(x) \varphi_{32}(0, x) dx = 0. \end{aligned} \quad (1.2.10)$$

Nous proposons ces deux théorèmes:

Théorème 2. Soient $T > 0$ et (l_e, N_e, f_{pe}) un équilibre constant,

$$F(l_e, N_e, f_{pe}) = 0 \quad (1.2.11)$$

avec $0 < f_{pe} < 1$, $0 < l_e < L$. Sous l'hypothèse de compatibilité en $(0, 0)$

$$\frac{F_{in}(0)}{\theta(N(0))} = f_p^0(0). \quad (1.2.12)$$

il existe ε_0 (dépendant de T) tel que pour tout $\varepsilon \in (0, \varepsilon_0]$, si

$$\|f_p^0(\cdot) - f_{pe}\|_{W^{1,\infty}} + \left\| \frac{F_{in}(\cdot)}{\theta(N(\cdot))} - f_{pe} \right\|_{W^{1,\infty}} + \|N(\cdot) - N_e\|_{W^{1,\infty}} + |l^0 - l_e| \leq \varepsilon. \quad (1.2.13)$$

le problème de Cauchy (1.2.1)-(1.2.4) admet une solution unique $(l, f_p, M_p, M_f, T_p, T_f) \in W^{1,\infty}(0, T) \times W^{1,\infty}(Q) \times (C^0([0, T]; L^2(0, 1)))^4$, avec:

$$\|f_p - f_{pe}\|_{W^{1,\infty}} + \|l - l_e\|_{W^{1,\infty}} \leq C_{\varepsilon_0} \cdot \varepsilon, \quad (1.2.14)$$

$$\|M_p\|_{C^0([0, T]; L^2(0, 1))} \leq C_{\varepsilon_0} \cdot (\|M_p^0\|_{L^2} + \|M_{in}\|_{L^2}), \quad (1.2.15)$$

$$\|T_p\|_{C^0([0, T]; L^2(0, 1))} \leq C_{\varepsilon_0} \cdot (\|T_p^0\|_{L^2} + \|T_{in}\|_{L^2}), \quad (1.2.16)$$

$$\|M_f\|_{C^0([0, T]; L^2(0, 1))} \leq C_{\varepsilon_0} \cdot (\|M_p^0\|_{L^2} + \|M_{in}\|_{L^2} + \|M_f^0\|_{L^2}), \quad (1.2.17)$$

$$\|T_f\|_{C^0([0, T]; L^2(0, 1))} \leq C_{\varepsilon_0} \cdot (\|T_p^0\|_{L^2} + \|T_{in}\|_{L^2} + \|T_f^0\|_{L^2}), \quad (1.2.18)$$

où C_{ε_0} est une constante dépendant de ε_0 mais indépendant de ε .

Théorème 3. Sous les hypothèses du Théorème 2, supposons que $f_p^0(\cdot) \in H^2(0, 1)$, $\frac{F_{in}(\cdot)}{\theta(N(\cdot))} \in H^2(0, T)$, et la condition de compatibilité suivante en $(0, 0)$ vérifiée:

$$f_{p_x}^0(0) + \frac{l(0)}{\zeta N(0)} \cdot \frac{F'_{in}(0)\theta(N(0)) - F_{in}(0)\theta'(N(0))N'(0)}{\theta^2(N(0))} = 0. \quad (1.2.19)$$

alors il existe ε_0 (dépendant de T) tel que pour tout $\varepsilon \in (0, \varepsilon_0]$, si

$$\|f_p^0(\cdot) - f_{pe}\|_{H^2(0, 1)} + \left\| \frac{F_{in}(\cdot)}{\theta(N(\cdot))} - f_{pe} \right\|_{H^2(0, T)} + \|N(\cdot) - N_e\|_{W^{1,\infty}} + |l^0 - l_e| \leq \varepsilon, \quad (1.2.20)$$

le problème de Cauchy (1.2.1)-(1.2.4) admet une solution unique $(l, f_p, M_p, M_f, T_p, T_f) \in W^{1,\infty}(0, T) \times C^0([0, T]; H^2(0, 1)) \times (C^0([0, T]; L^2(0, 1)))^4$ avec :

$$\|f_p - f_{pe}\|_{C^0([0, T]; H^2(0, 1))} \leq C_{\varepsilon_0} \cdot \varepsilon, \quad (1.2.21)$$

où C_{ε_0} est une constante dépendant de ε_0 mais indépendant de ε .

1.3 Stabilisation de l'interface par une approche de commande prédictive

Cette partie traite de la stabilisation de la position de l'interface par une régulation du débit d'alimentation en matière dans une extrudeuse. Ce débit entrant agit sur l'équation de transport du taux de remplissage dans la zone partiellement remplie définie sur un domaine variable dans le temps. Il apparaît dans ce contexte un retard du au temps de propagation de l'entrée et ce retard est fonction du taux de remplissage à l'interface $f_p(l(t), t)$. Le problème de commande est représenté par la stabilisation un système à retard sur l'entrée. Les systèmes à retard sur l'entrée ne sont pas fréquemment utilisés pour les problèmes de contrôle en génie des procédés même si les modèles dynamiques de différents procédés laissent apparaître des délais de propagation significatifs [39, 12, 151, 152, 31]. Généralement, les problèmes de régulation des systèmes d'équation de transport se ramènent à des problèmes de stabilisation de systèmes à retards. En effet, une résolution de des equations aux dérivées partielles par la méthode des caractéristiques permet de transformer les EDPs en des systèmes d'équations aux dérivées ordinaires comportant un retard [65, 125, 4, 3]. Dans cette section nous utilisons cette méthode des caractéristiques pour transformer le système original en un système à retard sur l'entrée équivalent.

1.3.1 Les équations de conservation de masse dans une extrudeuse

La modélisation de l'extrudeuse fait apparaître deux zones géométriques dans lesquelles la matière est transportée à des vitesse différentes. Ces deux zones sont séparées par une interface mobile dont la dynamique est dictée par une équation aux dérivées ordinaires obtenue par un bilan de masse dans la zone entièrement remplie. Ici, nous rappelons les équations issues du bilan de masse dans les zones partiellement et entièrement remplies. La zone partiellement remplie est définie dans le domaine spatial $[0, l(t)[$ et la zone entièrement remplie dans $]l(t), L]$ (L représente la longueur de l'extrudeuse et $l(t)$ la position de l'interface).

- En représentant la variation de la masse dans la zone partiellement remplie par le taux de remplissage $f_p(x, t)$, le bilan de masse est représenté par une équation de transport dont la vitesse est déterminée par la vitesse de rotation $N(t)$ et le pas ξ de la vis. Sous l'hypothèse d'une continuité de débit à l'entrée $\{x = 0\}$, la condition frontière associée au taux de remplissage se déduit de la vitesse de convection, du volume disponible V_{eff} , de la masse volumique ρ_0 , et du débit d'alimentation $F_{in}(t)$:

$$\begin{cases} \frac{\partial f_p}{\partial t}(x, t) = -\xi N(t) \frac{\partial f_p}{\partial x}(x, t) & x \in [0, l(t)[\\ f_p(0, t) = f_p^{in}(t) = \frac{F_{in}(t)}{\rho_0 \xi N(t) V_{eff}} \end{cases} \quad (1.3.1)$$

- Dans la zone entièrement remplie la vitesse de convection est proportionnelle au débit de sortie de filière $F_d(t)$. Le bilan de masse dans cette zone permet d'obtenir l'équation

d'évolution de la position de l'interface $l(t)$:

$$\begin{cases} \frac{dl(t)}{dt} = \frac{F_d(t) - \rho_0 N(t) V_{eff} f_p(l(t), t)}{\rho_0 S_{eff} (1 - f_p(l(t), t))} \\ l(0) = l^0 \quad 0 < l^0 < L, \end{cases} \quad (1.3.2)$$

Le débit $F_d(t)$ est une fonction des caractéristiques géométriques de la filière K_d , de la viscosité η et de la pression en L , $P(L, t)$.

$$\begin{cases} F_d(t) = \frac{K_d}{\eta} \Delta P(t) \\ \Delta P(t) = (P(L, t) - P_0), \end{cases} \quad (1.3.3)$$

P_0 est la pression atmosphérique.

Dans cette partie nous considérons que la relation de couplage est définie par une continuité de la pression à l'interface. Alors:

$$\Delta P(t) = \frac{\eta V_{eff} N(t) \rho_0 (L - l(t))}{(B \rho_0 + K_d (L - l(t)))} \quad (1.3.4)$$

1.3.2 Résolution de l'équation de transport

Considérons l'équation de transport (1.3.1) avec la condition frontière associée $f_p(0, t)$. La dérivée totale de la variable f_p s'écrit:

$$\frac{df_p(x(\tau), t)}{d\tau} = \frac{dt}{d\tau} \frac{\partial f_p(x(\tau), t)}{\partial t} + \frac{dx(\tau)}{d\tau} \frac{\partial f_p(x(\tau), t)}{\partial x}$$

Les solutions de l'équation (1.3.1), le long des caractéristiques sont données par:

$$\begin{cases} \frac{dt}{d\tau} = 1 \\ \frac{dx(\tau)}{d\tau} = \xi N(t) \\ \frac{df_p(x(\tau), t)}{d\tau} = 0 \end{cases} \quad (1.3.5)$$

Comme $N(t)$ est une fonction de t , le système (1.3.5) ne peut être résolu explicitement. En intégrant les equations caractéristiques:

$$\begin{pmatrix} x_1 & x_2 & x_3 \end{pmatrix} = \begin{pmatrix} t & x & f_p \end{pmatrix} \in \mathbb{R}^3$$

nous obtenons:

$$\begin{cases} x_1(\tau, s) = \tau + s \\ x_2(\tau, s) = \xi \int_s^{\tau+s} N(\tau') d\tau' \\ x_3(s) = f_p(s) \end{cases} \quad (1.3.6)$$

s étant la constante d'intégration. Soit $\bar{N}(t)$ la fonction primitive de $N(t)$, nous en déduisons :

$$\bar{N}(s) = \bar{N}(\tau + s) - \frac{x_2}{\xi} \quad (1.3.7)$$

Finalement:

$$s = \bar{N}^{-1}\left(\bar{N}(t) - \frac{x}{\xi}\right) \quad (1.3.8)$$

Toute fonction constante le long des caractéristiques s'exprime de la manière suivante:

$$f_p(x, t) = f_p\left(\bar{N}^{-1}\left(\bar{N}(t) - \frac{x}{\xi}\right)\right) \quad (1.3.9)$$

La solution satisfaisant la condition frontière associée à l'équation de transport (1.3.1) est donnée par:

$$f_p(x, t) = f_p^{in}\left(\bar{N}^{-1}\left(\bar{N}(t) - \frac{x}{\xi}\right)\right) \quad (1.3.10)$$

Cette solution peut être exprimée en fonction du débit d'alimentation en matière:

$$f_p^{in}\left(\bar{N}^{-1}\left(\bar{N}(t) - \frac{x}{\xi}\right)\right) = \frac{F_{in}\left(\bar{N}^{-1}\left(\bar{N}(t) - \frac{x}{\xi}\right)\right)}{\rho_0 N(t) V_{eff}}, \quad (1.3.11)$$

1.3.3 Système à retard sur l'entrée dépendant de l'état

Dans la suite nous considérons que la vitesse de rotation de la vis est constante $N(t) = N_0$. Le problème de commande consiste à stabiliser l'interface en agissant sur le débit d'alimentation en matière(1.3.11). Dans ce cas de figure, la solution de l'équation de transport s'écrit :

$$\begin{cases} f_p(x, t) = f_p^{in}\left(t - \frac{x}{N_0 \xi}\right) \\ f_p(l(t), t) = f_p^{in}\left(t - \frac{l(t)}{N_0 \xi}\right), \end{cases} \quad (1.3.12)$$

et l'équation de la dynamique d'interface devient :

$$\begin{cases} \frac{dl(t)}{dt} = \frac{F_d(t) - \rho_0 N_0 V_{eff} f_p^{in}\left(t - \frac{l(t)}{N_0 \xi}\right)}{\rho_0 S_{eff} \left[1 - f_p^{in}\left(t - \frac{l(t)}{N_0 \xi}\right)\right]} \\ F_d(t) = \frac{K_d}{\eta} \Delta P(t) \end{cases} \quad (1.3.13)$$

L'équation (1.3.13) définit un système à retard sur l'entrée dépendant de l'état et peut s'écrire sous la forme abstraite:

$$\begin{cases} \frac{dl(t)}{dt} = f(l(t), U(t - D(l(t)))) \\ U(t) = f_p^{in}(t) \end{cases} \quad (1.3.14)$$

où f est une fonction non-linéaire et $D(l(t))$ la fonction retard dépendant de l'état et agissant sur l'entrée $U(t)$. Le problème de stabilisation est résolu en utilisant le contrôleur prédictif proposé par [19, 20].

1.4 Systèmes Hamiltoniens à ports couplés par une interface mobile

De nombreux systèmes physiques décrits par des équations aux dérivées partielles admettent une formulation Hamiltonienne à ports et sont appelés systèmes Hamiltoniens à ports frontière [136, 98, 92]. Ces systèmes ont été étudiés sous différents aspects incluant l'existence de solution et la commande dans le cas linéaire [93, 87, 141, 155, 142, 73, 113, 94].

Ici nous explorons le couplage de deux systèmes Hamiltoniens à ports à travers une interface mobile. Cette classe de systèmes apparaît dans différents contextes liée aux procédés impliquant des changements de phase, des phénomènes d'évaporation etc. Dans cette étude nous considérons l'exemple de deux gaz séparés par un piston de masse nulle. L'approche proposée est basée sur les travaux de [61, 60, 10, 28] concernant les systèmes hyperboliques couplés par une interface fixe. Les auteurs proposent d'augmenter le système par une fonction couleur qui est définie comme étant la fonction caractéristique du domaine.

1.4.1 Définition d'un système Hamiltonien à ports pour deux lois de conservation

Dans un premier temps nous rappelons la définition d'un système Hamiltonien à ports frontière en considérant un système de deux lois de conservation défini par :

$$\partial_t x + \partial_z \mathcal{N}(x) = 0 \quad (1.4.1)$$

Nous rappelons que le système de deux lois de conservation (1.4.1) peut être exprimé sous la forme:

$$\partial_t x(z, t) = \mathcal{J} \delta_x \mathcal{H} \quad (1.4.2)$$

Où $\delta_x \mathcal{H}$ est la dérivée variationnelle d'une fonction Hamiltonienne correspondant à l'énergie totale du système. En effet le flux $\mathcal{N}(x)$ est donné par la relation suivante :

$$\mathcal{N}(x) = \begin{pmatrix} 0 & -1 \\ -1 & 0 \end{pmatrix} \begin{pmatrix} \delta_{x_1} \mathcal{H} \\ \delta_{x_2} \mathcal{H} \end{pmatrix} \quad (1.4.3)$$

et l'opérateur canonique Hamiltonien par l'égalité ci-dessous :

$$\mathcal{J} = \begin{pmatrix} 0 & -\partial_z \\ \partial_z^* & 0 \end{pmatrix} \quad (1.4.4)$$

L'équation (1.4.1) augmentée des variables de ports

$$\begin{pmatrix} f_\partial \\ e_\partial \end{pmatrix} = \begin{pmatrix} \delta_{x_2} \mathcal{H} \\ \delta_{x_1} \mathcal{H} \end{pmatrix} \Big|_{a,b} = \begin{pmatrix} 0 & 1 \\ 1 & 0 \end{pmatrix} \begin{pmatrix} \delta_{x_1} \mathcal{H} \\ \delta_{x_2} \mathcal{H} \end{pmatrix} \Big|_{a,b} \quad (1.4.5)$$

Définit un système Hamiltonien à ports frontière.

1.4.2 Interconnexion de deux systèmes Hamiltoniens à ports à travers une interface fixe

Nous considérons des systèmes Hamiltoniens à ports de deux lois de conservations définis sur les domaines spatiaux $[a, 0[$ et $]0, b]$ dénotés par les symboles $\{-; +\}$:

$$\partial_z x^i + \partial_z \mathcal{N}^i(x^i) \quad (1.4.6)$$

Nous définissons les fonctions couleurs qui sont des fonctions caractéristiques du domaine par:

$$c_0(z, t) = \begin{cases} 1 & z \in [a, 0[\\ 0 & z \in [0, b] \end{cases} \quad \text{and} \quad \bar{c}_0(z, t) = \begin{cases} 1 & z \in]0, b] \\ 0 & z \in [a, 0] \end{cases} \quad (1.4.7)$$

L'augmentation du système Hamiltonien par des variables couleurs satisfaisant les lois de conservation

$$\partial_t c = \partial_t \bar{c} = 0 \quad (1.4.8)$$

avec les conditions initiales c_0 and \bar{c}_0 et des conditions aux bords compatibles permet de définir un système Hamiltonien sur le domaine total $[a, b]$. Nous définissons le vecteur d'état étendu :

$$\tilde{x} = (x^T, c, \bar{c})^T \quad (1.4.9)$$

et la fonction Hamiltonienne $\mathcal{H}(x, c, \bar{c}) = \int_a^b H(x, c, \bar{c}) dz$ avec une densité d'énergie

$$H(x, c, \bar{c}) = c H^-(x) + \bar{c} H^+(x). \quad (1.4.10)$$

La dérivée variationnelle s'écrit :

$$\delta_{\tilde{x}} \mathcal{H}(\tilde{x}) = \begin{pmatrix} \delta_x \mathcal{H}(x, c, \bar{c}) \\ \delta_c \mathcal{H}(x, c, \bar{c}) \\ \delta_{\bar{c}} \mathcal{H}(x, c, \bar{c}) \end{pmatrix} = \begin{pmatrix} c \delta_x \mathcal{H}^-(x) + \bar{c} \delta_x \mathcal{H}^+(x) \\ \mathcal{H}^-(x) \\ \mathcal{H}^+(x) \end{pmatrix} \quad (1.4.11)$$

Considérons le système (1.4.12) :

$$\partial_t \tilde{x} = \mathcal{J}_a \delta_{\tilde{x}} \mathcal{H}(\tilde{x}) + I e_I \quad (1.4.12)$$

avec une application d'entrée définie par:

$$I^T = \begin{pmatrix} 0 & -1 & 0 & 0 \end{pmatrix} \quad (1.4.13)$$

et l'opérateur augmenté:

$$\mathcal{J}_a = \begin{pmatrix} 0 & \mathbf{d} & 0_2 \\ -\mathbf{d}^* & 0 & 0_2 \\ 0_2 & 0_2 \end{pmatrix} \quad (1.4.14)$$

L'opérateur \mathbf{d} est un opérateur différentiel non-linéaire, modulé par $c(z, t)$ and $\bar{c}(z, t)$ et défini par:

$$\mathbf{d} = -[\partial_z c + \partial \bar{c}.] \quad (1.4.15)$$

Son dual formel est:

$$\mathbf{d}^* = -\mathbf{d} + [(\partial_z c) - (\partial_z \bar{c})] \quad (1.4.16)$$

Proposition 1. *L'ensemble des relations \mathcal{D}_I associées au système de deux lois de conservation définis par les variables $\begin{pmatrix} x_1 \\ x_2 \end{pmatrix}$ sur le domaine spatial $[a, b] \ni z$ avec une interface au point $z = 0$ qui garantit la continuité de la variable d'effort e_2 et la discontinuité de la variable d'effort e_2 est défini par*

$$\mathcal{D}_I = \left\{ \left(\begin{pmatrix} \tilde{f} \\ f_I \\ f_\partial \end{pmatrix}, \begin{pmatrix} \tilde{e} \\ e_I \\ e_\partial \end{pmatrix} \right) \in \mathcal{F} \times \mathcal{E} / \right.$$

$$\left. \begin{pmatrix} \tilde{f} \\ f_I \end{pmatrix} = \begin{pmatrix} \mathcal{J}_a & I \\ -I^T & 0 \end{pmatrix} \begin{pmatrix} \tilde{e} \\ e_I \end{pmatrix} \right. \quad (1.4.17)$$

$$\left. \text{and } \begin{pmatrix} f_\partial \\ e_\partial \end{pmatrix} = \begin{pmatrix} 0 & 1 \\ (c + \bar{c}) & 0 \end{pmatrix} \begin{pmatrix} e_1 \\ e_2 \end{pmatrix} \Big|_{a,b} \right\}$$

avec les variables de flux $\tilde{f} = (f_1, f_2, f_c, f_{\bar{c}})^T$ et les variables d'effort $\tilde{e} = (e_1, e_2, e_c, e_{\bar{c}})^T$ associées au vecteur d'état étendu (1.4.9), et à l'opérateur différentiel augmenté \mathcal{J}_a défini par (1.4.14), les opérateurs \mathbf{d} , resp. \mathbf{d}^* définis par (1.4.15), resp. (1.4.16), le vecteur colonne I défini par (1.4.13), et l'espace produit $\mathcal{B} = \mathcal{F} \times \mathcal{E}$ avec $\mathcal{F} = L^2((a, b), \mathbb{R})^5 \times \mathbb{R}^2$ et $\mathcal{E} = \text{dom } \mathbf{d}^* \times \text{dom } \mathbf{d} \times L^2((a, b), \mathbb{R})^3 \times \mathbb{R}^2$ muni du produit bi-linéaire

$$\left\langle \begin{pmatrix} \tilde{f} \\ f_I \\ f_\partial \end{pmatrix}, \begin{pmatrix} \tilde{e} \\ e_I \\ e_\partial \end{pmatrix} \right\rangle = \int_a^b \tilde{e}^T \tilde{f} dz + e_\partial^T \Sigma f_\partial + \int_a^b e_I^T f_I dz \quad (1.4.18)$$

avec $e_\partial^T \Sigma f_\partial = e_\partial(a) f_\partial(a) - e_\partial(b) f_\partial(b)$, définit une structure de Dirac.

1.4.3 Interconnexion de deux systèmes Hamiltoniens à ports à travers une interface mobile

Pour une interface dont la position varie en fonction du temps nous définissons les fonctions couleur suivantes:

$$c_{l(t)}(z, t) = \begin{cases} 1 & z \in [a, l(t)[\\ 0 & z \in [l(t), b] \end{cases} \quad (1.4.19)$$

et

$$\bar{c}_{l(t)}(z, t) = \begin{cases} 1 & z \in]l(t), b] \\ 0 & z \in [a, l(t)] \end{cases} \quad (1.4.20)$$

Ces fonctions couleurs obéissent à des equations de transport dont la vélocité est donnée par la vitesse de l'interface $\dot{l}(t)$:

$$\partial_t c(z, t) = -\dot{l}(t) \partial_z c(z, t) \quad \text{and} \quad \partial_t \bar{c}(z, t) = -\dot{l}(t) \partial_z \bar{c}(z, t) \quad (1.4.21)$$

avec les conditions initiales:

$$c(z, 0) = c_{l(0)}(z, t) \quad \text{and} \quad \bar{c}(z, 0) = \bar{c}_{l(0)}(z, t) \quad (1.4.22)$$

Le système Hamiltonien associé aux deux systèmes de lois de conservation couplés par une interface mobile peut se définir en considérant un système étendu et augmenté des fonctions couleurs.

$$\partial_t \begin{pmatrix} x \\ c \\ \bar{c} \end{pmatrix} = \mathcal{J}_a \begin{pmatrix} \delta_x \mathcal{H}(x, c, \bar{c}) \\ \delta_c \mathcal{H}(x, c, \bar{c}) \\ \delta_{\bar{c}} \mathcal{H}(x, c, \bar{c}) \end{pmatrix} + I e_I + \dot{l}(t) \begin{pmatrix} c x & \bar{c} x \\ -1 & 0 \\ 0 & -1 \end{pmatrix} \partial_z \begin{pmatrix} c \\ \bar{c} \end{pmatrix} \quad (1.4.23)$$

l'application d'entrée à l'interface I est définie par (1.4.13).

L'application d'entrée associé à la dynamique de l'interface est définie par (1.4.24)

$$G(x, c, \bar{c}) = \begin{pmatrix} c x & \bar{c} x \\ -1 & 0 \\ 0 & -1 \end{pmatrix} \partial_z \begin{pmatrix} c \\ \bar{c} \end{pmatrix} \quad (1.4.24)$$

et sa sortie conjuguée e_l est définie par la relation:

$$e_l = \int_a^b \delta_{\tilde{x}} \mathcal{H}(\tilde{x})^T G(x, c, \bar{c}) dz$$

où:

$$e_l = \langle G({}^T x, c, \bar{c}) |, \delta_{\tilde{x}} \mathcal{H}(\tilde{x}) \rangle = \int_a^b \delta_{\tilde{x}} \mathcal{H}(\tilde{x})^T G(x, c, \bar{c}) dz \quad (1.4.25)$$

Proposition 2. *L'ensemble des relations \mathcal{D}_M associées au système de deux lois de conservation définis par les variables $\begin{pmatrix} x_1 \\ x_2 \end{pmatrix}$ sur le domaine spatial $[a, b] \ni z$ avec une interface mobile de vitesse \dot{l} qui garantit la continuité de la variable d'effort e_2 et la discontinuité de la variable d'effort e_2 est défini par:*

$$\mathcal{D}_M = \left\{ \left(\begin{pmatrix} \tilde{f} \\ f_I \\ e_l \\ f_\partial \end{pmatrix}, \begin{pmatrix} \tilde{e} \\ e_I \\ i \\ e_\partial \end{pmatrix} \right) \in \mathcal{F} \times \mathcal{E} / \right.$$

$$\left. \begin{pmatrix} \tilde{f} \\ f_I \\ -e_l \end{pmatrix} = \begin{pmatrix} \mathcal{J}_a & I & G(x, c, \bar{c}) \\ -I^T & 0 & 0 \\ -\langle G^T(x, c, \bar{c}) | & 0 & 0 \end{pmatrix} \begin{pmatrix} \tilde{e} \\ e_I \\ i \end{pmatrix} \right. \quad (1.4.26)$$

$$\left. \text{and } \begin{pmatrix} f_\partial \\ e_\partial \end{pmatrix} = \begin{pmatrix} 0 & 1 \\ (c + \bar{c}) & 0 \end{pmatrix} \begin{pmatrix} e_1 \\ e_2 \end{pmatrix}_{a,b} \right\}$$

avec les variables de flux $\tilde{f} = (f_1, f_2, f_c, f_{\bar{c}})^T$ et les variables d'effort $\tilde{e} = (e_1, e_2, e_c, e_{\bar{c}})^T$ associées au vecteur d'état étendu (1.4.9), l'opérateur différentiel \mathcal{J}_a défini par (1.4.14), des opérateurs \mathbf{d} , resp. \mathbf{d}^* définis par (1.4.15), resp. (1.4.16), le vecteur colonne I défini par (6.2.32), l'application en entrée G définie par (6.3.10) et son adjoint $\langle G^T |$ par (6.3.11) et l'espace produit $\mathcal{B} = \mathcal{F} \times \mathcal{E}$ avec $\mathcal{F} = L^2((a, b), \mathbb{R})^5 \times \mathbb{R} \times \mathbb{R}^9$ et $\mathcal{E} = \text{dom } \mathbf{d}^* \times \text{dom } \mathbf{d} \times L^2((a, b), \mathbb{R})^3 \times \mathbb{R} \times \mathbb{R}^9$ muni du produit bi-linéaire

$$\left\langle \begin{pmatrix} \tilde{f} \\ f_I \\ e_l \\ f_\partial \end{pmatrix}, \begin{pmatrix} \tilde{e} \\ e_I \\ i \\ e_\partial \end{pmatrix} \right\rangle = \int_a^b \tilde{e}^T \tilde{f} dz + \int_a^b e_I^T f_I dz + e_\partial^T \Sigma f_\partial - e_l i \quad (1.4.27)$$

avec $e_\partial^T \Sigma f_\partial = e_\partial(a) f_\partial(a) - e_\partial(b) f_\partial(b)$, définit une structure de Dirac.

Chapter 2

Introduction

2.1 Motivation and previous work

Balance equations provide the foundation for much of the physical-based modelling in fluid dynamics. They are also the starting point for developing qualitative understanding of phenomenological observations in fluid mechanics, heat transfer, mass transfer, and reaction engineering. Describing physical phenomena using variables that influence these behavior is the main issue of modelling and a large class of physical systems are characterized by a spatio-temporal dynamics. Physical systems obey to physical laws expressing conservation of certain quantities (mass, momentum, energy) and can be represented by partial differential equations. These infinite dimensional systems which are generally deduced from the conservation laws appear in modelling of transport and diffusion phenomena. In this context, the analysis of coupled PDEs through an interface is not current in the literature which concern to the study of these infinite dimensional systems. The lack of physical model which express clearly the interface structure and the coupling conditions can be considered as the real challenge in modelling point of view. It is clear that, in addition to the definition of each model of conservation laws, an interfacial model must be constructed in order to precise the nature of the informations that are exchanged at the coupling region. This interfacial model may be formulated for instance, when imposing the continuity of a given set of variables or a given linear or nonlinear function of variables while preserving physically a coherent description of processes. In this aspect, lot of studies which are related to coupled hyperbolic systems of conservation laws through an fixed interface exist in the literature. In [27], the coupling problem is considered in the space domain \mathbb{R} which is separated by a thin interface \mathcal{I} located at $\{0\}$. The system is described on each side of the interface by 1D hyperbolic systems of conservation law with different equations of state.

One may consider two cases of coupling formulation:

- The first one which is conservative, is called a *flux coupling methods* in the sense that the solution performs continuous flow at the interface. This approach is considered

when the conservation laws are described by discontinuous coefficients in the domains $\mathbb{R}^{-,*}$ and $\mathbb{R}^{+,*}$ [78, 71, 62, 32, 16].

- The second approach is related to *state coupling methods* which consist to impose the continuity of the state variables at the interface. Then, the relation between the traces of the solution on both sides of the interface can be interpreted in terms of two sets of boundary conditions. The left trace of the first conservation laws which are defined in $\mathbb{R}^{-,*}$ serves as boundary condition for the second one. Also, right trace of the second conservation laws which are defined in $\mathbb{R}^{+,*}$ stand as a boundary condition for the first one [8, 9, 11, 61, 60].

For physical problems the requirement of continuity of all the unknowns variables of the system is quite impossible. For example, considering a flow in tubes of different sections, a pressure drop is observed at the discontinuities of the medium [7]. An alternative model suggested by this observation is the *state coupling methods*: the interface requires continuity of a set of variables which are nonlinear transformation of the state variables, selected according to the physical constraints.

The mathematical and numerical studies of this class of systems calls for interesting questions in the last decades. Such fixed interface problems typically appear in nuclear reactor and steam generators at the phase change. They also concern the fluid dynamic modelling in porous and non-porous media, and are very frequent in networks traffic flow modelling (supply chains connecting several suppliers, a vertical manhole with two horizontal tubes) [120].

However, control techniques which are dedicated to coupled infinite dimensional systems by a fixed interface is very difficult to implement. Networks of flow transportation is the major example which is explored in control theory concerning these systems. For an irrigation canal which is connected to secondary canals and reservoirs, the control is located at the interfaces which interconnect different sub-systems. The objectives of such control strategies is usually the regulation of water levels close to a given reference set-point [17, 5, 123, 95], with input values being minimized, or changes in inputs being minimized [17, 143]. The inputs are here acting at the interface which is a gate modelling the pressure discontinuity in different region of the network. So the regulation is performed by opening gates at these points using model predictive controllers, feedback or feedforward controllers. Usually, due to the complexity and size of water networks, control of such systems is not performed in a centralized way. Distributed control composed by local controllers which are designed in such way that they take into account the effects of local actions on the overall system performance are developed. Then, control strategy is based on a potential cooperation, negotiation and communication between many controllers as in all transportation networks systems [107].

This thesis is devoted to the analysis of PDEs which are coupled through a moving interface by extrusion process modelling. The interface dynamic is given by an ordinary differential equation and the PDEs are defined in two complementary time-varying domains. Such sys-

tems arises in many applications like multi-phase flow, crystal growth, freeze drying process modelling [50, 51, 66, 119, 138, 26, 47], mixing systems (model of torus reactor including a well-mixed zone and a transport zone), Diesel Oxidation Catalyst [116]. For moving interface problems, one should also define the transmission conditions at the interface: the coupling aspect is formulated using a continuity argument as it will be shown in *Chapter 6*. As for fixed interface, there exists infinite manner for modelling the interconnection between the two sub-systems of conservation laws based on conservation of a physical quantity. The main difference between fixed and moving interface problem appears in the analysis of interfacial topological changes which are introduced by the interface motion. In the case of extrusion processes, the system should take into account thermal and friction effect as well as other factors which derive from modelling aspect. The coupled system may be also exposed to oscillations at the moving junction which can generate numerical instability in computations. Over the last two decades, there has been an ongoing quest for new computational methods to solve multi-phase flows and applications include the study of condensation and several phase change processes. This thrust has been motivated in part by the energy industry because those processes allow fluids to store and release large amounts of heat energy. The main challenges for a direct numerical simulation come from the fact that the interface location must be calculated as part of the process solution and discontinuities in materials properties across the interface must be preserved. The first attempt at advanced numerical simulations deals with the simulation of a two dimensional thin film boiling using moving triangular grids [147]. The others approaches as front tracking [46, 133] allow to track explicitly the interface by a moving front on a fixed mesh. Also, simulations are carried out using a level set approach [114] as well as volume of fluid approach [70],[45]. These numerical methods will be discussed succinctly in *Chapter 3* which is dedicated to the modelling and the numerical computation of the extrusion process model. Note that the advantage of the level set method is that topological changes are handled naturally without special treatments.

Mathematical analysis of such systems is generally performed using coordinates change which allows to treat the problem in a fixed domain. In *Chapter 4* we propose such kind of transformations in order to deal with the cauchy problem of the extruder process model.

Over the last few years, the problem of controlling coupled PDEs with time-varying domains has become subject to very great interest. In [116] a boundary control problem is formulated for the outlet temperature control in Diesel Oxidation Catalyst process. As it is described in [116] the distributed reactive gaseous system takes into account a moving interface model which separates the upstream reactive zone from the downstream transport zone. The author of [116] points out that the mobile interface dynamic in this process stand as a function of measured disturbances and the control variable. Also, the control problem is tackled using Laplace transformation to build a transfer function as a modified Bessel function which can be translated in the time domain. Then, the input/output relation obeys a straightforward open-loop control law: given histories for the output temperature, one can simply determine

the corresponding inlet temperature histories. For nonlinear Stefan problem control strategy based on the resolution of the inverse problem is proposed in [116]. In many cases concerning control of quasi-linear parabolic PDEs with moving interface, standard Galerkin's method is used to derive an approximate finite dimensional one, for applying classical control strategy as feedback [52, 13, 14]. In *Chapter 5* we suggest to treat moving interface problem using delay system framework.

2.2 Organization and contribution of the thesis

The thesis is divided into four chapters:

- *Chapter 3* is devoted to the modelling of an extrusion process as coupled transport equations through moving interface. The model derives from mass and energy balance in an extrusion process and is formulated as two non-autonomous systems of transport equations coupled by a moving interface which is described by an ordinary differential equation. Two coupling relations are proposed for mass balance equation. The first one states the continuity of pressure and the second one is based on momentum flux continuity at the mobile interface. The analysis of these two coupling relations is performed in *Chapter 5*
- *Chapter 4* is dedicated to a mathematical analysis of transport equations which are defined in complementary time-varying domains. We illustrate how fixed point argument and contraction mapping principle can be used in order to state the well-posedness of such coupled hyperbolic Cauchy problem using the extrusion process model. Our strategy is based on a change of coordinates which allows to express the system on a fixed domain. This normalization generates fictive convection terms depending on the interface dynamic in the transport equations. We obtain the existence, uniqueness and regularity of the weak solution for Cauchy problem.
- In *Chapter 5*, an analysis of 1D hyperbolic partial differential equation with moving interface as a delay system is proposed. The model derives from the mass balance of an extrusion process that describes the mass transport by hyperbolic partial differential equation coupled with an ordinary differential equation. The ordinary differential equation represents the interface motion. Solving the transport equation by the method of characteristics, we obtain a state-dependent-input-delay control problem. The stabilization of the system around an equilibrium is obtained using a state predictor.
- *Chapter 6* is an extension of our analysis on moving interface problem to a particular class of conservation laws. We consider the port-Hamiltonian formulation of systems of two conservation laws defined on two complementary intervals of some interval of the real line and coupled by a moving interface. We recall first how two port Hamiltonian

systems coupled by an interface may be expressed as a port Hamiltonian systems augmented with two variables being the characteristic functions of the two spatial domains. Then, we consider the case of a moving interface and show that it may be expressed as the previous port Hamiltonian system augmented with an input, being the velocity of the interface and define a conjugated output variable. We give some structure to the interface relations defining the dynamics of the displacement of the interface and with the simple example of two gases coupled by a moving piston we discuss the passivity property.

The thesis concludes with some final remarks and perspectives on future work in *Chapter 7*.

2.3 Publications

1. International Journal papers

DIAGNE M., DOS SANTOS MARTINS V., COUENNE F., MASCHKE B., JALLUT C., *Modélisation d'un procédé d'extrusion par deux systèmes d'équations d'évolution couplés par une interface mobile*. Méthodes numériques et applications des systèmes à paramètres répartis, JESA, VOL 45/7-10 2011, pp.665-691.

DIAGNE M., B. MASCHKE, *Port Hamiltonian formulation of a system of two conservation laws with a moving interface*, February 2013 (accepted in European Journal of Control).

2. International conference papers

DIAGNE M., DOS SANTOS MARTINS V., COUENNE F., MASCHKE B., *Well-posedness of the model of an extruder in infinite dimension*, 50th IEEE Conference on Decision and Control and European, Control Conference, Orlando, FL, USA on December 12-15 2011, (num 1926).

DOS SANTOS MARTINS V., DIAGNE M., COUENNE F., MASCHKE B., *Stabilité d'un procédé d'extrusion par deux systèmes d'équations d'évolution couplés par une interface mobile*, Conférence Internationale Francophone d'Automatique (CIFA 2012), Conférence IEEE, Grenoble, France, on July 4-6 2012, (num 174) .

DIAGNE M., MASCHKE B., *Boundary Port Hamiltonian Systems of Conservation Laws Coupled by a Moving Interface*, 4th IFAC Workshop on Lagrangian and Hamiltonian Methods for Non Linear Control, LHMNLC, Bertinoro, University of Bologna,

Italy, on August 29-31, 2012.

DIAGNE M., COUENNE F., MASCHKE B., *Mass Transport Equation with Moving Interface and Its Control As an Input Delay System* *Time Delay Systems*, 11th Workshop on Time-Delay Systems Time Delay Systems, Volume 11, Part 1, February 04-06, Grenoble, France, 2013.

3. National conference papers

DIAGNE M., COUENNE F., MASCHKE B., *Two-zone model of an extruder and its control as an input delay system*, Récents Progrès en Génie des Procédés, Numéro 104 - ISSN: 1775-335X ; ISBN: 978-2-910239-78-7, Ed. SFGP, Paris, France 2013.

Chapter 3

Extrusion processes modelling for control

3.1 Introduction

Extruders are designed to process highly viscous materials. They are mainly used in the chemical industries for polymer processing as well as in the food industries. An extruder is made of a barrel, the temperature of which is regulated. One or two Archimedean screws are rotating inside the barrel. The extruder is equipped with a die where the material comes out of the process (Fig. 3.1.1). The extruder is of particular interest due to its modular geometry allowing the control of capacities of mixing along the machine. Another interesting property of the extruder is that the fill ratio along the axial direction of the screws can be less than one in some part of the system according to the screw configuration and the operating conditions. For modelling purposes, the main phenomenon is obviously the fluid flow which may be considered as highly viscous Newtonian or non-Newtonian fluid flows interacting with heat transfer and possibly chemical reactions. These processes occur within a complex non-stationary volume delimited by the barrel and the rotating screw. Another point is that the fluid viscosity may significantly change due to composition and temperature changes.

The most important part of the extruder is the screw configuration which modulates extensively the mechanical energy. Direct pitch screws promote the transport by having conveying effect and reverse pitch screws which restrict the convection phenomena are useful for melting effect.

- Single-screw extruders are limited in their ability to transport high viscous material and have poor mixing capability. To improve the mixing effect distributive mixing elements called mixers blocks are often incorporated in the screw design. Generally the mixing section is a restrictive region where the material is subjected to high stresses that for a short time. A typical single-screw extruder consists of three zones: feeding zone which is essentially a transport zone, mixing zone and finishing zone (cooking zone for food

processing).

- Twin-screw extruders provide a high degree of heat transfer (Fig. 3.1.2). This type of extruders can be classified on the basis of direction of screw rotation in counter-rotating and co-rotating twin-screw extruders. Counter-rotating screws move in opposing directions and co-rotating screws move in the same direction. Counter-rotating screws are not widely used in food industry although they are excellent conveyors. They are good in processing relatively non viscous materials requiring low speed and long resident time. The main advantages of a co-rotating configuration which are commonly used in the snack food industry are the self-cleaning capacity, the excellent mixing quality and the very high degassing rate.

Both counter- and co-rotating screws can be either intermeshing or non-intermeshing. In an intermeshing configuration one screw penetrates the channel of the second screw, producing a positive pumping action, efficient mixing and self-cleaning capacity. Non-intermeshing screws do not engage or interfere with each other and depend on friction as single-screw extruders. They are not designed for mixing and are similar to single-screw extruders, even if they have higher capacities.

In the literature there exists no result about the control of an infinite dimensional model of an extruder. In this chapter, the proposed model offers the perspective to develop control methods for these processes using dynamic physical models.

The studies performed on the automated control of extruders are based on experimental data from pilot-scale units to develop transfer functions for controller design. The ultimate control systems involved manipulation of screw speed, feed rate, inlet solvent fraction, and barrel temperature. The models were developed to control motor torque, solvent content, product temperature, specific mechanical energy, viscosity, residence time and die flow, etc. As an example, the screw speed and temperature of the mixing zone determine the amount of cooking, moisture, extent of mixing, and exiting temperature of the final product. The transport phenomena occurring in the extruder lead to different models taking into account the delay corresponding to the time each particle spends in the barrel section (residence time). This suggests that the transport phenomena occurring in the extruder can be included in a specific delay system framework which offers many control strategies in order to obtain desired properties of extruded material. A number of control methodologies have been proposed to regulate the product quality for those processes. A simple methodology can be a single-input single-output (SISO) feedback control linking the output at the die to the input parameter such as the screw speed. In [85, 69, 85, 99, 54, 105, 127, 132] proportional integral derivative *PID* feedback controllers are performed through different models which are deduced from experimental data under specific operating conditions for food and polymer extrusion. In context of food extrusion a multi-variables predictive control which allows to track both input and output for a given set point is proposed by [145] as a Dual Target Predictive

Controller (*DTPC*). The predictive capabilities of (*DTPC*) are provided by an on-line system identification. Predictive controllers are also implemented for many applications as in [108, 130, 68, 67].

As far as modelling issues are concerned, one can find many papers devoted to steady-state modelling for design purpose, [139], but works devoted to dynamic modelling of extruders are less common, [80, 81, 75, 76, 37]. For control purposes, one can mainly cite the following works:

- [37] proposes a finite dimensional model based on a flow representation made of a series of Continuous Stirred Tank Reactors (CSTR) with variable back-flows. This approach allows simulating the filling process of the machine as well as all the other state-variables. This model has been validated in the case of the polymerization of ϵ -Caprolactone.
- An infinite dimensional model has been developed in [86, 89, 88] within the context of food processing. In this case, the *Fully and Partially Filled Zones* are defined in advance. These two zones are modelled by transport equations with different velocities. A moving interface obeying an ordinary differential equation interconnects the two infinite dimensional systems. Those models remained undeveloped for control because the authors do not explicitly express all constraints, particularly at the interface. The same methods are used in [117] to describe the extraction of solvent in a vegetable matter. The authors represent the liquid accumulation in porous matter. They consider otherwise, transport (*Partially Filled*) and pressing (*Fully Filled*) *Zones* without discussing the interconnection through the interface which separate the two zones. Transport equations are also used in [131] for modelling the solid fusion by extrusion under stationary conditions.

In this chapter, a non-linear infinite dimensional 1D model of an extruder is developed. The model is inspired by [86, 89, 88] and is focused on the analysis of interface relations as transmission conditions. The obtained model is simulated using finite volume method adapted to a moving interface system by extending the variables with a color function. The color function is associated to the time varying domains as a characteristic function which also obey to a transport equation. The velocity of transport is here given by the mobile interface motion.

3.1.1 Organization of the chapter

The organization of this chapter is as follows: first in Section 2.2, we present a geometric decomposition of the extruder by defining a *Partially* and a *Fully Filled Zone*. Then, we obtain a bi-zone model of the process by defining two zones which are coupled by a moving interface. In Section 2.3, we propose a model of the *Partially Filled Zone* by considering extrusion of homogeneous material and Section 2.4 is dedicated to the modelling of *Fully Filled Zone*. In section 2.5 we present the dynamics of the moving interface and two classes

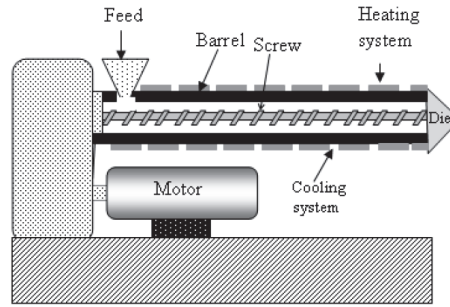


Figure 3.1.1: Schematic description of an extruder

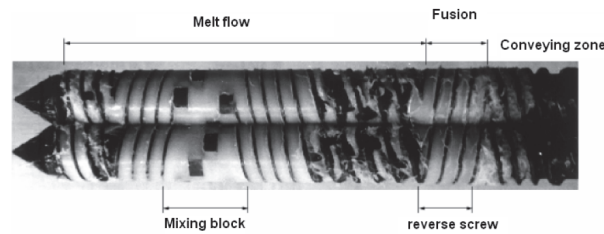


Figure 3.1.2: conveying, melting, mixing zones in a twin-screw extruder [2]

of coupling relations. Section 2.6 is devoted to the discussion on numerical computation and the simulation of the interface dynamics, filling ratio and temperature variables.

3.1.2 Contributions

The main contribution of this chapter is the formulation of a dynamic input/output 1D model of an extrusion process. The modelling objective is to analyze evolution of temperature, die pressure and filling ratio under some operating conditions. The model is based on structural decomposition of the extruder in two zones. These zones which are *Partially* and *Fully Filled* arise from the geometric structure of the machine. Expressing conservation of mass and energy in these two zones, one obtains a system of two non-autonomous transport equations which are interconnected by an ordinary differential equation on the moving interface. The specificity of the interface relations is discussed using continuity of pressure and continuity of momentum flux. Numerical method which is inspired from the height function method is performed using color function. The color function which stand as characteristic function of the complementary time-varying domains allows to extend the definition of variables in the total domain. Simulations are presented to illustrate the coherence of this physical model relating heat and mass transport in nonhomogeneous media.

3.2 Bi-zone model of an extruder

3.2.1 Zones defined by the pressure gradient

The complexity of screw configuration in an extruder makes difficult the design a non-isothermal flow model [25]. In [24], an analysis of the flow in the channel of co-rotating twin-screws with the same speed is developed and the authors show how a reasonable flow analysis can be made by writing a single screw extrusion process as an equivalent model. In an extruder, the net flow at the die exit is mainly due to the flow of material in the longitudinal direction if one neglects the clearance between the screw and the barrel and the vibrations. Therefore, the flow dynamic which is dominated by the convection effect in the direction of screw axis is sufficient to represent the material flow. This means that the transverse flow corresponding to a recirculation of the material in the plane perpendicular to the screw channel is neglected. From a macroscopic point of view, a 1D model describes clearly the material transport in an extruder. So, the material is driven from the feed to the die by the pumping effect of the screw rotation. It becomes clear that the geometric structure of the die influences the material transport along the extruder. Therefore, the material is accumulated behind the die and fills completely the available volume in this region. This spatial domain where the extruder is completely filled is called the *Fully Filled Zone* (FFZ). The flow in this *Fully Filled Zone* depends on the pumping capacity of the screw and also on the pressure flow. The pressure gradient which appears due to the die restriction is given by Navier-Stokes equation which provides a mathematical model of the fluid motion. The extruder which is initially empty, may also comprise a spatial domain that is not completely filled by the material. This region which corresponds to a conveying region is called *Partially Filled Zone* (PFZ). In this domain, there is no pressure build-up. This means that the pressure gradient is zero and the pressure inside the barrel is approximatively equal to the atmospheric pressure. The transport velocity of the material can be controlled by the screw speed and the feed rate. In an extrusion process with a complex geometry of the screws, there exist alternating *Partially* and *Fully Filled Zones*. In the remainder of the thesis, we shall assume that the geometry of the equivalent screw is uniform and that there exist only one *Partially Filled Zone* and one *Fully Filled Zone*. These two zones are coupled by an interface which characterizes the spatial domains where the pressure gradient is null or not (and accordingly where the extruder is *Partially or Fully Filled*). The moving interface is assumed to be thin, i.e. reduced to a point. In the sequel the spatial domain of the extruder will be taken to be the real interval $[0, L]$ where $L > 0$ is the length of the extruder. Denoting by $l(t) \in [0, L]$, the position of the thin interface, the domain of the *Partially Filled Zone* is $[0, l(t)[$ and the *Fully Filled Zone* is defined in interval $]l(t), L]$. The interface is moving according to the volume of material which is accumulated in the *Fully Filled* region. It is clear, that the interface which separates these two zones is a function of the difference between feed and die rates. In

conclusion we shall consider three interdependent dynamics which described the evolution of the material in the *Partially and Fully Filled Zones* (PFZ and FFZ) and the evolution of the interface position.

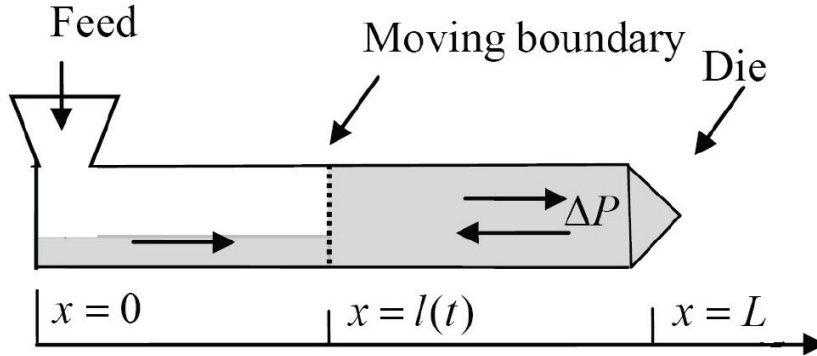


Figure 3.2.1: Bi-zone model of an extruder

3.2.2 Modelling assumptions and definition of the variables

3.2.2.1 Modelling assumptions

We shall assume that the extruded melt is composed of some species blended with water and that it forms an incompressible homogeneous mixture. For example, in food extrusion processes the water content is an important factor which characterizes the quality of extruded material. We also make the following assumptions:

- the twin-screw mechanism is approximated by a single screw and the relative motion of the screws is not taken into account.
- the flow is one-dimensional and strictly convective in the down barrel direction.
- the heat capacity C_p and the density ρ_0 are assumed to be constant,
- the screw pitch ξ is uniform along the extruder,
- there is no reaction which occurs along the process,
- the extruder is divided in time-varying spatial zones where the material fills completely or not the effective volume V_{eff} [86, 89].
- there exists an interface $l(t)$ between the *Partially Filled Zone* and the *Fully Filled Zone* corresponding to discontinuity of the filled volume (or filled volume fraction also called filling ratio);
- the *Partially Filled Zone* is submitted to atmospheric pressure P_0 .

3.2.2.2 Definition of the variables

let us remind that extrusion processes are used for the production of various products which may vary in their physical structures, composition and functional properties. Depending on the desired material and the desired properties of the product, the extrusion process can combine different functions: transport of material, mixing, compression, shear, chemical reactions, heating, cooling, cooking, drying and formatting. Each of these functions can be exploited to various degrees by the appropriate choice of the control parameters and the design of the machine. For a food extrusion process, the transformation mechanisms that occur lead to consider the following variables:

1. **The filling ratio:** This rate is defined as the ratio between the volume occupied by the material (V_o) and the free volume or effective volume between the barrel and the screw. Effective volume (V_{eff}) is the total volume that can be occupied by material.

$$f(x, t) = \frac{V_o(x, t)}{V_{eff}} \quad (x, t) \in (\mathbb{R}^+ \times \mathbb{R}^+) \quad (3.2.1)$$

Remark 1. In the *Partially Filled Zone*, the partial filling characteristic implies that the volume occupied by material is less than the total available volume:

$$0 < f_p(x, t) < 1.$$

The FFZ has an occupied volume equal to the free volume and $f_f(x, t) = 1$.

2. **The moisture content** is the fraction of water stored in the material which is conveyed. This rate is defined as the ratio between the volume of water V_e and the effective volume V_{eff} :

$$M(x, t) = \frac{V_e(x, t)}{V_{eff}} \quad \forall (x, t) \in (\mathbb{R}^+ \times \mathbb{R}^+) \quad (3.2.2)$$

Remark 2. The moisture content is always less than 1 for both two zones and its evolution affects the viscosity $\eta(x, t)$ along the extruder. This rate determines the quality of the product see e.g [68], where the author considers the moisture content to evaluate volume expansion during cooking popcorn process.

3. **The temperature:** $T(x, t)$ depends on exchanges of heat between the barrel and the extruded material and also on the viscous dissipation phenomena due to the transformation of mechanical energy into heat.

4. **The Pressure:** in the *Partially Filled Zone* the pressure is supposed to be equal to air pressure P_0 whereas in the completely filled zone, $P(x, t)$ depends on the reflux flow due to geometric characteristics of the die.
5. **The viscosity** $\eta(x, t)$ stands as a function of temperature and moisture depending on the considered zone.

For the coupled system the filling ratio f_p , the temperature (T_p and T_f), the moisture (M_p and M_f), viscosity (η_p and η_f), and pressure P are the variables. The screw speed $N(t)$, barrel temperature T_b and feed rate $F_{in}(t)$ are the input variables.

3.3 Model of the Partially Filled Zone

3.3.1 Mass balance in the Partially Filled Zone

The mass balance equations in the PFZ, is written on the spatial domain $[0, l(t)[$, in terms of the filling ratio $f_p(x, t)$ (the filled volume fraction which may be related to the total mass density) [86] where $l(t)$ is the position of the thin interface which separates the PFZ and FFZ zones. A local analysis of the flow in one component of the screw is performed to obtain the flow dynamics in the *Partially Filled Zone*.

We have assumed that the extruded material is composed by a homogeneous mixture and no chemical transformation is operating in the process. So, no species are produced or destroyed and the variation of the amount of material in time is derived as the change of inflow and outflow through the cross section S_{eff} defining an elementary volume in this area. This cross section is the effective section between the screw and the barrel. The variation in the elementary volume between x_2 and x_1 with $(0 < x_1 < x_2 < l(t))$ in cartesian coordinates (x, y, z) (Fig. 3.3.1).

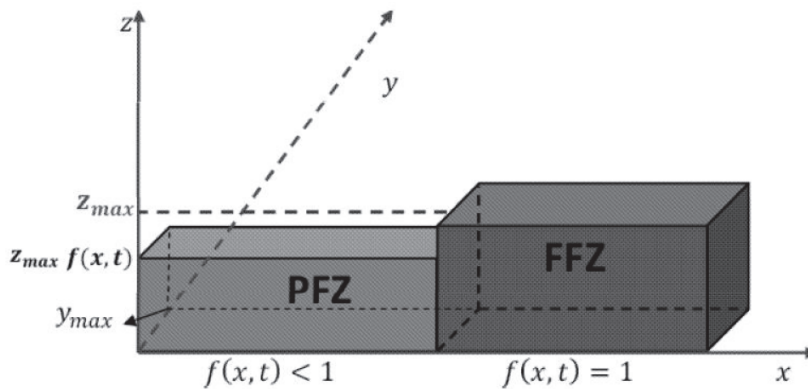


Figure 3.3.1: Cartesian representation of the effective volume V_{eff}

$$\frac{d}{dt} \int_{x_1}^{x_2} \int_0^{z_{max}f_p(x,t)} \rho_0 y_{max} dz dx = F(x_1, t) - F(x_2, t) \quad (3.3.1)$$

$F(x_1)$ and $F(x_2)$ are the inflow and outflow at x_1 and x_2 respectively. The right term of equation (3.3.1) can be written in an integral form using the divergence operator (in the 1D case it reduces to the differential operator ∂_x):

$$F(x_1, t) - F(x_2, t) = \int_{x_1}^{x_2} \partial_x F(x, t) dx \quad (3.3.2)$$

Developing equation (3.3.1) and using Leibniz formula we obtain the following equality:

$$\int_{x_1}^{x_2} \left[\rho_0 y_{max} z_{max} \partial_t f_p(x, t) + \int_0^{z_{max}f_p(x,t)} \frac{d}{dt} (\rho_0 y_{max} z_{max}) dz \right] dx = - \int_{x_1}^{x_2} \partial_x F(x, t) dx$$

ρ_0 , y_{max} , and z_{max} are constant and the product $y_{max} z_{max}$ corresponds to the effective section S_{eff} (Fig. 3.3.1). Thus, equation (3.3.1) implies that:

$$\rho_0 S_{eff} \partial_t f_p(x, t) = -\partial_x F(x, t) \quad (3.3.3)$$

Now extending the local formulation of the mass balance to a global one in the *Partially Filled Zone* we consider the transport phenomena for one screw element of pitch ξ . In this case, the inflow is due to the convection of the extruded material from the upstream channel to the current channel and the outflow is determined by the transport from the current channel to the downstream channel (Fig. 3.3.2):

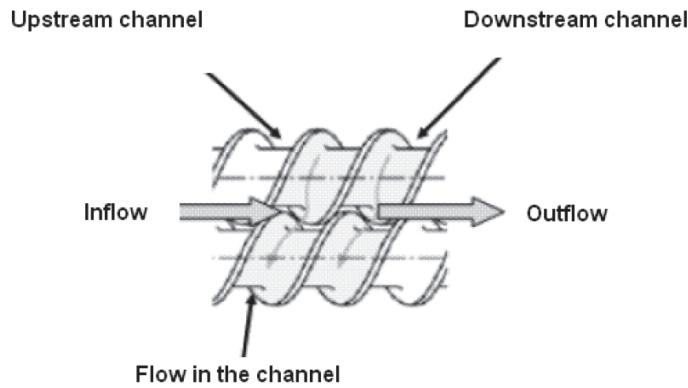


Figure 3.3.2: Description of the flow in a twin-screw extruder [35]

- The effective volume for a screw element is given by the following relation:

$$V_{eff} = \xi S_{eff} \quad (3.3.4)$$

- $F(x, t)$ is the material flow at the spatial coordinates x for a given time t . It could be expressed as a function of the filling ratio $f_p(x, t)$ and the screw speed $N(t)$:

$$F(x, t) = N(t)\rho_0V_{eff}f_p(x, t) \quad (3.3.5)$$

Using the definition of the effective volume (3.3.4) and the flow of matter (3.3.5) in this situation, we obtain the following transport equation which described the transport of the homogeneous material in the down barrel direction. The transport velocity which depends on the screw pitch ξ is the transversal component of the rotational velocity $N(t)$.

$$\partial_t f_p(x, t) = -\xi N(t)\partial_x f_p(x, t) \quad (t, x) \in (\mathbb{R}^+, [0, l(t)[) \quad (3.3.6)$$

$$(3.3.7)$$

- $f_p(x, t)$ filling ratio in *Partially Filled Zone*;
- $N(t)$ screw speed ;
- ξ uniform pitch of the screw.

3.3.2 Moisture balance in the Partially Filled Zone

The moisture content in the *Partially Filled Zone* $M_p(x, t)$ is the fraction of water in the transported homogeneous mixture. It represents the amount of water stored in the processing material and can be assimilated to the fraction of water in the effective volume. The moisture content has the same behavior as the homogeneous mixture because the mass density is supposed to be constant. Therefore, its evolution is also described by a transport equation as previously (3.3.9):

$$\partial_t M_p(x, t) = -\xi N(t)\partial_x M_p(x, t) \quad (t, x) \in (\mathbb{R}^+, [0, l(t)[) \quad (3.3.8)$$

$$(3.3.9)$$

3.3.3 Energy balance in the Partially Filled Zone

The energy balance allows to describe the evolution of the temperature along the extruder. There are two major effects which affect temperature behavior of the melt:

1. **The mechanical energy** provided by the rotation of the screw, which results in deformations of the extruded material. Usually, a drive unit with variable speed causes rotation of the screw. This mechanical power generates heat under the shearing effect: it is the power generated by viscous dissipation. We would like to mention that heat produced by the internal friction of screws affects the viscosity $\eta(x, t)$ and consequently modifies the behavior of matter. The shearing effect is particularly important in the channel and in different geometric area of screw circuit. Especially, the area between

the top of screws thread and the inner surface of the barrel. The thermal power Q_c generated by viscous dissipation per unit occupied volume V_o is a function of the viscosity $\eta(x, t)$, a geometrical constant C (depending on shear in different areas of screw circuit), the screw speed $N(t)$ (which is related to mechanical energy) and viscous dissipation factor γ . As in [86] the γ parameter is approximated by a linear function in the filling ratio (ϑ is a given constant):

$$\begin{cases} Q_c = \frac{\gamma(x,t)C\eta(x,t)N^2(t)}{f(x,t)V_{eff}} \\ \gamma(x, t) = \vartheta + (1 - \vartheta)f_p(x, t) \end{cases} \quad (3.3.10)$$

In the *Partially Filled Zone* the viscosity $\eta_p(x, t)$ for an unplastized material is given by equation (3.3.11) as in [89]. The viscosity decays when the moisture content increases. Given the initial viscosity η_p^0 , the power law is given by the following equation (β_p is a constant depending on rheological properties of the extruded material):

$$\eta_p(x, t) = \eta_p^0 e^{-\beta_p M_p(x, t)} \quad (3.3.11)$$

2. **The heat flow** is supplied by the temperature of the barrel surrounding the screw. This barrel is equipped with a heating system composed by electric circuits. Also, the circulation of a thermal fluid (hot water, steam, oil or fluids special) in channels and a system of cooling by circulation of fluid (air, water or oil) influence the barrel temperature $T_b(x, t)$. A heat flow ϕ_e is exchanged between the barrel and the mixture through a jacket surface S_e in accordance with a coefficient depending on the properties of the extruded material.

$$\phi_e = \frac{\alpha S_e (T_b(x, t) - T_p(x, t))}{V_{eff}} \quad (3.3.12)$$

- T_b is the barrel temperature;
- T_p is the temperature in the PFZ;
- α coefficient of exchange;
- S_e surface of exchange.

The first laws of thermodynamics law states that the variation of energy per unit of time for a closed system is equal to the power of the external forces plus the external heat exchanged between the system and its environment. Defining $u(x, t)$ as the internal energy per unit of volume and $h(x, t)$ as the enthalpy, we obtain the following relation:

$$u(x, t) = h(x, t) - P(x, t) \quad (3.3.13)$$

$P(x, t)$ is the pressure which is supposed to be uniform. The variation of internal energy $u(x, t)$ per unit of volume depends on the enthalpy inflow and outflow $F(x, t)$ and sources

terms such as viscous dissipation $Q_c(x, t)$ and convective heat from the barrel to the mass ϕ_e . Its expression is given by the following relation:

$$\rho_0 S_{eff} \partial_t (u f_p) dx = [Fh]_{x+dx}^x - \rho_0 S_{eff} P_0 \partial_x f_p dx + (Q_c + \phi_e) S_{eff} f_p dx \quad (3.3.14)$$

Using (3.3.13) and defining the flux $F(x, t)$ as the enthalpy flux which crosses the section S_{eff} in the *Partially Filled Zone* with transport velocity $\xi N(t)$, (3.3.14) is rewritten as:

$$\rho_0 \partial_t [(h - P) f_p] = -\rho_0 \xi N(t) \partial_x (h f_p) - \rho_0 P_0 \partial_t f_p + Q_c f_p + \phi_e f_p \quad (3.3.15)$$

Since the pressure in the *Partially Filled Zone* is equivalent to the air pressure P_0 , (3.3.15) becomes:

$$\partial_t h = -\xi N(t) \partial_x h + \frac{Q_c}{\rho_0} + \frac{\phi_e}{\rho_0} \quad (3.3.16)$$

The relation between the enthalpy and the temperature T_p of the homogeneous mixture with constant mass density is given by :

$$\partial h = C_p \partial T_p \quad (3.3.17)$$

C_p is a the specific heat capacity. Combining (3.3.10), (3.3.11), (3.3.12), (3.3.16) and (3.3.17), one obtains the following nonlinear time varying transport equation with source terms:

$$\begin{cases} \partial_t T_p(x, t) = -\xi N(t) \partial_x T_p(x, t) + \frac{\lambda \eta_p(x, t) N^2(t)}{\phi f_p(x, t)} + \frac{\theta}{\phi} (T_b - T_p(x, t)) \\ \theta = \alpha S_e \quad \lambda = \gamma C \quad \phi = \rho_0 C_p V_{eff} \\ \eta_p(x, t) = \eta_p^0 e^{-\beta_p M_p(x, t)} \quad (t, x) \in (\mathbb{R}^+, [0, l(t)]) \end{cases} \quad (3.3.18)$$

γ and C are supposed to be constant.

3.4 Model of the Fully Filled Zone

3.4.1 The momentum balance of the Fully Filled Zone

In this section, the characteristics of the flow in the *Fully Filled Zone* are analyzed. The main aspect is that the speed of transportation is essentially determined by the outlet flow rate depending on the pressure at the die. In the *Fully Filled Zone* the pressure is generated to overcome die section offering flow restriction and the location of the peak pressure coincides with the beginning of the restriction. The length of the *Fully Filled Zone* is a function of the pressure needed for the melt to flow across the die. In this zone the flow has two components:

- the first component is generated by the pumping effect of the screw. In most cases, this is a forward flow, but it could be a backward flow if a reverse screw element is used.

- the second component is the pressure flow, which could be a backward flow (called leakage backflow) if there is a forward pressure build-up, but could also be a forward flow if there is a forward pressure drop.

The *Fully Filled Zone* is defined in the spatial domain $]l(t), L]$, where L is the length of the extruder. By definition the mass balance states that mass accumulated in the *Fully Filled Zone* is the difference between the inflow and the outflow mass as previously. This is a consequence of constant density, and it means that the net forward mass $F_d(t)$ is constant across this zone. The available volume is completely filled and the filling ratio have no dynamic: $f_f = 1$.

The momentum balance equation in the *Fully Filled Zone* is expressed in term of pressure gradient and yields the following equation for the pressure:

$$\partial_x P(x, t) = \eta_f(x, t) \frac{\rho_0 V_{eff} N(t) - F_d(t)}{B \rho_0}; \quad (t, x) \in (\mathbb{R}^+,]l(t), L] \quad (3.4.1)$$

B is a coefficient of pressure flow and $\eta_f(x, t)$ is the melt viscosity in the *FFZ* [89]. $\eta_f(x, t)$ is a decreasing exponential function depending on the moisture content $M_f(x, t)$ and the temperature $T_f(x, t)$. δ and β_f are moisture content and temperature constants of viscosity respectively.

$$\eta_f(x, t) = \eta_f^0 e^{-\beta_f M_f(x, t)} e^{-\delta T_f(x, t)} \quad (3.4.2)$$

Remark 3. The pressure gradient defined by the equation (3.4.1) appears in the *Fully Filled Zone*. The discontinuity of the pressure (the *Partially Filled Zone* is submitted to atmospheric pressure P_0) determines the position of the interface which separates the two zones. Thus, the interface $l(t)$ arises from a change of causality between the filling ratio and the pressure from the *Partially Filled Zone* to the *Fully Filled Zone*. Recall that the filling ratio is related to the fraction of volume which is occupied by the extruded material and the pressure corresponds to its conjugate variable.

Integrating the equation (3.4.1), we can derive the value of the pressure at the die exit $P(L, t)$.

$$P(L, t) - P(l(t), t) = \int_{l(t)}^L \eta_f(x, t) \frac{\rho_0 V_{eff} N(t) - F_d(t)}{B \rho_0} dx \quad (3.4.3)$$

Remark 4. It becomes clear that the coupling relations at the interface depend on the possible solutions of equation (3.4.3). This equation interconnects the two zones and the pressure at the interface position $P(l(t), t)$ should be expressed by taking into account the influence of the *Partially Filled Zone*. This aspect will be analyzed under a simplified assumption in the section 3.5.2 dedicated to the interface relations. In our sense, the formulation of an analytical solution of the integral (3.4.3) with respect to the distributed viscosity $\eta_f(x, t)$ is a difficult point for the construction of explicit coupling relation by (3.4.3).

The net forward flow is determined by the die conductance K_d and viscosity η_d by the following relation

$$\begin{cases} F_d(t) = \frac{K_d}{\eta_d} \Delta P(t) \\ \Delta P(t) = (P(L, t) - P_0) \\ \eta_d = \eta_f(L, t) \end{cases} \quad (3.4.4)$$

η_d is equal to $\eta_f(x, t)$ at the die entry.

Remark 5. For a Newtonian fluid which flows in a tube of length \mathbf{L} and radius R (Fig. 3.4.1) K_d is given by the following equation:

$$K_d = \frac{\pi R^4}{8 \mathbf{L}} \quad (3.4.5)$$

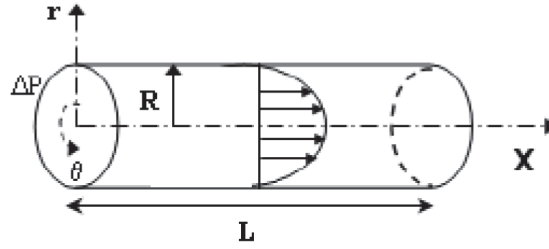


Figure 3.4.1: Poiseuille flow in a tube [38]

3.4.2 Moisture balance in the Fully Filled Zone

The moisture content $M_f(x, t)$ is also defined as the fraction of water in the extruded material, see the *Partially Filled Zone*. This variable obeys a similar transport equation (3.3.9) with a different velocity. The flow in this zone is the net forward flow and for an uniform screw the velocity $v(t)$ of the convection is proportional to $F_d(t)$:

$$v(t) = \frac{1}{S_{eff}} \frac{F_d(t)}{\rho_0} = \frac{\xi F_d}{\rho_0 V_{eff}} \quad (3.4.6)$$

Then the moisture content balance equation stands as:

$$\partial_t M_f(x, t) = -\frac{\xi F_d(t)}{\rho_0 V_{eff}} \partial_x M_f(x, t) \quad (t, x) \in (\mathbb{R}^+,]l(t), L] \quad (3.4.7)$$

3.4.3 Energy balance in the Fully Filled Zone

In this the *Fully Filled Zone*, the thermal phenomena are identical to those which occur in the *Partially Filled Zone*. As for moisture content equation (3.4.7), the heat transport velocity is given by equation (3.4.6). Viscous dissipation and heat exchange have to be considered as source terms. The viscous heat generation is much important in this zone due to the mixing effect. One should point out that the permanent contact between the melt and the barrel increases the heat exchange with the mixture. Here, the viscosity depends on both temperature and moisture evolutions as it is shown by equation (3.4.2). Recalling, equation (3.3.14)(with $f_p = 1$), and the melt viscosity (3.4.2) the following equations are obtained to describe the temperature evolution $T_f(x, t)$:

$$\begin{cases} \partial_t T_f(x, t) = -\frac{\xi F_d(t)}{\rho_0 V_{eff}} \partial_x T_f(x, t) + \frac{\lambda \eta_f(x, t) N^2(t)}{\phi} + \frac{\theta}{\phi} (T_b - T_f(x, t)) \\ \theta = \alpha S_e \quad \lambda = \gamma C \quad \phi = \rho_0 C_f V_{eff} \\ \eta_f(x, t) = \eta_f^0 e^{-\beta_f M_f(x, t)} e^{-\delta T_f(x, t)} \quad (t, x) \in (\mathbb{R}^+,]l(t), L]) \end{cases} \quad (3.4.8)$$

As for the *Partially Filled Zone*, the coefficients γ and C are supposed to be constant.

3.5 Description of the interface

3.5.1 Dynamics of the moving interface

The interface that separates the *Partially Filled Zone* to the *Fully Filled Zone* is located at the position $l(t)$ where the pressure changes from air pressure to greater than air pressure and the pressure gradient changes from zero to positive value (and the filling ratio changes from values strictly less than *one* to *one*). The position of the interface will, in general, change due to the difference between the incoming and outgoing mass flow rates. For a nonuniform screw profile, interfaces are determined from the screw geometry as the end point of the restrictive sections [88]. However, the location of the interfaces is in general, unknown and must be calculated along with the solution of the model equations. In this section we calculate the equation associated with the interface $l(t)$ for a uniform screw profile. The variation of the position of the interface is derived from the local mass balance at the interface. We consider a fixed domain $[l^-, l^+]$ strictly containing the position of the interface that is $l^- < l(t) < l^+$ for some time interval and define all functions $f_p(x, t)$ and $F(x, t)$ as left continuous.

Then, the mass balance is written as follows:

$$\frac{d}{dt} \int_{l^-}^{l^+} \int_0^{z_{max} f(x, t)} \rho_0 y_{max} dz dx = F(l^-) - F(l^+) = \Delta F \quad (3.5.1)$$

Remind that the filling ratio $f(x, t)$ is :

- $f_p(x, t)$ in the *Partially Filled Zone* ($x \in [l^-, l(t)[$),

- $f_f(x, t) = 1$ in *Fully Filled Zone* ($x \in]l(t), l^+]$).

Thus equation (3.5.1) is rewritten as:

$$\int_0^{z_{max}f_p(x,t)} \left[\frac{d}{dt} \int_{l^-}^{l(t)} \rho_0 y_{max} dx dz + \frac{d}{dt} \int_{l(t)}^{l^+} \rho_0 y_{max} \right] dx dz = \Delta F \quad (3.5.2)$$

Developing this integral (3.5.2) and using $f(l^+, t) = f_f = 1$, we deduce the following relation:

$$\frac{dl(t)}{dt} (\rho_0 S_{eff} (f_p(l^-, t) - 1)) + \underbrace{\int_{l^-}^{l^+} \frac{d}{dt} \int_0^{z_{max}f_p(x,t)} \rho_0 y_{max} dz dx}_{\star} = \Delta F \quad (3.5.3)$$

$$\star = \int_{l^-}^{l^+} \rho_0 y_{max} z_{max} \partial_t f(x, t) dx \quad (3.5.4)$$

$$\star = \int_{l^-}^{l(t)} \rho_0 y_{max} z_{max} \frac{\partial f_p(x, t)}{\partial t} dx + \int_{l(t)}^{l^+} \rho_0 y_{max} z_{max} \frac{\partial f_f(x, t)}{\partial t} dx \quad (3.5.5)$$

let us remind that the filling ratio is defined by $f_p(x, t)$ in the *PFZ* and is equal to 1 in the *FFZ*, then (3.5.3) is rewritten as:

$$\frac{dl(t)}{dt} \rho_0 S_{eff} (f_p(l^-, t) - 1) + \int_{l^-}^{l(t)} \rho_0 S_{eff} \frac{\partial f(x, t)}{\partial t} dx = \Delta F$$

Using the transport equation of the filling ratio (3.3.7), one obtains equation (3.5.6):

$$\frac{dl(t)}{dt} \rho_0 S_{eff} (f_p(l^-, t) - 1) + \int_{l^-}^{l(t)} \xi N(t) \rho_0 S_{eff} \frac{\partial f_p(x, t)}{\partial x} dx = \Delta F \quad (3.5.6)$$

Which can be rewritten as:

$$\frac{dl(t)}{dt} \rho_0 S_{eff} (f_p(l^-, t) - 1) + \xi N(t) \rho_0 S_{eff} (f_p(l(t)) - f_p(l^-, t)) = \Delta F \quad (3.5.7)$$

By considering the first order approximation of the filling ratio $f_p(l^-, t)$ and the flow rate $F(l^-, t)$ in (3.5.7) we find (3.5.8):

$$\begin{aligned} & \frac{dl(t)}{dt} \left(f_p(l(t), t) + (l(t) - l^-) \frac{\partial f_p(l(t), t)}{\partial x} - 1 \right) + \xi N(t) \left((l(t) - l^-) \frac{\partial f_p(l(t), t)}{\partial x} \right) \\ &= \frac{1}{\rho_0 S_{eff}} \left[F(l(t), t) - (l(t) - l^-) \frac{\partial F(l(t), t)}{\partial x} - F(l^+, t) \right] \end{aligned} \quad (3.5.8)$$

When $l^- \rightarrow l(t)$, the equation (3.5.8) becomes:

$$\frac{dl(t)}{dt} = \frac{F(l^+) - F(l(t), t)}{\rho_0 S_{eff} (1 - f_p(l(t), t))} \quad (3.5.9)$$

In the *Fully Filled Zone* the net flow rate is uniform and equal to the net flow at the die $F_d(t)$ which is a function of the pressure gradient (3.4.4). The flow rate $F(l(t), t)$ is defined by the maximum pumping capacity of the screw which is reduced to the effective fraction of convected material at the left limit of the interface.

$$F(l(t), t) = \rho_0 \xi N(t) V_{eff} f_p(l(t), t) \quad (3.5.10)$$

Finally the ordinary differential equation of the moving interface is:

$$\frac{dl(t)}{dt} = \frac{F_d(t) - \rho_0 \xi N(t) V_{eff} f_p(l(t), t)}{\rho_0 S_{eff} (1 - f_p(l(t), t))} \quad (3.5.11)$$

Remark 6. The term $(1 - f_p(l(t), t))$ shows that the extruded material can only fill the fraction of volume which is unoccupied.

Secondly, the condition $0 < f_p(l(t), t) < 1$ is necessary to have a well-posed differential equation.

3.5.2 Interface relations

Throughout this chapter we build a simplified model of the extrusion process based on the conservation of mass, energy and momentum. The model is described by considering two zones which are linked by a moving interface. It shows that the filling ratio is discontinuous from the PFZ to the FFZ:

- $0 < f_p(x, t) < 1$ in the *Partially Filled Zone (PFZ)*
- $f_f = 1$ in the *Partially Filled Zone (FFZ)*

It thus becomes necessary to describe the coupling between the two zones by physical coupling relations ensuring consistency of the model. As stated in the introduction, these relations are established under some continuity assumptions of state or flux variables or some functions of state variables. In this section we discuss coupling relations based on the continuity of the state variables or momentum flux. The interconnection is performed under the assumption of constant viscosity η along the extruder. This hypothesis allows to solve explicitly the equation for the pressure gradient which is a function of the distributed viscosity (3.4.1) and (3.4.3) see Remark 4. Then, the dynamics of temperature and moisture are not influenced the net flow. The system is now "decoupled" because the interface dynamics (3.5.11) depends on the filling ratio at the interface $f_p(l(t), t)$.

3.5.2.1 Coupling relations for moisture content and temperature evolutions

The temperature and the moisture content are supposed to be continuous at the interface. This assumption is physically coherent under a constant viscosity. In our perspective, the strong assumption concerning the viscosity is considered because we focus our analysis on

the particular structure of the system consisting of transport equations related by a moving interface.

$$\begin{cases} T_p(l^-, t) = T_f(l^+, t) \\ M_p(l^-, t) = M_f(l^+, t) \end{cases} \quad (3.5.12)$$

3.5.2.2 Coupling relations for total mass balance equation

The coupling relation for the homogeneous mixture mass balance are established considering two alternatives.

3.5.2.2.1 Continuity of pressure at the interface The assumption of the continuity of pressure at the interface is a *state coupling relation*. Knowing that the pressure in the *Partially Filled Zone* is equal to atmospheric pressure P_0 we find the equality: $P(l^+, t) = P_0$. By integrating the equation of the pressure gradient (3.4.1), we express the die pressure $P(L, t)$ or the net flow rate $F_d(t)$ as a function which is strictly determined by the screw speed $N(t)$ and the position of the interface $l(t)$. Recall that the value of the filling ratio determines the interface position $l(t)$ (3.5.11).

$$\begin{cases} P(L, t) = P_0 + \frac{\eta V_{eff} N(t) \rho_0 (L - l(t))}{(B \rho_0 + K_d (L - l(t)))} \\ F_d(t) = \frac{K_d V_{eff} N(t) \rho_0 (L - l(t))}{(B \rho_0 + K_d (L - l(t)))} \end{cases} \quad (3.5.13)$$

recall B and K_d are some geometric parameters of the screw and the die respectively.

3.5.2.2.2 Continuity of the flux of momentum flux The second assumption is based on the continuity of momentum flux which is given by the following relation:

$$F(l^-, t) v(l^-, t) + P_0 f_p(l^-, t) S_{eff} = F_d(t) v(l^+, t) + P(l^+, t) S_{eff}, \quad (3.5.14)$$

where

$$\begin{cases} F(l^-, t) = \rho_0 N(t) V_{eff} f(l^-, t) \\ v(l^-, t) = \xi N(t) \\ v(l^+, t) = \frac{\xi F_d(t)}{\rho_0 V_{eff}}. \end{cases} \quad (3.5.15)$$

Deducing $P(l^+, t)$ from integrating (3.4.1) and computing equation (3.5.14), we find:

$$\Delta P(L, t) = \nu \left[-\left[1 + \frac{K_d}{B \rho_0} (L - l(t)) \right] + \sqrt{\Delta(l(t), N(t), f_p(l(t), t))} \right], \quad (3.5.16)$$

where $\nu = \frac{\eta_f^2 \rho_0 S_{eff}^2}{2 K_d^2}$ and $\Delta P(L, t) = P(L, t) - P_0$,

$$\Delta(l(t), N(t), f_p(l(t), t)) = \left[1 + \frac{K_d}{B \rho_0} (L - l(t)) \right]^2 + \Omega(f_p(l(t), t), N(t), l^+) \quad (3.5.17)$$

$$\text{and } \Omega = \left(\frac{2\rho_0}{\nu} \right) \left(\frac{\eta_f V_{eff} N(t)}{B\rho_0} (L - l(t)) + \xi^2 N^2(t) f_p(l(t), t) - (1 - f_p(l(t), t)) \frac{P_0}{\rho_0} \right)$$

The equation (3.5.16) restricts the solution of the system because it induces a positivity constraint. Indeed, the die flow rate which depends on the pressure $P(L, t)$ should be positive and this condition is satisfied if $P(L, t) > P_0$. Then, it becomes necessary to define a critical value of the filling ratio $f_{pc}(l(t), t)$ as:

$$f_{pc}(l(t), t) > \frac{P_0 - \frac{\eta V_{eff} N(t)}{B} (L - l(t))}{\rho_0 \xi^2 N^2(t) + P_0} \quad (3.5.18)$$

3.6 Control problem associated to the extrusion process model

Here we recall the equations which define the model of both *Partially and Fully Filled Zones* in the extruder. An analysis of the global system leads to a control problem for the design of extruded material. The control variables associated to this extrusion process model are:

- the boundary conditions at $x = 0$ for filling ratio, moisture content and temperature which are defined by:

$$f_p^{in}(t) = f_p(0, t) = \frac{F_{in}(t)}{\rho_0 N(t) V_{eff}}, \quad M_p(0, t) = M_{in}(t), \quad T_p(0, t) = T_{in}(t), \quad (3.6.1)$$

respectively. $F_{in}(t)$ is the feed rate,

- $T_b(x, t)$, the barrel temperature
- and $N(t)$ the screw speed.

Under the assumption of constant viscosity η , the control objective is to design the temperature $T_f(L, t)$ and the die pressure $P(L, t)$. Under the hypothesis of constant viscosity, the moisture content dynamics can be neglected in the control point of view because its evolution influences essentially the viscosity design as it is shown by equations (3.3.11) and (3.4.2).

In the both following equations (3.6.2) and (3.6.4), ξ , θ , ϕ and λ are parameters depending on the screw geometry, the barrel characteristics and the material properties (see Section 3.3.3). We mention that at the initial time $t = 0$, we assume the existence of both *Partially and Fully Filled Zones* in the spatial domains $[0, l_0)$ and $(l_0, L]$ respectively. L is the length of the extruder, l_0 being the initial position of the moving interface. Thus, the system defined in the coupled domains $[0, l(t))$ and $(l(t), L]$ is given by the following equations:

1. For the *Partially Filled Zone*, filling ratio, moisture content and temperature dynamics are given by equations (3.3.7), (3.3.9) and (3.3.18) respectively on the spatial domain $[0, l(t)]$:

$$\partial_t \begin{pmatrix} f_p \\ M_p \\ T_p \end{pmatrix} (x, t) = -\xi N(t) \partial_x \begin{pmatrix} f_p \\ M_p \\ T_p \end{pmatrix} (x, t) + \begin{pmatrix} 0 \\ 0 \\ \Omega_p(f_p, N, T_p, T_b) \end{pmatrix} \quad (3.6.2)$$

where the source term (3.3.18) is given by the equation :

$$\Omega_p(f_p, N, T_p, T_b) = \frac{\lambda \eta N^2(t)}{\phi f_p(x, t)} + \frac{\theta}{\phi} (T_b(x, t) - T_p(x, t)). \quad (3.6.3)$$

2. For the *Fully Filled Zone*, the moisture content and the temperature are given by equations (3.4.7) and (3.4.8) respectively, on the spatial domain $(l(t), L]$:

$$\partial_t \begin{pmatrix} M_f \\ T_f \end{pmatrix} (x, t) = -\frac{\xi F_d(t)}{\rho_0 V_{eff}} \partial_x \begin{pmatrix} M_f \\ T_f \end{pmatrix} (x, t) + \begin{pmatrix} 0 \\ \Omega_f(N, T_f, T_b) \end{pmatrix} \quad (3.6.4)$$

$\Omega_f(N, T_f, T_b)$ is the source term which is given by the following equality:

$$\Omega_f(N, T_f, T_b) = \frac{\lambda \eta N^2(t)}{\phi} + \frac{\theta}{\phi} (T_b(x, t) - T_f(x, t)) \quad (3.6.5)$$

Recall that the die net flow $F_d(t)$ is a function of the pressure at the die exit (3.4.4):

$$F_d(t) = \frac{K_d}{\eta} \Delta P(t) \quad \Delta P(t) = (P(L, t) - P_0) \quad (3.6.6)$$

3. For interface coupling relations the temperature and the moisture content are supposed to be continuous at the interface. We consider two coupling conditions concerning the pressure (or the filling ratio) which is a discontinuous variable:

- the first one derives from the continuity of momentum flux at the interface $l(t)$ (for the parameter see equations (3.5.17) and (3.5.18)):

$$\Delta P(L, t) = \nu \left[-\left[1 + \frac{K_d}{B \rho_0} (L - l(t)) \right] + \sqrt{\Delta(l(t), N(t), f_p(l(t), t))} \right], \quad (3.6.7)$$

where Δ is the difference between the pressure at L and the atmospheric pressure, L being the extruder length ($P(L, t) - P_0$). This coupling relation generates a constraint on the filling ratio ($\Delta P(t)$ should be positive (in some sense the square roots term on Δ should be positive). Thus :

$$f_{pc}(l(t), t) > \frac{P_0 - \frac{\eta V_{eff} N(t)}{B} (L - l(t))}{\rho_0 \xi^2 N^2(t) + P_0}, \quad (3.6.8)$$

Where $f_{pc}(l(t), t)$ represents the minimal value of the filling ratio for a coherent physical model.

- the second one is constructed under the hypothesis of the continuity of pressure at interface $l(t)$. Thus:

$$\begin{cases} \Delta P(t) = \frac{\eta V_{eff} N(t) \rho_0 (L-l(t))}{(B\rho_0 + K_d(L-l(t)))} \\ F_d(t) = \frac{K_d V_{eff} N(t) \rho_0 (L-l(t))}{(B\rho_0 + K_d(L-l(t)))}. \end{cases} \quad (3.6.9)$$

4. The dynamics of the moving interface $l(t)$ is deduced from a local mass balance and it follows :

$$\begin{cases} \frac{dl(t)}{dt} = \frac{F_d(t) - \rho_0 V_{eff} N(t) (1 - f_p(t, l(t)))}{\rho_0 S_{eff} (1 - f_p(t, l(t)))} \\ l(0) = l^0 \end{cases} \quad (3.6.10)$$

3.7 Open loop simulations of mass and energy balance equations

3.7.1 Description of the simulated extrusion process model

In this part, we perform simulations for the mass and energy balance of the extrusion process model. We impose constant screw speed N_0 , feed rate F_{in} , inlet temperature T_{in} and barrel temperature T_b . We point out that F_{in} and T_{in} are the boundary conditions associated to the filling ratio and the temperature transport equations.

Screw speed	$N_0 = 325/60 rpm.s^{-1}$
Feed rate	$F_{in} = 135/3600 kg.s^{-1}$
Filling ratio	$f_p^{in} = \frac{F_{in}}{\rho_0 V_{eff} N_0} = 0.3148$
Barrel temperature	$T_b = 330K$
Inlet temperature	$T_{in} = 293K$
Extruder length	$L = 2m$

Table 3.1: Input values N_0 , f_p^{in} , T_{in} , T_b

The initial conditions are defined for the filling ratio, the interface position and the temperature along the extruder as f_p^0 , l^0 , T_p^0 and T_f^0 respectively.

Initial filling ratio	$f_p^0 = 0.3$
Initial interface position	$l^0 = 1m$
Initial temperature along the extruder	$T^0 = T_p^0 = T_f^0 = 293K$

Table 3.2: Initial conditions f_p^0 , l^0 , T^0

Now, considering the initial and boundary data which are defined in (Tab. 3.1) and (Tab. 3.2), we define the following the simulated system composed by:

1. The filling ratio and the temperature dynamics in the *Partially Filled Zone* $x \in [0, l(t)]$:

$$\partial_t \begin{pmatrix} f_p \\ T_p \end{pmatrix} (x, t) = -\xi N_0 \partial_x \begin{pmatrix} f_p \\ T_p \end{pmatrix} (x, t) + \begin{pmatrix} 0 \\ \Omega_p(f_p, T_p) \end{pmatrix}, \quad (3.7.1)$$

where the source term $\Omega_p(f_p, T_p)$ is given by the equation:

$$\Omega_p(f_p, T_p) = \frac{\lambda \eta N_0^2}{\phi f_p(x, t)} + \frac{\theta}{\phi} (T_b - T_p(x, t)). \quad (3.7.2)$$

2. The temperature dynamics in the *Fully Filled Zone* $x \in (l(t), L]$:

$$\partial_t T_f(x, t) = -\frac{\xi F_d(t)}{\rho_0 V_{eff}} \partial_x T_f(x, t) + \Omega_f(T_f), \quad (3.7.3)$$

where

$$\Omega_f(T_f) = \frac{\lambda \eta N_0^2(t)}{\phi} + \frac{\theta}{\phi} (T_b - T_f(x, t)). \quad (3.7.4)$$

3. Interface relations which consist of continuity of temperature ($T_p(l^-, t) = T_f(l^+, t)$) and pressure at the coupling point $l(t)$. As for (3.7.5), we find:

$$\begin{cases} P(L, t) = P_0 + \frac{\eta V_{eff} N_0 \rho_0 (L-l(t))}{(B \rho_0 + K_d (L-l(t)))} \\ F_d(t) = \frac{K_d V_{eff} N_0 \rho_0 (L-l(t))}{(B \rho_0 + K_d (L-l(t)))}. \end{cases} \quad (3.7.5)$$

4. The moving interface whose dynamics is given by the following equation:

$$\frac{dl(t)}{dt} = \frac{F_d(t) - \rho_0 \xi N_0 V_{eff} f_p(l(t), t)}{\rho_0 S_{eff} (1 - f_p(l(t), t))} \quad (3.7.6)$$

Remark 7. In the case of continuity of momentum flux at the interface, the initial condition must be chosen with respect to the minimal value of the filling ratio f_{pc} (3.6.8).

3.7.2 Numerical computation by finite volume method

There is a fairly extensive literature on numerical analysis of partial differential equations with time-varying domains. Most of the numerical works have been focused on multi-phase flow problems including the inter-phase coupling terms which require specific treatment by numerical algorithms. A very important feature of multi-phase flow simulations is the interface between materials and phases, and it is often crucial to track such interfaces at each step of the computation. There exist two classes of numerical representations which allow to perform numerical experiments on moving interface problems:

- For Lagrangian representation, the mesh deforms with the material and automatically maintain interfaces. These representations fail if the mesh is excessively deformed by topological changes because the mesh reconstitution for each step is strongly based on the interface form.

- For Eulerian representation, the material moves through a stationary mesh and requires special procedures to track precisely the interfaces position in the flow.

In fluid dynamics, however, both Lagrangian and Eulerian coordinates have been used with considerable success. Because each coordinates representation has advantages and disadvantages, the choice of which representation to use depends on the characteristics of the problem to be solved. The two representations differ, however, in the manner in which the fluid elements are moved to their next positions after their new velocities have been computed. In the Lagrangian case the grid simply moves with the computed element velocities, while in an Eulerian calculation it is necessary to compute the flow of fluid through the mesh.

By definition the interface is a boundary which separates two different physical regions. In many cases, the numerical analysis is based on the use of marker-cells, volume of fluids, height functions or Level Set methods which allow to keeping track of the interface position [70, 45, 46, 133]. Also, there exist many algorithms which are developed to rebuild the interface along the numerical calculation specially for volume of fluid methods one can mention works of [111, 115, 124]. Here we present a brief description of the height function method. The idea behind the height function method is to define the interface distance from a reference line as a function of position along the reference line. For example, in a rectangular mesh of cells of width δx and height δy one might define the vertical height (h) of the interface above the bottom of the mesh in each column of cells. This would approximate a curve $h = f(x, t)$ by assigning values of h to discrete values of x . This representation is extremely efficient, requiring only a one-dimensional storage array to record the surface height values. Likewise, the evolution of the surface only requires the updating of the one-dimensional array. Then, the time evolution of the height function is governed by a kinematic equation expressing the fact that the surface must move with the fluid:

$$\partial_t h + u \partial_x h = v \quad (3.7.7)$$

where (u, v) are the fluid velocity components in the (x, y) coordinates direction.

Numerical analysis of the extruder model which is described by coupled hyperbolic systems in complementary time-varying domains through an interface is very similar to fluid-structure coupling problems. Thus the height function methods presented previously may be relevant in this case. Indeed, we consider a fixed mesh on which a color function whose value are 1 or 0 according to the *Partially Filled Zone* and the *Fully Filled Zone*. It is important to note that the position of the interface can be calculated explicitly by integrating the color function over the whole domain $[0, L]$ if appropriate initial conditions are chosen. Here we define the color function as the characteristic function of the domain:

$$c(x, t) = \begin{cases} 1 & x \in [0, l(t) [\\ 0 & x \in [l(t), L] \end{cases} \quad (3.7.8)$$

We mention that the characteristic function (3.7.8) is the solution of the transport equation whose velocity corresponds to the dynamics of the interface.

$$\frac{\partial}{\partial t}c(x, t) = -\dot{l}(t) \frac{\partial}{\partial x}c(x, t) \quad (3.7.9)$$

with the following initial conditions:

$$c(x, 0) = \begin{cases} 1 & x \in [0, l_0[\\ 0 & x \in [l_0, L] \end{cases} \quad (3.7.10)$$

l_0 being the position of the interface at time $t = 0$.

All the states and flux variables which describe the extruder model in PFZ and FFZ are extended over the whole domain $[0, L]$, using color function (3.7.8) and its complement as follows:

$$\begin{cases} \mathcal{N}(x, t) = c(x, t)\mathcal{N}_p(x, t) + (1 - c(x, t))\mathcal{N}_f(x, t) \end{cases} \quad (3.7.11)$$

The finite volume method which is generally well adapted to the numerical calculation of the transport equations is used to simulated the system. The numerical scheme is applied on a fixed mesh considering the extended variables which arise from a linear combination (3.7.11).

3.7.3 Simulations results

- The interface position $l(t)$

Recall that the extruder length is $L = 2m$. The figure (Fig. 3.7.1) shows the evolution

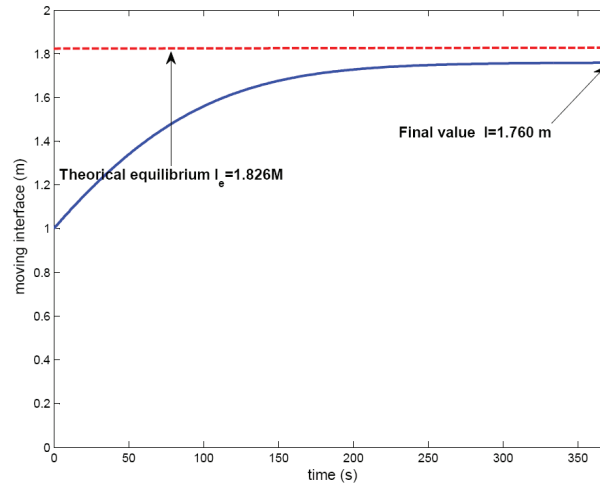


Figure 3.7.1: Moving interface position $l(t)$

of the interface $l(t)$ from the initial position $l_0 = 1m$ to $l(t_1) = 1.760m$, $t_1 = 350s$. The equilibrium position of the interface $l_e = 1.826m$ is given by:

$$l_e = L - \frac{B\rho_0 f_{in}^p}{K_d(1 - f_{in}^p)}, \quad (3.7.12)$$

where f_{in}^p is the inlet filling ratio deduced from the value of the feed rate F_{in} (see Tab. 3.1). We remark that at time $t = 350s$ the interface converges to the equilibrium with an error equal to 6.6%

- The filling ratio evolution at different spatial coordinates

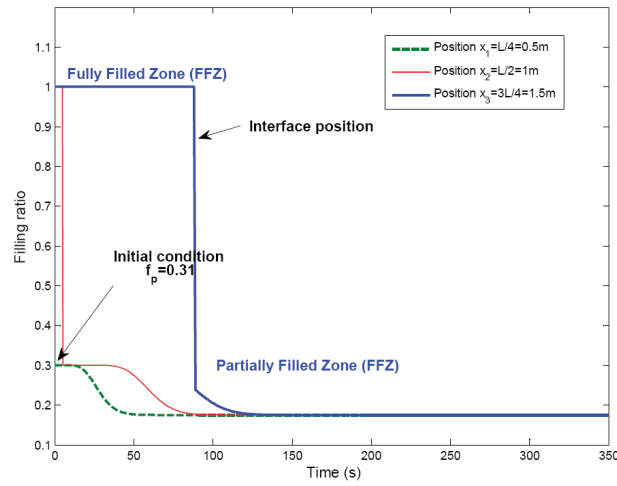


Figure 3.7.2: Filling ratio evolution

Figure (Fig. 3.7.2) shows its evolution the evolution of the filling ratio $f_p(x, t)$ at different spatial coordinates: $x_1 = L/50 = 0.5m$, $x_2 = L/2 = 1m$ and $x_3 = 3L/4 = 1.5m$.

- First, at time $t = 0$, $f_p(t)$ has a constant initial value which is $f_p^0 = 0.3$ (Tab. 3.2). Recall that the extruder length is $L = 2m$. Consequently, the coordinates x_1 , belongs to the *Partially Filled Zone* and the positions x_2 and x_3 belong to the *Fully Filled Zone*.
- Secondly, the interface moves increasingly starting from the initial value $l^0 = 1m$ to its final value $l(t_1) = 1.760m$ ($t_1 = 350s$) (Fig. 3.7.1). Then, the coordinates x_2 and x_3 which initially belong to *Fully Filled Zone* passe into the *Partially Filled Zone* due to the evolution of the interface position. The discontinuity of the filling ratio appears clearly in the simulation results (Fig. 3.7.2) and the value of the filling ratio at position x_2 and x_3 at times when occurs the change zone is determined by the transport in the *Partially Filled Zone* velocity ξN_0 and the inlet filling ratio f_{in}^p .

- Finally at positions x_1 x_2 x_3 , the final value of the filling ratio is $f_p = 0.1749$. We observe that delay of propagation of the boundary input f_{in}^p also appears in the simulation (Fig. 3.7.2): the input acts on the initial value after a delay which depends on the speed and the pitch of the screw which are the constant "parameters" N_0 and ξ , respectively.

- The temperature in *Partially and Fully Filled Zones*

Recall that the barrel temperature is fixed at $T_b = 330K$, the initial value of temperature along the extruder is $T^0 = 293K$ and the inlet temperature is $T_{in} = 293K$ (continuity of temperature at the entry of the extruder). Using the previous arguments we observe that at the initial time t_0 :

- the spatial coordinate $x_1 = L/4 = 0.5m$ belongs to the *Partially Filled Zone*,
- and the positions $x_2 = 3L/4 = 1.5m$ and $x_3 = L = 2m$ belong to the *Fully Filled Zone*

The figure (Fig. 3.7.3) shows that:

- at the spatial coordinate $x_3 = L = 2m$ which belongs to the *Fully Filled Zone*, the temperature reaches its final value $T(L, t_1) = 355K$, ($t_1 = 350s$);
- at the spatial coordinate $x_3 = L = 2m$ which belongs to the *Partially Filled Zone* the temperature increases from the initial value and reaches its final value $T(x_3, t_1) = 361K$.
- The evolution of the temperature at the spatial coordinate $x_2 = 3L/4 = 1.5m$ is particular due to the change of zone.

Remark 8. At time $t_1 = 350s$ the value of the temperature in the *Partially Filled Zone* is superior to its value in the *Fully Filled Zone* and both temperatures that we observe in (Fig. 3.7.3) are greater than the barrel temperature. The extruders includes generally a cooling system which regulate the heat flux between the barrel and the material. Normally, in a real extruder, the shear is more important in the *Fully Filled Zone* and we should observe the opposite phenomenon. The strong assumption of constant viscosity which mitigates the effect of the power generated by viscous dissipation.

- The evolution of temperature profile at different times

The figure (Fig. 3.7.4) is a screenshot of the temperature along the extruder at different times t_1 , t_2 , t_3 and t_4 . It allows to observe the evolution of temperature profiles depending on the interface position. For each captured time, the "dot" shows the position of the interface. The peak from which the temperature starts to decrease rapidly corresponds to the position of the interface at the time when the temperature profile is captured.

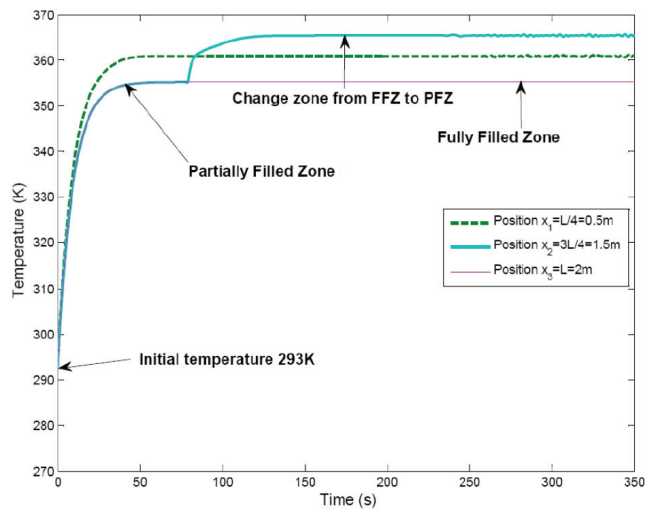


Figure 3.7.3: Temperature evolution

3.8 Conclusion

In this chapter the model of an extrusion process has been presented. The model is derived from balance laws expressing conservation of mass, moisture content and energy. Firstly, we describe the flow in a nonhomogeneous medium which corresponds to the geometric structure of the extruder. We explain how a gradient of pressure is build-up in some *Fully Filled Zone* due to the accumulation of material behind the die. Then, by a structural decomposition of the extruder, we obtain transport equations in *Partially and Fully Filled Zone* in the time-varying domains $[0, l(t)[$ and $]l(t), L]$ respectively. The obtained model is composed by nonlinear hyperbolic systems with source terms and a mobile interface $l(t)$ stands as an interconnection component. The main difficulty in such system arises from the definition of the coupling conditions between the two zones. We propose two coupling relations at the moving interface by means of state and flux coupling methods. The first transmission condition is based on a pressure continuity hypothesis and the second one is obtained assuming the continuity of momentum flux. An analysis of the proposed coupling relations shows how the system is constrained in the case of the continuity of momentum flux. Another interesting point in this chapter concerns the brief analysis of numerical methods concerning fluids dynamics. The color function which is proposed in [27] permits to extend the definition of variables of each zone in the whole domain $[0, L]$ and a finite volume method is performed for simulations. The results illustrate the dynamics of moving interface, filling ratio and temperature along the process. The position of the moving interface appears clearly in the simulation as a point of discontinuity. In the next chapter, an mathematical analysis will be performed in order to prove the well-posedness of the Cauchy problem of the extruder process model.

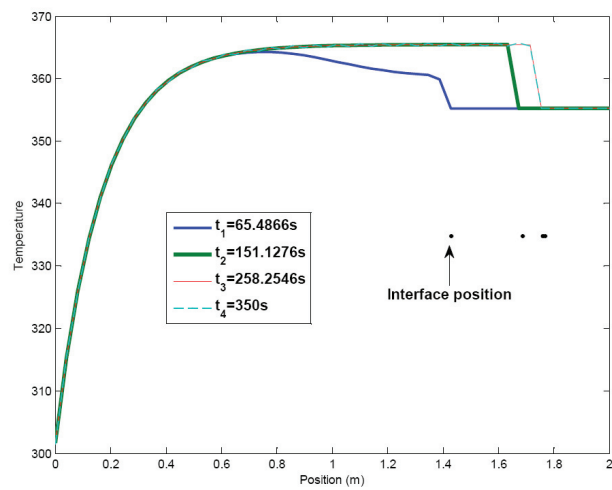


Figure 3.7.4: Temperature and interface position

Chapter 4

The Cauchy problem for coupled hyperbolic systems through a moving interface

4.1 Introduction

The mathematical analysis of mobile interfaces in the context of moving boundary problems have been an active subject in the last decades and their mathematical understanding continues to be an important interdisciplinary tool for the scientific applications. Such class of partial differential equations arises in many applications devoted to modelling of biological systems and reaction diffusion processes. In this context, [36] study the global existence of solutions to a coupled parabolic-hyperbolic system with moving boundary representing cell mobility. A similar type of nonlinear moving-boundary problem consisting of a hyperbolic equation and a parabolic equation for modelling blood flow through viscoelastic arteries [33] and tumor growth [44] is study in terms of well-posedness. General reaction-absorption-diffusion processes involves also moving boundary as it is stated in [122]. In order to prove local existence and uniqueness of a solution for such problem, the key of the resolution is to transform the system with moving boundary into a system defined on a fixed domain. Then, the results of many studies dedicated to hyperbolic system of conservation laws may be useful for establishing the existence, uniqueness, regularity and continuous dependence of solutions. The well-posedness study of hyperbolic systems of conservation laws which are defined on fixed domains is proposed in [22, 90, 146, 41, 126] (and the references therein) in the content of weak solutions. In this chapter we apply the method proposed in [126, 41] to prove the existence and the uniqueness of solutions for the extrusion process model after a change of coordinates which allows to express the system in a fixed domain $(0, 1)$. In [126] a scalar conservation law that models a highly re-entrant manufacturing system is studying as a generalization of [41]. The proof of the existence and uniqueness of the weak solution of the

corresponding Cauchy problem with initial and boundary data is given using a fixed point argument. We mention that first results concerning the well-posedness of extrusion processes as transport equations coupled via complementary time varying domains is proposed in [49]. In [49] The mathematical analysis is performed for the linearized model of the extruder and the well-posedness is proved using perturbation theory on the linear operator [79]. Here we are interested in the nonlinear model of the extruder which is described by conservation laws of *Chapter 3*.

We consider the cauchy problem for extruder model composed of two systems of conservation laws together with an ordinary differential equation. Using *Banach fixed point theorem*, we prove the well-posedness directly on the nonlinear model. Recall that the model is based on the decomposition of the extruder in *Partially and Fully Filled Zones*. Let us recall the transport equations of mass, moisture content and energy in an extruder. **In this chapter we define ζ as the screw pitch and $\xi(t)$ as the characteristic curves.**

1. For the *Partially Filled Zone*, we consider the filling ratio f_p , the moisture content M_p and the temperature T_p as the state variables.
 - The transport equations which are associated to these variables are defined at time $t \in [0, T]$, and position $x \in [0, l(t))$ where $l(t)$ represents the moving interface between the two zones (3.3.7), (3.3.9), (3.3.18). The filling ratio f_p and the moisture M_p are strictly positive functions which are less than one according to the modelling assumptions.

$$\partial_t \begin{pmatrix} f_p \\ M_p \\ T_p \end{pmatrix} = -\alpha_p(N)\partial_x \begin{pmatrix} f_p \\ M_p \\ T_p \end{pmatrix} + \begin{pmatrix} 0 \\ 0 \\ \Omega_p(f_p, N, T_p, T_b) \end{pmatrix} \quad (4.1.1)$$

where

$$\alpha_p(N) = \zeta N. \quad (4.1.2)$$

The source term (3.3.18) is given by the equation :

$$\Omega_p(f_p, N, T_p, T_b) = C_1(T_p - T_b) + g_1(N, f_p), \quad (4.1.3)$$

with

$$C_1 := -\frac{\theta}{\phi}, \quad (4.1.4)$$

$$g_1 := \frac{\lambda\eta N^2(t)}{\phi f_p(x, t)}. \quad (4.1.5)$$

The definition of the variables above (4.1.3) can be found in section 3.3.3.

2. For the *Fully Filled Zone*, we consider the moisture M_f and temperature T_f as states variables.

- The transport equations which are associated to these variables are defined at time $t \in [0, T]$, and position $x \in (l(t), L]$ where L is the length of the extruder (3.4.7), (3.4.8). The moisture content is the fraction of water which takes values in $]0, 1]$.

$$\partial_t \begin{pmatrix} M_f \\ T_f \end{pmatrix} = -\alpha_f(N, l, f_p) \partial_x \begin{pmatrix} M_f \\ T_f \end{pmatrix} + \begin{pmatrix} 0 \\ \Omega_f(N, T_f, T_b) \end{pmatrix} \quad (4.1.6)$$

where

$$\alpha_f(N, l, f_p) = \frac{\zeta F_d(t)}{\rho_0 V_{eff}} \quad (4.1.7)$$

The source term is given by the equation:

$$\Omega_f(N, T_f, T_b) = C_1(T_f - T_b) + g_2(N), \quad (4.1.8)$$

with

$$g_2 := \frac{\lambda \eta N^2(t)}{\rho_0 V_{eff} c_p}$$

The definition of the variables above (4.1.8) can be found in section 3.3.3. Assuming the continuity of momentum flux at the interface $l(t)$, the net flow $F_d(t)$ is a function of $l(t)$, $f_p(t, l(t))$ and $N(t)$ and under hypothesis of constant viscosity η , we find:

$$\Delta P(L, t) = \nu \left[-\left[1 + \frac{K_d}{B\rho_0} (L - l(t)) \right] + \sqrt{\Delta(l(t), N(t), f_p(l(t), t))} \right], \quad (4.1.9)$$

where $\nu = \frac{\eta_f^2 \rho_0 S_{eff}^2}{2K_d^2}$ and $\Delta P(L, t) = P(L, t) - P_0$,

$$\Delta(l(t), N(t), f_p(l(t), t)) = \left[1 + \frac{K_d}{B\rho_0} (L - l(t)) \right]^2 + \Omega(f_p(l(t), t), N(t), l^+) \quad (4.1.10)$$

$$\begin{aligned} \text{and } \Omega &= \left(\frac{2\rho_0}{\nu} \right) \left(\frac{\eta_f V_{eff} N(t)}{B\rho_0} (L - l(t)) \right. \\ &\quad \left. + \zeta^2 N^2(t) f_p(l(t), t) - (1 - f_p(l(t), t)) \frac{P_0}{\rho_0} \right) \end{aligned}$$

$$F_d(t) = \frac{K_d}{\eta} (P(L, t) - P_0), \quad (4.1.11)$$

3. The moving interface $l(t)$ dynamic is deduced from a total mass balance and is:

$$\begin{cases} \dot{l}(t) = F(l(t), N(t), f_p(t, l(t))), & 0 < t < T, \\ l(0) = l^0, \end{cases} \quad (4.1.12)$$

where

$$F(l(t), N(t), f_p(t, l(t))) = \frac{F_d(t) - \rho_0 V_{eff} N(t) (1 - f_p(t, l(t)))}{\rho_0 S_{eff} (1 - f_p(t, l(t)))}. \quad (4.1.13)$$

Recall that the *Partially and Fully Filled Zones* exist if the positivity constraint is satisfied:

$$\implies f_{pc}(t, l(t)) > \frac{1}{\zeta^2 N^2(t) + \frac{P_0}{\rho_0}} \left(\frac{P_0}{\rho_0} - K_2(L - l(t)) \right) \quad (4.1.14)$$

For the system defined by (4.1.1), (4.1.6) (4.1.9) and (4.1.12) , we define:

- the initial conditions as:

$$(f_p(0, x), M_p(0, x), T_p(0, x))^T = (f_p^0(x), M_p^0(x), T_p^0(x))^T, \quad 0 \leq x \leq l^0, \quad (4.1.15)$$

$$(M_f(0, x), T_f(0, x))^T = (M_f^0(x), T_f^0(x))^T, \quad l^0 \leq x \leq L. \quad (4.1.16)$$

Here we assume that f_p^0 satisfied:

$$0 < \gamma_0 \leq \|f_p^0\|_{L^\infty} \leq \gamma_1 < 1. \quad (4.1.17)$$

- the boundary conditions as:

$$(f_p(t, 0), M_p(t, 0), T_p(t, 0))^T = \left(\frac{F_{in}(t)}{\theta(N(t))}, M_{in}(t), T_{in}(t) \right)^T, \quad t \in (0, T), \quad (4.1.18)$$

where

$$\theta(N(t)) = \rho_0 V_{eff} N(t).$$

$F_{in}(t)$ is the feed rate. $F_{in}(t)$ and $N(t)$ are known functions of time t .

- and the interface coupling relation for temperature and moisture as:

$$(M_p(t, l(t)), T_p(t, l(t)))^T = (M_f(t, l(t)), T_f(t, l(t)))^T. \quad (4.1.19)$$

The aim of this part is to analyze the well-posedness of the system which is defined by equations (4.1.1) (4.1.6) and (4.1.12) with associated initial and boundary data (4.1.15), (4.1.16) and 4.1.18) respectively. The interface relations are described by (4.1.19) and the momentum flux continuity equations (4.1.9), (4.1.10) and (4.1.11).

4.1.1 Organization of the chapter

The organization of this chapter is as follows/ First in Section 3.2, using a change of variables, we transform the time-varying spatial domain problem into a fixed domain problem. In Section 3.3 we present the main results on the existence and uniqueness of solutions in $W^{1,\infty}$ (*Theorem 3*) and H^2 (*Theorem 4*) spaces. In Section 3.4 we give the proof of *Theorem 3* and finally in Section 3.5 we give an idea of the proof of *Theorem 4*.

4.1.2 Contributions

In this chapter, we prove the existence, uniqueness and regularity of the weak solution to the free boundary Cauchy problem (4.1.1), (4.1.6), (4.1.12), (4.1.15), (4.1.16), (4.1.18), (4.1.19). To tackle this free boundary problem, we make a change of variables on the spatial variables and transform the time-varying spatial domain into a fixed domain. Here, we use *Banach fixed point theorem* to prove the existence of weak solutions in $W^{1,\infty}$ and H^2 .

4.2 Model expressed in fixed spatial domain

The main difficulty of the well-posedness study arises from the moving domains $[0, l(t)[$ and $]l(t), L]$, $l(t)$ being the interface dynamics. In order to deal with this system of balance equations in fixed domains, a classical change of spatial variables is performed for the two zones leading to two systems of conservation laws with additive fictitious convection terms in the transport velocities. Now the *Partially and Fully Filled Zone* equations are defined on $Q := (0, T) \times (0, 1)$.

1. For *Partially Filled Zone (PFZ)*, after the change of variables from $(0, l(t))$ to the interval $(0, 1)$, see [48], via

$$y(t, x) := \frac{x}{l(t)},$$

we normalize the system (4.1.1) to a new system defined on $Q := (0, T) \times (0, 1)$. For the sake of simplicity, we still denote the space variable y as x and unknown the functions as (f_p, M_p, T_p) , the velocity term as α_p and the source term as Ω_p . We have

$$\partial_t \begin{pmatrix} f_p(t, x) \\ M_p(t, x) \\ T_p(t, x) \end{pmatrix} + \alpha_p(t, x) \partial_x \begin{pmatrix} f_p(t, x) \\ M_p(t, x) \\ T_p(t, x) \end{pmatrix} = \begin{pmatrix} 0 \\ 0 \\ \Omega_p(f_p, N, T_p, T_b) \end{pmatrix} \quad (4.2.1)$$

with

$$\begin{aligned} \alpha_p(t, x) &= \frac{1}{l(t)} (\zeta N(t) - x \dot{l}(t)) \\ &= \frac{1}{l(t)} (\zeta N(l(t)) - x F(l(t), N(t), f_p(t, 1))). \end{aligned} \quad (4.2.2)$$

The source term is given by the same relation (4.1.3):

$$\Omega_p(f_p, N, T_p, T_b) = C_1(T_p - T_b) + g_1(N, f_p), \quad (4.2.3)$$

2. For the *Fully Filled Zone (FFZ)*, after the change of variables from $(l(t), L)$ onto the interval $(0, 1)$

$$y(t, x) := \frac{x - l(t)}{L - l(t)},$$

system (4.1.6) can be normalized to a new system defined on $Q := (0, T) \times (0, 1)$. For the sake of simplicity, we still denote the space variable y as x and unknown functions as (M_f, T_f) , the velocity term as α_f and the source term as Ω_f .

$$\partial_t \begin{pmatrix} M_f(t, x) \\ T_f(t, x) \end{pmatrix} + \alpha_f(t, x) \partial_x \begin{pmatrix} M_f(t, x) \\ T_f(t, x) \end{pmatrix} = \begin{pmatrix} 0 \\ \Omega_f(N, T_f, T_b) \end{pmatrix}, \quad (4.2.4)$$

with

$$\begin{aligned}\alpha_f(t, x) &= \frac{1}{L - l(t)} \left(\frac{\zeta F_d(t)}{\rho_0 V_{eff}} + (x - 1) \dot{l}(t) \right), \\ &= \frac{1}{L - l(t)} \left(\frac{\zeta F_d(t)}{\rho_0 V_{eff}} + (x - 1) F(l(t), N(t), f_p(t, 1)) \right),\end{aligned}\quad (4.2.5)$$

where

$$F_d(t) := F_d(l(t), N(t), f_p(t, 1))$$

is defined by (4.1.11). The source term is also given by the same relation (4.1.8).

$$\Omega_f(N, T_f, T_b) = C_1(T_f - T_b) + g_2(N), \quad (4.2.6)$$

From (4.1.18) and (4.1.19), we rewrite the interface relations as the boundary conditions associated to the coupled equations in fixed domains:

$$(f_p(t, 0), M_p(t, 0), T_p(t, 0))^T = \left(\frac{F_{in}(t)}{\theta(N(t))}, M_{in}(t), T_{in}(t) \right)^T, \quad t \in (0, T) \quad (4.2.7)$$

$$(M_f(t, 0), T_f(t, 0))^T = (M_p(t, 1), T_p(t, 1))^T, \quad t \in (0, T). \quad (4.2.8)$$

Remark 9. Now, the convection velocities $\alpha_p(x, t)$ (for *PFZ* zone) and $\alpha_f(x, t)$ (for *FFZ* zone) depend on the spatial coordinate x and are functions of the interface position and velocity. Recall that the interface dynamics is a nonlinear function of $F_d(t)$ and $f_p(l(t), t)$ which are the die net flow rate and the filling ratio at the interface, respectively.

Consequently, in both *Partially and Fully Filled Zones* the net flow rate $F_d(t)$, filling ratio at the interface $f_p(l(t), t)$ and the screw speed $N(t)$ must be considered in the convection terms: the interface dynamic is a nonlinear function of these functions.

In summary, we consider a coupled system composed of an *Ordinary Differential Equation (ODE)* for moving interface

$$\begin{cases} \dot{l}(t) = F(l(t), N(t), f_p(t, 1)), & t \in (0, T) \\ l(0) = l^0, \end{cases} \quad (4.2.9)$$

a transport equation for filling ratio

$$\begin{cases} \partial_t f_p(t, x) + \alpha_p(t, x) \partial_x f_p(t, x) = 0, & (t, x) \in (0, T) \times (0, 1) \\ f_p(0, x) = f_p^0(x), & x \in (0, 1) \\ f_p(t, 0) = \frac{F_{in}(t)}{\theta(N(t))}, & t \in (0, T) \end{cases} \quad (4.2.10)$$

two transport equations for the moisture contains

$$\begin{cases} \partial_t M_p(t, x) + \alpha_p(t, x) \partial_x M_p(t, x) = 0, & (t, x) \in (0, T) \times (0, 1) \\ \partial_t M_f(t, x) + \alpha_f(t, x) \partial_x M_f(t, x) = 0, & (t, x) \in (0, T) \times (0, 1) \\ M_p(0, x) = M_p^0(x), \quad M_f(0, x) = M_f^0(x), & x \in (0, 1) \\ M_p(t, 0) = M_{in}(t), \quad M_f(t, 0) = M_p(t, 1), & t \in (0, T) \end{cases} \quad (4.2.11)$$

and two transport equations for the temperature

$$\begin{cases} \partial_t T_p(t, x) + \alpha_p(t, x) \partial_x T_p(t, x) = \Omega_p, & (t, x) \in (0, T) \times (0, 1) \\ \partial_t T_f(t, x) + \alpha_f(t, x) \partial_x T_f(t, x) = \Omega_f, & (t, x) \in (0, T) \times (0, 1) \\ T_p(0, x) = T_p^0(x), \quad T_f(0, x) = T_f^0(x), & x \in (0, 1) \\ T_p(t, 0) = T_{in}(t), \quad T_f(t, 0) = T_p(t, 1), & t \in (0, T) \end{cases} \quad (4.2.12)$$

In the whole chapter, unless otherwise specified, we always assume that $l^0 \in (0, L)$, $f_p^0 \in W^{1,\infty}(0, 1)$, $M_p^0, T_p^0, M_f^0, T_f^0 \in L^2(0, 1)$, $M_{in}, T_{in} \in L^2(0, T)$, $F_{in}, N \in W^{1,\infty}(0, T)$ and $T_b \in L^\infty(Q)$. For the sake of simplicity, we denote from now on $\|f\|_{L^\infty}$ ($\|f\|_{W^{1,\infty}}$, $\|f\|_{L^2}$, resp.) as the L^∞ ($W^{1,\infty}$, L^2 , resp.) norm of the function f with respect to its unknowns.

$$\|F\|_{W^{1,\infty}} := \sum_{|\alpha| \leq 1} \operatorname{ess\,sup}_{\substack{l_e - \varepsilon_1 < x_1 < l_e + \varepsilon_1 \\ N_e - \varepsilon_1 < x_2 < N_e + \varepsilon_1 \\ f_{pe} - \varepsilon_1 < x_3 < f_{pe} + \varepsilon_1}} |D^\alpha F(x_1, x_2, x_3)|.$$

4.3 Main Results

We recall from [40, Section 2.1], the usual definition of a weak solution to Cauchy problem (4.2.9)-(4.2.12).

Definition 1. Let $T > 0$ be given. A weak solution of Cauchy problem (4.2.9)-(4.2.12) is a vector function $(l, f_p, M_p, M_f, T_p, T_f) \in W^{1,\infty}(0, T) \times W^{1,\infty}(Q) \times (C^0([0, T]; L^2(0, 1)))^4$, such that for every $\tau \in [0, T]$, every test function φ_1 , $\varphi_2 = (\varphi_{21}, \varphi_{22})$, $\varphi_3 = (\varphi_{31}, \varphi_{32}) \in C^1([0, T] \times [0, 1])$ such that

$$\varphi_i(\tau, x) = 0, \quad \forall x \in [0, 1], \quad i = 1, 2, 3, \quad (4.3.1)$$

$$\varphi_i(t, 1) = 0, \quad \forall t \in [0, T], \quad i = 1, 2, 3, \quad (4.3.2)$$

one has

$$l(t) = l^0 + \int_0^t F(l(s), N(s), f_p(s, 1)) ds, \quad t \in (0, \tau), \quad (4.3.3)$$

$$\begin{aligned} \int_0^\tau \int_0^1 f_p(\partial_t \varphi_1 + \partial_x(\alpha_p \varphi_1)) dx dt + \int_0^1 f_p^0(x) \varphi_1(0, x) dx \\ + \int_0^\tau \frac{F_{in}(t)}{\theta(N(t))} \alpha_p(t, 0) \varphi_1(t, 0) dt = 0, \end{aligned} \quad (4.3.4)$$

$$\begin{aligned} \int_0^\tau \int_0^1 M_p(\partial_t \varphi_{21} + \partial_x(\alpha_p \varphi_{21})) dx dt + \int_0^\tau \int_0^1 M_f(\partial_t \varphi_{22} + \partial_x(\alpha_f \varphi_{22})) dx dt \\ + \int_0^\tau \alpha_p(t, 0) M_{in}(t) \varphi_{21}(t, 0) dt + \int_0^\tau \alpha_f(t, 0) M_p(t, 1) \varphi_{22}(t, 0) dt \\ + \int_0^1 M_p^0(x) \varphi_{21}(0, x) dx + \int_0^1 M_f^0(x) \varphi_{22}(0, x) dx = 0, \end{aligned} \quad (4.3.5)$$

$$\begin{aligned}
& \int_0^\tau \int_0^1 T_p(\partial_t \varphi_{31} + \partial_x(\alpha_p \varphi_{31})) dx dt + \int_0^\tau \int_0^1 T_f(\partial_t \varphi_{32} + \partial_x(\alpha_f \varphi_{32})) dx dt \\
& + \int_0^\tau \int_0^1 \Omega_p \varphi_{31} dx dt + \int_0^\tau \int_0^1 \Omega_f \varphi_{32} dx dt \\
& + \int_0^\tau \alpha_p(t, 0) T_{in}(t) \varphi_{31}(t, 0) dt + \int_0^\tau \alpha_f(t, 0) T_p(t, 1) \varphi_{32}(t, 0) dt \\
& + \int_0^1 T_p^0(x) \varphi_{31}(0, x) dx + \int_0^1 T_f^0(x) \varphi_{32}(0, x) dx = 0.
\end{aligned} \tag{4.3.6}$$

We have the following two theorems

Theorem 3. *Let $T > 0$. Let (l_e, N_e, f_{pe}) be a constant equilibrium,*

$$F(l_e, N_e, f_{pe}) = 0 \tag{4.3.7}$$

with $0 < f_{pe} < 1$, $0 < l_e < L$. Assume that the compatibility condition at $(0, 0)$ holds

$$\frac{F_{in}(0)}{\theta(N(0))} = f_p^0(0). \tag{4.3.8}$$

Then, there exists ε_0 (depending on T) such that for any $\varepsilon \in (0, \varepsilon_0]$, if

$$\|f_p^0(\cdot) - f_{pe}\|_{W^{1,\infty}} + \left\| \frac{F_{in}(\cdot)}{\theta(N(\cdot))} - f_{pe} \right\|_{W^{1,\infty}} + \|N(\cdot) - N_e\|_{W^{1,\infty}} + |l^0 - l_e| \leq \varepsilon. \tag{4.3.9}$$

Cauchy problem (4.2.9)-(4.2.12) admits a unique solution $(l, f_p, M_p, M_f, T_p, T_f) \in W^{1,\infty}(0, T) \times W^{1,\infty}(Q) \times (C^0([0, T]; L^2(0, 1)))^4$, and the following estimates hold

$$\|f_p - f_{pe}\|_{W^{1,\infty}} + \|l - l_e\|_{W^{1,\infty}} \leq C_{\varepsilon_0} \cdot \varepsilon, \tag{4.3.10}$$

$$\|M_p\|_{C^0([0, T]; L^2(0, 1))} \leq C_{\varepsilon_0} \cdot (\|M_p^0\|_{L^2} + \|M_{in}\|_{L^2}), \tag{4.3.11}$$

$$\|T_p\|_{C^0([0, T]; L^2(0, 1))} \leq C_{\varepsilon_0} \cdot (\|T_p^0\|_{L^2} + \|T_{in}\|_{L^2}), \tag{4.3.12}$$

$$\|M_f\|_{C^0([0, T]; L^2(0, 1))} \leq C_{\varepsilon_0} \cdot (\|M_p^0\|_{L^2} + \|M_{in}\|_{L^2} + \|M_f^0\|_{L^2}), \tag{4.3.13}$$

$$\|T_f\|_{C^0([0, T]; L^2(0, 1))} \leq C_{\varepsilon_0} \cdot (\|T_p^0\|_{L^2} + \|T_{in}\|_{L^2} + \|T_f^0\|_{L^2}), \tag{4.3.14}$$

where C_{ε_0} is a constant depending on ε_0 , but independent of ε .

Theorem 4. *Under the assumptions of Theorem 3, we assume further that $f_p^0(\cdot) \in H^2(0, 1)$, $\frac{F_{in}(\cdot)}{\theta(N(\cdot))} \in H^2(0, T)$, and the compatibility condition at $(0, 0)$ holds*

$$f_{px}^0(0) + \frac{l(0)}{\zeta N(0)} \cdot \frac{F'_{in}(0)\theta(N(0)) - F_{in}(0)\theta'(N(0))N'(0)}{\theta^2(N(0))} = 0. \tag{4.3.15}$$

Then, there exists ε_0 (depending on T) such that for any $\varepsilon \in (0, \varepsilon_0]$, if

$$\|f_p^0(\cdot) - f_{pe}\|_{H^2(0, 1)} + \left\| \frac{F_{in}(\cdot)}{\theta(N(\cdot))} - f_{pe} \right\|_{H^2(0, T)} + \|N(\cdot) - N_e\|_{W^{1,\infty}} + |l^0 - l_e| \leq \varepsilon, \tag{4.3.16}$$

Cauchy problem (4.2.9)-(4.2.12) has a unique solution $(l, f_p, M_p, M_f, T_p, T_f) \in W^{1,\infty}(0, T) \times C^0([0, T]; H^2(0, 1)) \times (C^0([0, T]; L^2(0, 1)))^4$ with the additional estimate

$$\|f_p - f_{pe}\|_{C^0([0, T]; H^2(0, 1))} \leq C_{\varepsilon_0} \cdot \varepsilon, \tag{4.3.17}$$

where C_{ε_0} is a constant depending on ε_0 , but independent of ε .

Remark 10. The solution we obtained in Theorem 3 or in Theorem 4 is called semi-global solution since it exists on any preassigned time interval $[0, T]$ if (l, f_p) has some kind of smallness (depending on T), see [90, 146]. On the other hand, we do not require any smallness on M_p, M_f, T_p and T_f since their equations are linear.

Remark 11. We have the hidden regularity that $(M_p, M_f, T_p, T_f) \in (C^0([0, 1]; L^2(0, T)))^4$ both in Theorem 3 and in Theorem 4. Similarly, we also have $f_p \in C^0([0, 1]; H^2(0, T))$ in Theorem 4.

For the proof of Remark 11, one can refer to [41, 126].

4.4 Proof of Theorem 1

Sketch of the prove of Theorem 3:

1. In Section 4.4.1 we apply *contraction mapping principle* to prove the existence and uniqueness of $l(t)$ and $f_p(t, 1)$ for t small. With the existence of $l(t)$ and $f_p(t, 1)$ we construct the local solution of Cauchy problem (4.2.9)-(4.2.10) using the definition 1 [40, Section 2.1].
2. In section 4.4.2, we extend the local solution of (4.2.9) to the semi-global one.
3. With the existence of $l(t)$ and $f_p(t, x)$, we next solve the moisture equation (4.2.11) in Section 4.4.3
4. Finally we solve the temperature equation (4.2.12) in Section 4.4.4.

4.4.1 Local solution to Cauchy problem (4.2.9)-(4.2.10)

Lemma 4.4.1. $\exists \varepsilon_1 > 0$ suitably small, $\exists \delta_1 = \delta_1(\varepsilon_1, \|f_p^0 - f_{pe}\|_{W^{1,\infty}}, |l^0 - l_e|)$, $\forall \varepsilon \in (0, \varepsilon_1]$, $\forall f_p^0 \in W^{1,\infty}(0, 1)$, $\forall F_{in}, N \in W^{1,\infty}(0, T)$, $\forall l^0 \in (0, L)$ with

$$\|f_p^0(\cdot) - f_{pe}\|_{W^{1,\infty}} + \left\| \frac{F_{in}(\cdot)}{\theta(N(\cdot))} - f_{pe} \right\|_{W^{1,\infty}} + \|N(\cdot) - N_e\|_{W^{1,\infty}} + |l^0 - l_e| \leq \varepsilon, \quad (4.4.1)$$

Cauchy problem (4.2.9)-(4.2.10) admits a unique local solution on $[0, \delta_1]$, which satisfies the estimates:

$$\|f_p(t, \cdot) - f_{pe}\|_{W^{1,\infty}} \leq C_{\varepsilon_1} \cdot \varepsilon, \quad \forall t \in [0, \delta_1], \quad (4.4.2)$$

$$|l(t) - l_e| \leq C_{\varepsilon_1} \cdot \varepsilon, \quad \forall t \in [0, \delta_1]. \quad (4.4.3)$$

where C_{ε_1} is a constant depending on ε_1 , but independent of ε .

Proof of Lemma 4.4.1: We first apply contraction mapping principle to prove the existence and uniqueness of $l(t)$ and $f_p(t, 1)$ for t small. With the existence of $l(t)$ and $f_p(t, 1)$, we then

construct a local solution to Cauchy problem (4.2.9)-(4.2.10). Next, we prove the solution we constructed is indeed the unique weak solution to Cauchy problem (4.2.9)-(4.2.10). Finally, we derive the estimates (4.4.2)-(4.4.3) of the local solution.

Step 1. Fixed point argument We choose ε_1 such that

$$0 < \varepsilon_1 < \min\{l_e, L - l_e\}. \quad (4.4.4)$$

We denote

$$\|F\|_{W^{1,\infty}} := \sum_{|\alpha| \leq 1} \operatorname{ess\,sup}_{\substack{l_e - \varepsilon_1 < x_1 < l_e + \varepsilon_1 \\ N_e - \varepsilon_1 < x_2 < N_e + \varepsilon_1 \\ f_{pe} - \varepsilon_1 < x_3 < f_{pe} + \varepsilon_1}} |D^\alpha F(x_1, x_2, x_3)|, \quad (4.4.5)$$

$$\Psi(t) := (l(t), f_p(t, 1)), \quad t \in [0, T].$$

For any given $\delta > 0$ small enough (which will be defined later), let us define a domain candidate as a closed subset of $C^0([0, \delta])$ with respect to C^0 norm.

$$\Omega_\delta := \left\{ \Psi \in C^0([0, \delta]) : \|\Psi\|_{C^0([0, \delta])} := \max\{\|l\|_{C^0([0, \delta])}, \|f_p(\cdot, 1)\|_{C^0([0, \delta])}\} \leq L + 1 \right\}, \quad (4.4.6)$$

Let us define a map $\mathfrak{F} := (\mathfrak{F}_1, \mathfrak{F}_2)$, where $\mathfrak{F} : \Omega_\delta \rightarrow C^0([0, \delta])$, $\Psi \mapsto \mathfrak{F}(\Psi)$ as

$$\mathfrak{F}_1(l)(t) = l^0 + \int_0^t F(l(s), N(s), f_p(s, 1)) ds, \quad (4.4.7)$$

$$\mathfrak{F}_2(f_p)(t, 1) = f_p^0(\xi_2(0)), \quad (4.4.8)$$

where ξ_2 (see Fig 4.4.1) represents the characteristic curve passing through $(t, 1)$

$$\begin{cases} \frac{d\xi_2(s)}{ds} = \alpha_p(N(s), \xi_2(s), l(s), f_p(s, 1)), & 0 \leq s \leq t \\ \xi_2(t) = 1. \end{cases} \quad (4.4.9)$$

From (4.2.2), we solve the linear ODE (4.4.9)

$$\xi_2(s) = e^{\int_s^t \frac{F(l(\sigma), N(\sigma), f_p(\sigma, 1))}{l(\sigma)} d\sigma} - \int_s^t \frac{\zeta N(\sigma)}{l(\sigma)} \cdot e^{-\int_\sigma^s \frac{F(l(s), N(s), f_p(s, 1))}{l(s)} ds} d\sigma, \quad 0 \leq s \leq t. \quad (4.4.10)$$

It is obvious that \mathfrak{F} maps into Ω_δ itself if

$$0 < \delta < \min\{T_1, T\}, \quad (4.4.11)$$

where T_1 satisfies

$$\xi(T_1) = 1. \quad (4.4.12)$$

Here ξ represents the characteristic curve passing through $(0, 0)$ (see Fig 4.4.1)

$$\begin{cases} \frac{d\xi}{ds} = \alpha_p(N(s), \xi(s), l(s), f_p(s, 1)), & 0 \leq s \leq t, \\ \xi(0) = 0. \end{cases} \quad (4.4.13)$$

We solve the linear ODE (4.4.13)

$$\xi(s) = - \int_s^0 \frac{\zeta N(\sigma)}{l(\sigma)} \cdot e^{-\int_\sigma^s \frac{F(l(s), N(s), f_p(s, 1))}{l(s)} ds} d\sigma, \quad 0 \leq s \leq t. \quad (4.4.14)$$

Now we prove that, if δ is small enough, \mathfrak{F} is a contraction mapping on Ω_δ with respect to the C^0 norm. Let $\Psi = (l, f_p), \bar{\Psi} = (\bar{l}, \bar{f}_p) \in \Omega_\delta$, for any fixed $t \in [0, \delta]$, we have

$$\begin{aligned} |\mathfrak{F}_1(\bar{l})(t) - \mathfrak{F}_1(l)(t)| &= \left| \int_0^t F(\bar{l}(s), N(s), \bar{f}_p(s, 1)) ds - \int_0^t F(l(s), N(s), f_p(s, 1)) ds \right| \\ &\leq \delta \|F\|_{W^{1, \infty}} (\|\bar{l} - l\|_{C^0([0, \delta])} + \|\bar{f}_p(\cdot, 1) - f_p(\cdot, 1)\|_{C^0([0, \delta])}). \end{aligned} \quad (4.4.15)$$

Define the characteristic curve $\bar{\xi}_2$

$$\bar{\xi}_2(s) = e^{\int_s^t \frac{F(\bar{l}(\sigma), N(\sigma), \bar{f}_p(\sigma, 1))}{\bar{l}(\sigma)} d\sigma} - \int_s^t \frac{\zeta N(\sigma)}{\bar{l}(\sigma)} \cdot e^{-\int_\sigma^s \frac{F(\bar{l}(\sigma), N(\sigma), \bar{f}_p(\sigma, 1))}{\bar{l}(\sigma)} ds} d\sigma, \quad 0 \leq s \leq t, \quad (4.4.16)$$

then for any $t \in [0, \delta]$

$$\begin{aligned} &|\mathfrak{F}_2(\bar{f}_p)(t, 1) - \mathfrak{F}_2(f_p)(t, 1)| \\ &= \left| f_p^0 \left(e^{\int_0^t \frac{F(\bar{l}(\sigma), N(\sigma), \bar{f}_p(\sigma, 1))}{\bar{l}(\sigma)} d\sigma} - \int_0^t \frac{\zeta N(\sigma)}{\bar{l}(\sigma)} \cdot e^{-\int_\sigma^0 \frac{F(\bar{l}(\sigma), N(\sigma), \bar{f}_p(\sigma, 1))}{\bar{l}(\sigma)} ds} d\sigma \right) \right. \\ &\quad \left. - f_p^0 \left(e^{\int_0^t \frac{F(l(\sigma), N(\sigma), f_p(\sigma, 1))}{l(\sigma)} d\sigma} - \int_0^t \frac{\zeta N(\sigma)}{l(\sigma)} \cdot e^{-\int_\sigma^0 \frac{F(l(\sigma), N(\sigma), f_p(\sigma, 1))}{l(\sigma)} ds} d\sigma \right) \right| \\ &\leq \|f_p^0\|_{W^{1, \infty}} \left\{ \left| e^{\int_0^t \frac{F(\bar{l}(\sigma), N(\sigma), \bar{f}_p(\sigma, 1))}{\bar{l}(\sigma)} d\sigma} - e^{\int_0^t \frac{F(l(\sigma), N(\sigma), f_p(\sigma, 1))}{l(\sigma)} d\sigma} \right| \right. \\ &\quad \left. + \int_0^t \left| \frac{\zeta N(\sigma)}{\bar{l}(\sigma)} \cdot e^{-\int_\sigma^0 \frac{F(\bar{l}(\sigma), N(\sigma), \bar{f}_p(\sigma, 1))}{\bar{l}(\sigma)} ds} - \frac{\zeta N(\sigma)}{l(\sigma)} \cdot e^{-\int_\sigma^0 \frac{F(l(\sigma), N(\sigma), f_p(\sigma, 1))}{l(\sigma)} ds} \right| d\sigma \right\} \\ &\leq \|f_p^0\|_{W^{1, \infty}} \left\{ e^{\frac{\delta \|F\|_{W^{1, \infty}}}{l_e - \varepsilon_1}} \int_0^t \left| \frac{F(\bar{l}, N, \bar{f}_p)l - F(N, l, f_p)\bar{l}(\sigma)}{\bar{l}l} \right| d\sigma \right. \\ &\quad + \int_0^t \left| \frac{\zeta N(\sigma)(l(\sigma) - \bar{l}(\sigma))}{\bar{l}(\sigma)l(\sigma)} e^{\int_0^\sigma \frac{F(\bar{l}(s), N(s), \bar{f}_p(s, 1))}{\bar{l}(s)} ds} \right| d\sigma \\ &\quad \left. + \int_0^t \frac{\zeta N(\sigma)}{l(\sigma)} e^{\frac{\delta \|F\|_{W^{1, \infty}}}{l_e - \varepsilon_1}} \left(\int_0^\sigma \left| \frac{F(\bar{l}, N, \bar{f}_p)l - F(N, l, f_p)\bar{l}}{\bar{l}l} \right| ds \right) d\sigma \right\} \\ &\leq \|f_p^0\|_{W^{1, \infty}} \left\{ e^{\frac{\delta \|F\|_{W^{1, \infty}}}{l_e - \varepsilon_1}} \int_0^t \left| \frac{F(\bar{l}, N, \bar{f}_p)(l - \bar{l}) - \bar{l}(F(\bar{l}, N, \bar{f}_p) - F(N, l, f_p))}{\bar{l}l} \right| d\sigma \right. \\ &\quad + \int_0^t \left| \frac{\zeta N(\sigma)(l(\sigma) - \bar{l}(\sigma))}{\bar{l}(\sigma)l(\sigma)} e^{\int_0^\sigma \frac{F(\bar{l}(s), N(s), \bar{f}_p(s, 1))}{\bar{l}(s)} ds} \right| d\sigma \\ &\quad \left. + \int_0^t \frac{\zeta N(\sigma)}{l(\sigma)} e^{\frac{\delta \|F\|_{W^{1, \infty}}}{l_e - \varepsilon_1}} \left(\int_0^\sigma \left| \frac{F(\bar{l}, N, \bar{f}_p)(l - \bar{l}) - \bar{l}(F(\bar{l}, N, \bar{f}_p) - F(N, l, f_p))}{\bar{l}l} \right| ds \right) d\sigma \right\}. \end{aligned} \quad (4.4.17)$$

Since $t \in [0, \delta]$, $l < l_e - \varepsilon_1$, $\bar{l} < l_e - \varepsilon_1$ and noting (4.4.5), from (4.4.17), we obtain

$$\begin{aligned}
& |\mathfrak{F}_2(\bar{f}_p)(t, 1) - \mathfrak{F}_2(f_p)(t, 1)| \\
& \leq \|f_p^0\|_{W^{1,\infty}} \left\{ \delta e^{\frac{\delta \|F\|_{W^{1,\infty}}}{l_e - \varepsilon_1}} \left(\frac{\|F\|_{W^{1,\infty}}}{l_e - \varepsilon_1} (\|\bar{l} - l\|_{C^0([0,\delta])} + \|\bar{f}_p - f_p\|_{C^0([0,\delta])}) + \frac{\|F\|_{W^{1,\infty}}}{(l_e - \varepsilon_1)^2} \|\bar{l} - l\|_{C^0([0,\delta])} \right) \right. \\
& \quad + \frac{\delta^2 \zeta \|N\|_{L^\infty}}{l_e - \varepsilon_1} e^{\frac{\delta \|F\|_{W^{1,\infty}}}{l_e - \varepsilon_1}} \left(\frac{\|F\|_{W^{1,\infty}}}{l_e - \varepsilon_1} (\|\bar{l} - l\|_{C^0([0,\delta])} + \|\bar{f}_p - f_p\|_{C^0([0,\delta])}) + \frac{\|F\|_{W^{1,\infty}}}{(l_e - \varepsilon_1)^2} \|\bar{l} - l\|_{C^0([0,\delta])} \right) \\
& \quad \left. + \frac{\delta \zeta \|N\|_{L^\infty}}{(l_e - \varepsilon_1)^2} e^{\frac{\delta \|F\|_{W^{1,\infty}}}{l_e - \varepsilon_1}} \|\bar{l} - l\|_{C^0([0,\delta])} \right\}. \tag{4.4.18}
\end{aligned}$$

Hence, from (4.4.15) and (4.4.18), we have

$$\begin{aligned}
& \|\mathfrak{F}(\bar{\Psi}) - \mathfrak{F}(\Psi)\|_{C^0([0,\delta])} \\
& = \max \left\{ \|\mathfrak{F}_1(\bar{l})(\cdot) - \mathfrak{F}_1(l)(\cdot)\|_{C^0([0,\delta])}, \|\mathfrak{F}_2(\bar{f}_p)(\cdot, 1) - \mathfrak{F}_2(f_p)(\cdot, 1)\|_{C^0([0,\delta])} \right\} \\
& \leq \delta \max \{ \|\bar{l} - l\|_{C^0([0,\delta])}, \|\bar{f}_p - f_p\|_{C^0([0,\delta])} \} \\
& \quad \cdot \left\{ 2\|F\|_{W^{1,\infty}} + \|f_p^0\|_{W^{1,\infty}} \cdot e^{\frac{\delta \|F\|_{W^{1,\infty}}}{l_e - \varepsilon_1}} \cdot \left(\left(2\frac{\|F\|_{W^{1,\infty}}}{l_e - \varepsilon_1} + \frac{\|F\|_{W^{1,\infty}}}{(l_e - \varepsilon_1)^2} \right) \left(1 + \frac{\delta \zeta \|N\|_{L^\infty}}{l_e - \varepsilon_1} \right) \right. \right. \\
& \quad \left. \left. + \frac{\zeta \|N\|_{L^\infty}}{(l_e - \varepsilon_1)^2} \right) \right\} \\
& \leq \delta C_{\varepsilon_1} \cdot \max \left\{ \|\bar{l} - l\|_{C^0([0,\delta])}, \|\bar{f}_p - f_p\|_{C^0([0,\delta])} \right\}. \tag{4.4.19}
\end{aligned}$$

We choose δ_1 (depending on $\varepsilon_1, \|f_p^0\|_{W^{1,\infty}}, \|F\|_{W^{1,\infty}}, \|N\|_{L^\infty}$) be small enough such that

$$\|\mathfrak{F}(\bar{\Psi}) - \mathfrak{F}(\Psi)\|_{C^0([0,\delta_1])} \leq \frac{1}{2} \|\bar{\Psi} - \Psi\|_{C^0([0,\delta_1])}. \tag{4.4.20}$$

By means of the contraction mapping principle, there exists a unique fixed point $\Psi = \mathfrak{F}(\Psi)$ in Ω_{δ_1} .

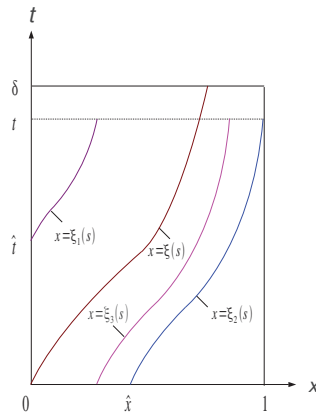


Figure 4.4.1: The characteristics ξ , ξ_1 , ξ_2 and ξ_3 .

Step 2. Construction of a weak solution By fixed point argument, we get the existence and uniqueness of local solution $l(t)$ and $f_p(t, 1)$. Next, we construct local solution to (4.2.10) by characteristic method.

For any fixed $t \in [0, \delta_1]$, when $0 \leq x \leq \xi(t)$, we define the characteristic curve $\xi_1(s)$ as (see Fig 4.4.1)

$$\xi_1(s) = xe^{\int_s^t \frac{F(l(\sigma), N(\sigma), f_p(\sigma, 1))}{l(\sigma)} d\sigma} - \int_s^t \frac{\zeta N(\sigma)}{l(\sigma)} \cdot e^{-\int_\sigma^s \frac{F(l(s), N(s), f_p(s, 1))}{l(s)} ds} d\sigma. \quad (4.4.21)$$

We define \hat{t} as (see Fig 4.4.1)

$$\xi_1(\hat{t}) = 0. \quad (4.4.22)$$

For any given $l \in \Omega_{\delta_1, M}$, when $\xi(t) \leq x \leq 1$, we define the characteristic curve $\xi_3(s)$ as (see Fig 4.4.1)

$$\xi_3(s) = xe^{\int_s^t \frac{F(l(\sigma), N(\sigma), f_p(\sigma, 1))}{l(\sigma)} d\sigma} - \int_s^t \frac{\zeta N(\sigma)}{l(\sigma)} \cdot e^{-\int_\sigma^s \frac{F(l(s), N(s), f_p(s, 1))}{l(s)} ds} d\sigma. \quad (4.4.23)$$

We define \hat{x} as (see Fig 4.4.1).

$$\hat{x} = \xi_3(0). \quad (4.4.24)$$

We have

$$\frac{\partial \hat{t}}{\partial t} = \frac{-\alpha_p(t, x)l(\hat{t})}{\zeta N(\hat{t})} \cdot e^{\int_{\hat{t}}^t \frac{F(l(\sigma), N(\sigma), f_p(\sigma, 1))}{l(\sigma)} d\sigma}, \quad (4.4.25)$$

$$\frac{\partial \hat{t}}{\partial x} = \frac{-l(\hat{t})}{\zeta N(\hat{t})} \cdot e^{\int_{\hat{t}}^t \frac{F(l(\sigma), N(\sigma), f_p(\sigma, 1))}{l(\sigma)} d\sigma}. \quad (4.4.26)$$

$$\frac{\partial \hat{x}}{\partial t} = -\alpha_p(t, x) \cdot e^{\int_0^t \frac{F(l(\sigma), N(\sigma), f_p(\sigma, 1))}{l(\sigma)} d\sigma}, \quad (4.4.27)$$

$$\frac{\partial \hat{x}}{\partial x} = e^{\int_0^t \frac{F(l(\sigma), N(\sigma), f_p(\sigma, 1))}{l(\sigma)} d\sigma}. \quad (4.4.28)$$

Now, we construct a solution for the filling ratio f_p for PFZ zone as

$$f_p(t, x) = \begin{cases} \frac{F_{in}(\hat{t})}{\theta(N(\hat{t}))}, & 0 \leq x \leq \xi(t), \\ f_p^0(\hat{x}), & \xi(t) \leq x \leq 1, \end{cases} \quad (4.4.29)$$

where \hat{t} and \hat{x} are define by (4.4.22) and (4.4.24).

Next, we prove the solution defined by (4.4.29) is indeed a weak solution to Cauchy problem (4.2.10). That is to prove that solutions defined above satisfy (4.3.4).

Let $\tau \in [0, \delta_1]$ and any $\varphi_1 \in C^1([0, \tau] \times [0, 1])$ with $\varphi_1(\tau, x) \equiv 0$ and $\varphi_1(t, 1) \equiv 0$ be given, we have

$$\begin{aligned} A &:= \int_0^\tau \int_0^1 f_p(t, x)(\varphi_{1t}(t, x) + (\alpha_p \varphi_1(t, x))_x) dx dt \\ &= \int_0^\tau \int_0^{\xi(t)} \frac{F_{in}(\hat{t})}{\theta(N(\hat{t}))} (\varphi_{1t}(t, x) + (\alpha_p \varphi_1(t, x))_x) dx dt \\ &\quad + \int_0^\tau \int_{\xi(t)}^1 f_p^0(\hat{x}) (\varphi_{1t}(t, x) + (\alpha_p \varphi_1(t, x))_x) dx dt. \end{aligned}$$

By (4.4.26) and (4.4.28), we obtain

$$\begin{aligned}
A &= \int_0^\tau \int_0^t \frac{F_{in}(\hat{t})}{\theta(N(\hat{t}))} \cdot \frac{\zeta N(\hat{t})}{l(\hat{t})} e^{-\int_{\hat{t}}^t \frac{F(s)}{l(s)} ds} (\varphi_{1t}(t, \xi_1(t)) + (\alpha_p(t, \xi_1(t))\varphi_1(t, \xi_1(t)))_x) d\hat{t} dt \\
&\quad + \int_0^\tau \int_0^{1-\int_0^t \alpha_p(s, \xi_2(s)) ds} f_p^0(\hat{x}) \cdot e^{-\int_0^t \frac{F(s)}{l(s)} ds} (\varphi_{1t}(t, \xi_3(t)) + (\alpha_p(t, \xi_3(t))\varphi_1(t, \xi_3(t)))_x) d\hat{x} dt \\
&= \int_0^\tau \int_0^t \frac{F_{in}(\hat{t})}{\theta(N(\hat{t}))} \cdot \frac{\zeta N(\hat{t})}{l(\hat{t})} e^{-\int_{\hat{t}}^t \frac{F(s)}{l(s)} ds} \left(\frac{d\varphi_1(t, \xi_1(t))}{dt} - \frac{F(t)}{l(t)} \varphi_1(t, \xi_1(t)) \right) d\hat{t} dt \\
&\quad + \int_0^\tau \int_0^{1-\int_0^t \alpha_p(s, \xi_2(s)) ds} f_p^0(\hat{x}) \cdot e^{-\int_0^t \frac{F(s)}{l(s)} ds} \left(\frac{d\varphi_1(t, \xi_3(t))}{dt} - \frac{F(t)}{l(t)} \varphi_1(t, \xi_3(t)) \right) d\hat{x} dt \\
&= \int_0^\tau \int_0^t \frac{F_{in}(\hat{t})}{\theta(N(\hat{t}))} \cdot \frac{\zeta N(\hat{t})}{l(\hat{t})} \cdot \frac{d(\varphi_1(t, \xi_1(t))e^{-\int_{\hat{t}}^t \frac{F(s)}{l(s)} ds})}{dt} d\hat{t} dt \\
&\quad + \int_0^\tau \int_0^{1-\int_0^t \alpha_p(s, \xi_2(s)) ds} f_p^0(\hat{x}) \cdot \frac{d(\varphi_1(t, \xi_3(t))e^{-\int_0^t \frac{F(s)}{l(s)} ds})}{dt} d\hat{x} dt
\end{aligned}$$

By changing the order of integral, we have

$$\begin{aligned}
A &= \int_0^\tau \int_{\hat{t}}^\tau \frac{F_{in}(\hat{t})}{\theta(N(\hat{t}))} \cdot \frac{\zeta N(\hat{t})}{l(\hat{t})} \cdot \frac{d(\varphi_1(t, \xi_1(t))e^{-\int_{\hat{t}}^t \frac{F(s)}{l(s)} ds})}{dt} dt d\hat{t} \\
&\quad + \left(\int_0^{f(\tau)} \int_0^\tau + \int_{f(\tau)}^1 \int_0^{f^{-1}(\hat{x})} \right) f_p^0(\hat{x}) \cdot \frac{d(\varphi_1(t, \xi_3(t))e^{-\int_0^t \frac{F(s)}{l(s)} ds})}{dt} dt d\hat{x},
\end{aligned}$$

where

$$f(t) = 1 - \int_0^t \alpha_p(s, \xi_2(s)) ds$$

represents the coordinate that the characteristic curve ξ_2 intersects with x -axis and $f^{-1}(\hat{x})$ represents the time when the characteristic curve starting from $(0, \hat{x})$ arrives at the boundary $x = 1$. Consequently, for any $\beta \in [f(\tau), 1]$, ξ_2 and ξ_3 are identical to each other since they pass through the same point $(0, \beta)$, so we get

$$\xi_3(f^{-1}(\hat{x})) = \xi_2(f^{-1}(\hat{x})) = 1.$$

Finally, we get

$$\begin{aligned}
A &= - \int_0^\tau \frac{F_{in}(\hat{t})}{\theta(N(\hat{t}))} \cdot \frac{\zeta N(\hat{t})}{l(\hat{t})} \varphi_1(\hat{t}, 0) d\hat{t} - \int_0^{f(\tau)} f_p^0(\hat{x}) \varphi_1(0, \hat{x}) d\hat{x} - \int_{f(\tau)}^1 f_p^0(\hat{x}) \varphi_1(0, \hat{x}) d\hat{x} \\
&= - \int_0^\tau \frac{F_{in}(\hat{t})}{\theta(N(\hat{t}))} \cdot \frac{\zeta N(\hat{t})}{l(\hat{t})} \varphi_1(\hat{t}, 0) d\hat{t} - \int_0^1 f_p^0(\hat{x}) \varphi_1(0, \hat{x}) d\hat{x}.
\end{aligned}$$

This proves that f_p given by (4.4.29) satisfies (4.3.4) for every $\tau \in [0, \delta_1]$.

Step 3. Uniqueness of solution. Since the fixed point iteration yields the uniqueness of the fixed point $(l(t), f_p(t, 1))$ that determines the characteristic curves ξ_1 and ξ_3 . Then (4.2.10) becomes a linear forward Cauchy problem, it follows easily the uniqueness of $f_p(t, x)$.

Step 4. Priori estimate

From (4.4.1) and the expression of the solution for the filling ratio (4.4.29), it is easy to check that, for any $t \in [0, \delta_1]$

$$\|f_p(t, \cdot) - f_{pe}\|_{L^\infty} \leq \varepsilon. \quad (4.4.30)$$

From now on, we denote by C_{ε_1} various constants that may depend on ε_1 .

$$\begin{aligned} |\dot{l}(t)| &= |\dot{l}(t) - \dot{l}_e| = |F(l(t), N(t), f_p(t, 1)) - F(l_e, N_e, f_{pe})| \\ &\leq \|F\|_{W^{1,\infty}} |l(t) - l_e| + \|F\|_{W^{1,\infty}} |N(t) - N_e| \\ &\quad + \|F\|_{W^{1,\infty}} |f_p(t, 1) - f_{pe}|. \end{aligned} \quad (4.4.31)$$

Combining (4.4.1), (4.4.30) and (4.4.31), we get

$$|\dot{l}(t)| \leq C_{\varepsilon_1} |l(t) - l_e| + C_{\varepsilon_1} \varepsilon. \quad (4.4.32)$$

By (4.4.1) and using Grownwall's inequality, we get (4.4.3). Furthermore,

$$\begin{aligned} \left\| \frac{\partial f_p(t, x)}{\partial x} \right\|_{L^\infty} &\leq \left\| \frac{\partial \left(\frac{F_{in}(\hat{t})}{\theta(N(\hat{t}))} \right)}{\partial x} \right\|_{L^\infty} + \left\| \frac{\partial f_p^0(\hat{x})}{\partial x} \right\|_{L^\infty} \\ &\leq \left\| \frac{F_{in}(\cdot)}{\theta(N(\cdot))} - f_{pe} \right\|_{W^{1,\infty}} \cdot \left\| \frac{\partial \hat{t}}{\partial x} \right\|_{L^\infty} + \|f_p^0(\cdot) - f_{pe}\|_{W^{1,\infty}} \cdot \left\| \frac{\partial \hat{x}}{\partial x} \right\|_{L^\infty}. \end{aligned} \quad (4.4.33)$$

By (4.4.26), (4.4.28) and noting (4.4.1), we obtain (4.4.2).

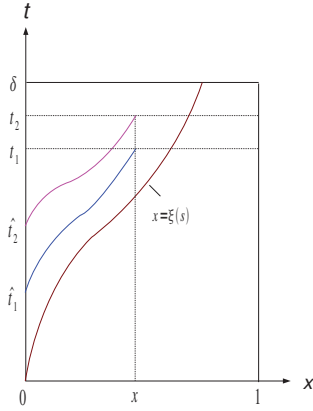


Figure 4.4.2: $x \in [0, \xi(t_1)]$.

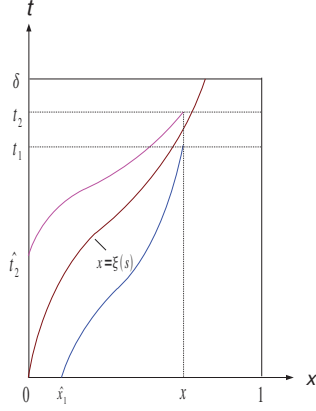


Figure 4.4.3: $x \in [\xi(t_1), \xi(t_2)]$.

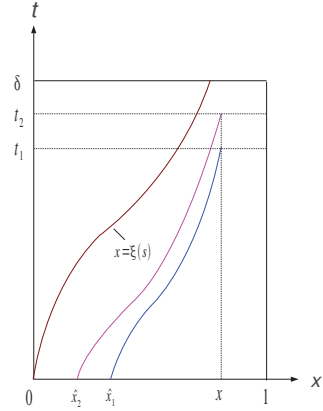


Figure 4.4.4: $x \in [\xi(t_2), 1]$.

4.4.2 Semi-global solution to Cauchy problem (4.2.9)-(4.2.10)

By (4.4.2) and (4.4.3) in Lemma 4.4.1, we take $\varepsilon_2 \leq \varepsilon_1$ such that $C_{\varepsilon_1} \cdot \varepsilon_2 \leq \varepsilon_1$. Then for any $\varepsilon \in (0, \varepsilon_2]$ and any initial-boundary data such that (4.4.1) holds, noting (4.4.19), Cauchy problem (4.2.9)-(4.2.10) admits a solution on $[0, \delta_1]$. Furthermore,

$$\|f_p(\delta_1, \cdot) - f_{pe}\|_{W^{1,\infty}(0,1)} \leq C_{\varepsilon_1} \cdot \varepsilon \leq \varepsilon_1, \quad (4.4.34)$$

$$|l(\delta_1) - l_e| \leq C_{\varepsilon_1} \cdot \varepsilon \leq \varepsilon_1. \quad (4.4.35)$$

Take $(l(\delta_1), f_p(\delta_1, 1))$ as new initial condition, noting (4.4.34) and (4.4.35), after repeating the process in the proof of Lemma 4.4.1, we could solve Cauchy problem (4.2.9) to (4.2.10) on $[\delta_1, 2\delta_1]$. For fixed $T > 0$, by at most $\lceil \frac{T}{\delta_1} \rceil + 1$ steps, we reduce the value of ε to ε_0 and apply Lemma 4.4.1 successively, then we extend local solution to large time interval, finally to $[0, T]$.

4.4.3 Solving the moisture equation (4.2.11) for PFZ zone and FFZ zone

With the existence of the interface $l(t)$ and $f_p(t, 1)$, $t \in [0, T]$, using characteristic method, we construct a solution M_p as

$$M_p(t, x) = \begin{cases} M_p^0(\hat{x}), & \xi(t) \leq x \leq 1, \quad t \in [0, T], \\ M_{in}(\hat{t}), & \text{else,} \end{cases} \quad (4.4.36)$$

with \hat{t} and \hat{x} defined by (4.4.22) and (4.4.24).

Next we prove that $M_p \in C^0([0, T]; L^2(0, 1))$. For any given $0 \leq t_1 < t_2 \leq \delta$, we prove that

$$\|M_p(t_2, x) - M_p(t_1, x)\|_{L^2(0,1)} \rightarrow 0, \quad \text{as } |t_2 - t_1| \rightarrow 0. \quad (4.4.37)$$

We estimate $\int_0^{\xi(t_1)} |M_p(t_2, x) - M_p(t_1, x)|^2 dx$, $\int_{\xi(t_1)}^{\xi(t_2)} |M_p(t_2, x) - M_p(t_1, x)|^2 dx$, $\int_{\xi(t_2)}^1 |M_p(t_2, x) - M_p(t_1, x)|^2 dx$ separately. For almost every $x \in [0, \xi(t_1)]$, by (4.4.36), we have (see Fig 4.4.2)

$$|M_p(t_2, x) - M_p(t_1, x)| = |M_{in}(\hat{t}_2) - M_{in}(\hat{t}_1)|, \quad (4.4.38)$$

where \hat{t}_1 and \hat{t}_2 are defined by

$$0 = xe^{\int_{\hat{t}_1}^{t_1} \frac{F(l(\sigma), N(\sigma), f_p(\sigma, 1))}{l(\sigma)} d\sigma} - \int_{\hat{t}_1}^{t_1} \frac{\zeta N(\sigma)}{l(\sigma)} \cdot e^{-\int_{\sigma}^{\hat{t}_1} \frac{F(l(s), N(s), f_p(s, 1))}{l(s)} ds} d\sigma, \quad (4.4.39)$$

$$0 = xe^{\int_{\hat{t}_2}^{t_2} \frac{F(l(\sigma), N(\sigma), f_p(\sigma, 1))}{l(\sigma)} d\sigma} - \int_{\hat{t}_2}^{t_2} \frac{\zeta N(\sigma)}{l(\sigma)} \cdot e^{-\int_{\sigma}^{\hat{t}_2} \frac{F(l(s), N(s), f_p(s, 1))}{l(s)} ds} d\sigma. \quad (4.4.40)$$

For the given $M_{in} \in L^2(0, T)$, we let $M_{in}^n \in C^1([0, T])$ be such that $M_{in}^n \rightarrow M_{in}$ in $L^2(0, T)$.

We have that for almost every $x \in [0, \xi(t_1)]$

$$\begin{aligned} |M_p(t_2, x) - M_p(t_1, x)| &\leq |M_{in}(\hat{t}_1) - M_{in}^n(\hat{t}_1)| + |M_{in}^n(\hat{t}_1) - M_{in}^n(\hat{t}_2)| \\ &\quad + |M_{in}^n(\hat{t}_2) - M_{in}(\hat{t}_2)|. \end{aligned} \quad (4.4.41)$$

>From (4.4.39) and (4.4.40), we get

$$\begin{aligned} &\int_{\hat{t}_1}^{t_1} \frac{\zeta N(\sigma)}{l(\sigma)} \cdot e^{-\int_{\sigma}^{\hat{t}_1} \frac{F(l(s), N(s), f_p(s, 1))}{l(s)} ds} d\sigma \\ &= e^{(\int_{\hat{t}_1}^{t_1} - \int_{\hat{t}_2}^{t_2}) \frac{F(l(\sigma), N(\sigma), f_p(\sigma, 1))}{l(\sigma)} d\sigma} \cdot \int_{\hat{t}_2}^{t_2} \frac{\zeta N(\sigma)}{l(\sigma)} \cdot e^{-\int_{\sigma}^{\hat{t}_2} \frac{F(l(s), N(s), f_p(s, 1))}{l(s)} ds} d\sigma. \end{aligned} \quad (4.4.42)$$

Hence, we have

$$\begin{aligned}
|\hat{t}_2 - \hat{t}_1| &\leq \frac{1}{D} \int_{\hat{t}_1}^{\hat{t}_2} \frac{\zeta N(\sigma)}{l(\sigma)} \cdot e^{-\int_{\sigma}^{\hat{t}_1} \frac{F(l(s), N(s), f_p(s,1))}{l(s)} ds} d\sigma \\
&= e^{(\int_{\hat{t}_1}^{\hat{t}_2} \frac{F(l(\sigma), N(\sigma), f_p(\sigma,1))}{l(\sigma)} d\sigma)} \int_{\hat{t}_2}^{\hat{t}_1} \frac{\zeta N(\sigma)}{l(\sigma)} \cdot e^{-\int_{\sigma}^{\hat{t}_2} \frac{F(l(s), N(s), f_p(s,1))}{l(s)} ds} d\sigma \\
&\quad - \int_{\hat{t}_2}^{\hat{t}_1} \frac{\zeta N(\sigma)}{l(\sigma)} \cdot e^{-\int_{\sigma}^{\hat{t}_1} \frac{F(l(s), N(s), f_p(s,1))}{l(s)} ds} d\sigma \\
&\quad + e^{(\int_{\hat{t}_1}^{\hat{t}_2} \frac{F(l(\sigma), N(\sigma), f_p(\sigma,1))}{l(\sigma)} d\sigma)} \int_{t_1}^{\hat{t}_2} \frac{\zeta N(\sigma)}{l(\sigma)} \cdot e^{-\int_{\sigma}^{\hat{t}_2} \frac{F(l(s), N(s), f_p(s,1))}{l(s)} ds} d\sigma \\
&= (e^{(\int_{\hat{t}_1}^{\hat{t}_2} \frac{F(l(\sigma), N(\sigma), f_p(\sigma,1))}{l(\sigma)} d\sigma)} - 1) \int_{\hat{t}_2}^{\hat{t}_1} \frac{\zeta N(\sigma)}{l(\sigma)} \cdot e^{-\int_{\sigma}^{\hat{t}_2} \frac{F(l(s), N(s), f_p(s,1))}{l(s)} ds} d\sigma \\
&\quad + \int_{\hat{t}_2}^{\hat{t}_1} \frac{\zeta N(\sigma)}{l(\sigma)} \cdot (e^{-\int_{\sigma}^{\hat{t}_2} \frac{F(l(s), N(s), f_p(s,1))}{l(s)} ds} - e^{-\int_{\sigma}^{\hat{t}_1} \frac{F(l(s), N(s), f_p(s,1))}{l(s)} ds}) d\sigma \\
&\quad + e^{(\int_{\hat{t}_1}^{\hat{t}_2} \frac{F(l(\sigma), N(\sigma), f_p(\sigma,1))}{l(\sigma)} d\sigma)} \int_{t_1}^{\hat{t}_2} \frac{\zeta N(\sigma)}{l(\sigma)} \cdot e^{-\int_{\sigma}^{\hat{t}_2} \frac{F(l(s), N(s), f_p(s,1))}{l(s)} ds} d\sigma, \quad (4.4.43)
\end{aligned}$$

where

$$D := \frac{\zeta(N_e - \varepsilon_1)}{l_e + \varepsilon_1}. \quad (4.4.44)$$

We get

$$|\hat{t}_2 - \hat{t}_1| \leq C|t_2 - t_1|. \quad (4.4.45)$$

Hence, from (4.4.38), (4.4.41) and (4.4.45), we get

$$\int_0^{\xi(t_1)} |M_p(t_2, x) - M_p(t_1, x)|^2 dx \leq C \|M_{in}^n - M_{in}\|_{L^2(0,T)}^2 + C_n |t_2 - t_1|^2. \quad (4.4.46)$$

Here and hereafter, we denote by C different constants which do not depend on x , t_1 , t_2 and n . We denote by C_n various constants which do not depend on x , t_1 and t_2 , but may depend on n .

For almost every $x \in [\xi(t_1), \xi(t_2)]$, by definition (4.4.36) of M_p , we have (see Fig 4.4.3)

$$|M_p(t_2, x) - M_p(t_1, x)| = |M_{in}(\hat{t}_2) - M_p^0(\hat{x}_1)|, \quad (4.4.47)$$

where \hat{t}_2 is defined by (4.4.40) and \hat{x}_1 are defined by

$$\hat{x}_1 = x e^{\int_0^{\hat{t}_1} \frac{F(l(\sigma), N(\sigma), f_p(\sigma,1))}{l(\sigma)} d\sigma} - \int_0^{\hat{t}_1} \frac{\zeta N(\sigma)}{l(\sigma)} \cdot e^{-\int_{\sigma}^0 \frac{F(l(s), N(s), f_p(s,1))}{l(s)} ds} d\sigma. \quad (4.4.48)$$

Noting (4.4.26) and (4.4.28), we have

$$\begin{aligned}
&\int_{\xi(t_1)}^{\xi(t_2)} |M_p(t_2, x) - M_p(t_1, x)|^2 dx \\
&\leq 2 \int_{\xi(t_1)}^{\xi(t_2)} |M_p(t_2, x)|^2 dx + 2 \int_{\xi(t_1)}^{\xi(t_2)} |M_p(t_1, x)|^2 dx \\
&= 2 \int_0^{\Gamma_2^{-1}(0)} |M_{in}(t)|^2 \cdot \frac{l(t)}{\zeta N(t)} \cdot e^{\int_t^{\hat{t}_2} \frac{F(l(\sigma), N(\sigma), f_p(\sigma,1))}{l(\sigma)} d\sigma} dt \\
&\quad + 2 \int_0^{\Gamma_1(0)} |M_p^0(x)|^2 \cdot e^{\int_0^{\hat{t}_2} \frac{F(l(\sigma), N(\sigma), f_p(\sigma,1))}{l(\sigma)} d\sigma} dx, \quad (4.4.49)
\end{aligned}$$

where Γ_1 and Γ_2 are defined by

$$\Gamma_1(s) = \xi(t_2) e^{\int_s^{t_1} \frac{F(N(\sigma), l(\sigma), f_p(\sigma, 1))}{l(\sigma)} d\sigma} - \int_s^{t_1} \frac{\zeta N(\sigma)}{l(\sigma)} \cdot e^{-\int_\sigma^s \frac{F(N(s), l(s), f_p(s, 1))}{l(s)} ds} d\sigma, \quad (4.4.50)$$

$$\Gamma_2(s) = \xi(t_1) e^{\int_s^{t_2} \frac{F(N(\sigma), l(\sigma), f_p(\sigma, 1))}{l(\sigma)} d\sigma} - \int_s^{t_2} \frac{\zeta N(\sigma)}{l(\sigma)} \cdot e^{-\int_\sigma^s \frac{F(N(s), l(s), f_p(s, 1))}{l(s)} ds} d\sigma. \quad (4.4.51)$$

From (4.4.10) and (4.4.50), we get

$$\begin{aligned} |\Gamma_1(0)| &= \left| \int_0^{t_2} \frac{\zeta N(\sigma)}{l(\sigma)} \cdot e^{\left(\int_0^{t_1} - \int_\sigma^{t_2}\right) \frac{F(N(s), l(s), f_p(s, 1))}{l(s)} ds} d\sigma \right. \\ &\quad \left. - \int_0^{t_1} \frac{\zeta N(\sigma)}{l(\sigma)} \cdot e^{-\int_\sigma^0 \frac{F(N(s), l(s), f_p(s, 1))}{l(s)} ds} d\sigma \right| \\ &\leq \int_0^{t_2} \frac{\zeta N(\sigma)}{l(\sigma)} \left| e^{\left(\int_0^{t_1} - \int_\sigma^{t_2}\right) \frac{F(N(s), l(s), f_p(s, 1))}{l(s)} ds} - e^{-\int_\sigma^0 \frac{F(N(s), l(s), f_p(s, 1))}{l(s)} ds} \right| d\sigma \\ &\quad + \int_{t_1}^{t_2} \frac{\zeta N(\sigma)}{l(\sigma)} \cdot e^{-\int_\sigma^0 \frac{F(N(s), l(s), f_p(s, 1))}{l(s)} ds} d\sigma \\ &\leq C \int_0^{t_2} \left(\int_0^{t_1} - \int_\sigma^{t_2} - \int_\sigma^0 \right) \frac{F(N(s), l(s), f_p(s, 1))}{l(s)} ds d\sigma + C|t_2 - t_1| \\ &\leq C|t_2 - t_1|. \end{aligned} \quad (4.4.52)$$

From (4.4.51), we get

$$0 = \xi(t_1) e^{\int_{\Gamma_2^{-1}(0)}^{t_2} \frac{F(N(\sigma), l(\sigma), f_p(\sigma, 1))}{l(\sigma)} d\sigma} - \int_{\Gamma_2^{-1}(0)}^{t_2} \frac{\zeta N(\sigma)}{l(\sigma)} \cdot e^{-\int_\sigma^{\Gamma_2^{-1}(0)} \frac{F(N(s), l(s), f_p(s, 1))}{l(s)} ds} d\sigma. \quad (4.4.53)$$

Hence,

$$\int_{\xi(t_1)}^{\xi(t_2)} |M_p(t_2, x) - M_p(t_1, x)|^2 dx \leq C|t_2 - t_1|. \quad (4.4.54)$$

For almost every $x \in [\xi(t_2), 1]$, by definition (4.4.36) of M_p , we have (see Fig 4.4.4)

$$|M_p(t_2, x) - M_p(t_1, x)| = |M_p^0(\hat{x}_2) - M_p^0(\hat{x}_1)|, \quad (4.4.55)$$

where \hat{x}_1 is defined by (4.4.48) and \hat{x}_2 is defined by

$$\hat{x}_2 = x e^{\int_0^{t_2} \frac{F(N(\sigma), l(\sigma), f_p(\sigma, 1))}{l(\sigma)} d\sigma} - \int_0^{t_2} \frac{\zeta N(\sigma)}{l(\sigma)} \cdot e^{-\int_\sigma^0 \frac{F(N(s), l(s), f_p(s, 1))}{l(s)} ds} d\sigma. \quad (4.4.56)$$

It is easy to get

$$|\hat{x}_2 - \hat{x}_1| \leq C|t_2 - t_1|. \quad (4.4.57)$$

For the given $M_p^0 \in L^2(0, 1)$, we let $M_p^{0n} \in C^1([0, 1])$ be such that $M_p^{0n} \rightarrow M_p^0$ in $L^2(0, 1)$.

From (4.4.55), we get

$$\begin{aligned} |M_p(t_2, x) - M_p(t_1, x)| &\leq |M_p^0(\hat{x}_2) - M_p^{0n}(\hat{x}_2)| + |M_p^{0n}(\hat{x}_2) - M_p^{0n}(\hat{x}_1)| \\ &\quad + |M_p^{0n}(\hat{x}_1) - M_p^0(\hat{x}_1)|. \end{aligned} \quad (4.4.58)$$

Noting (4.4.57), we have

$$\int_{\xi(t_2)}^1 |M_p(t_2, x) - M_p(t_1, x)|^2 dx \leq C \|M_p^{0n} - M_p^0\|_{L^2(0,1)}^2 + C_n |t_2 - t_1|^2. \quad (4.4.59)$$

Combining (4.4.46), (4.4.54) and (4.4.59), we get

$$\begin{aligned} \int_0^1 |M_p(t_2, x) - M_p(t_1, x)|^2 dx &\leq C \|M_{in}^n - M_{in}\|_{L^2(0,T)}^2 + C \|M_p^{0n} - M_p^0\|_{L^2(0,1)}^2 \\ &\quad + C_n |t_2 - t_1|^2 + C |t_2 - t_1|^2. \end{aligned} \quad (4.4.60)$$

Therefore by Lebesgue dominated convergence theorem, letting n large enough and then $|t_2 - t_1|$ small enough, the right hand side of (4.4.60) can be arbitrarily small. Thus, we get (4.4.37). This proves that the function M_p defined by (4.4.36) belongs to $C^0([0, T]; L^2(0, 1))$.

With the existence of the solution $M_p(t, x)$ for moisture equation for PFZ zone, we use the interface relation in (4.2.11) to solve the FFZ zone.

For any $s \in [0, T]$, we define the characteristic curve $\tilde{\xi}(s)$ (see Fig 4.4.5)

$$\tilde{\xi}(s) = - \int_s^0 \frac{1}{L - l(\sigma)} \left(\frac{\zeta F_d(\sigma)}{\rho_0 V_{eff}} - F(N(\sigma), l(\sigma), f_p(\sigma, 1)) \right) \cdot e^{\int_\sigma^s \frac{F(N(s), l(s), f_p(s, 1))}{L - l(s)} ds} d\sigma. \quad (4.4.61)$$

For any fixed (t, x) , when $0 \leq x \leq \tilde{\xi}(t)$ we define the characteristic curve $\tilde{\xi}_1(s)$ (see Fig 4.4.5)

$$\begin{aligned} \tilde{\xi}_1(s) &= x e^{-\int_s^t \frac{F(N(\sigma), l(\sigma), f_p(\sigma, 1))}{L - l(\sigma)} d\sigma} \\ &\quad - \int_s^t \frac{1}{L - l(\sigma)} \left(\frac{\zeta F_d(\sigma)}{\rho_0 V_{eff}} - F(N(\sigma), l(\sigma), f_p(\sigma, 1)) \right) \cdot e^{\int_\sigma^s \frac{F(N(s), l(s), f_p(s, 1))}{L - l(s)} ds} d\sigma. \end{aligned}$$

We define \tilde{t} as

$$\tilde{\xi}_1(\tilde{t}) = 0. \quad (4.4.62)$$

When $\tilde{\xi}(t) \leq x \leq 1$, we define the characteristic curve $\tilde{\xi}_3(t)$ (see Fig 4.4.5)

$$\begin{aligned} \tilde{\xi}_3(s) &= x e^{-\int_s^t \frac{F(N(\sigma), l(\sigma), f_p(\sigma, 1))}{L - l(\sigma)} d\sigma} \\ &\quad - \int_s^t \frac{1}{L - l(\sigma)} \left(\frac{\zeta F_d(\sigma)}{\rho_0 V_{eff}} - F(N(\sigma), l(\sigma), f_p(\sigma, 1)) \right) \cdot e^{\int_\sigma^s \frac{F(N(s), l(s), f_p(s, 1))}{L - l(s)} ds} d\sigma. \end{aligned}$$

We define \tilde{x} as

$$\tilde{x} := \tilde{\xi}_3(0). \quad (4.4.63)$$

Now, we construct a solution

$$M_f(t, x) = \begin{cases} M_f^0(\tilde{x}), & \tilde{\xi}(t) \leq x \leq 1, \quad t \in [0, T], \\ M_p(\tilde{t}, 1), & \text{else,} \end{cases} \quad (4.4.64)$$

where \tilde{t} and \tilde{x} are defined by (4.4.62) and (4.4.63).

By expression (4.4.64) of solution M_f , it is easy to check that $M_f \in C^0([0, T]; L^2(0, 1))$.

From (4.4.36), we get that for any fixed $t \in [0, T]$

$$\begin{aligned} \int_0^1 M_p^2(t, x) dx &\leq \int_0^1 (M_p^0(\hat{x}))^2 dx + \int_0^1 (M_{in}(\hat{t}))^2 dx \\ &= \int_0^1 (M_p^0(\hat{x}))^2 \left| \frac{\partial x}{\partial \hat{x}} \right| d\hat{x} + \int_0^T (M_{in}(\hat{t}))^2 \left| \frac{\partial x}{\partial \hat{t}} \right| d\hat{t}. \end{aligned} \quad (4.4.65)$$

By (4.4.26) and (4.4.28), we have

$$\left| \frac{\partial x}{\partial \hat{x}} \right| < 1, \quad \left| \frac{\partial x}{\partial \hat{t}} \right| < \frac{\zeta(N_e + \varepsilon_0)}{l_e - \varepsilon_0}. \quad (4.4.66)$$

Combining (4.4.65) and (4.4.66), we obtain (4.3.11). Similarly, we can obtain (4.3.13).

By the uniqueness of $(l(t), f_p(t, 1))$ which determines the characteristic curves ξ_1 , ξ_3 , $\tilde{\xi}_1$ and $\tilde{\xi}_3$, we conclude the uniqueness of M_p and M_f .

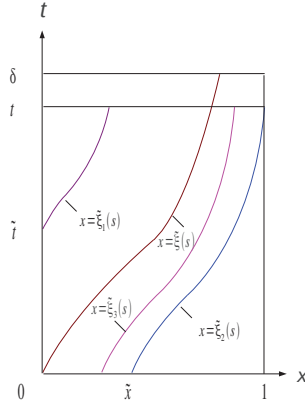


Figure 4.4.5: The characteristics $\tilde{\xi}$, $\tilde{\xi}_1$, $\tilde{\xi}_2$ and $\tilde{\xi}_3$.

4.4.4 Solving the temperature equation (4.2.12) for PFZ zone and FFZ zone

With the existence of the interface $l(t)$ and $f_p(t, 1)$, $t \in [0, \delta_1]$, using characteristic method, we construct a solution T_p as

$$T_p(t, x) = \begin{cases} T_p^0(\hat{x})e^{C_1 t} + \int_0^t e^{C_1(t-s)} \left(g_1(N(s), f_p(s, \xi_2(s))) - C_1 T_b(x, \xi_2(s)) \right) ds, & \xi(t) \leq x \leq 1, \\ T_{in}(\hat{t})e^{C_1 t} + \int_{\hat{t}}^t e^{C_1(t-s)} \left(g_1(N(s), f_p(s, \xi_1(s))) - C_1 T_b(x, \xi_1(s)) \right) ds, & \text{else,} \end{cases} \quad (4.4.67)$$

with \hat{t} and \hat{x} defined by (4.4.22) and (4.4.24).

With the existence of the solution for temperature equation for PFZ zone, we use the interface relation in (4.2.12) to solve the FFZ zone. We construct a solution T_f as

$$T_f(t, x) = \begin{cases} T_f^0(\tilde{x})e^{C_1 t} + \int_0^t e^{C_1(t-s)} \left(g_2(N(s)) - C_1 T_b(s, \tilde{\xi}_2(s)) \right) ds, & \tilde{\xi}(t) \leq x \leq 1, \\ T_p(\tilde{t}, 1)e^{C_1 t} + \int_{\tilde{t}}^t e^{C_1(t-s)} \left(g_2(N(s)) - C_1 T_b(s, \tilde{\xi}_1(s)) \right) ds, & \text{else,} \end{cases} \quad (4.4.68)$$

where \tilde{t} and \tilde{x} are defined by (4.4.62) and (4.4.63).

Similarly as we did for M_p and M_f , one can easily conclude that (4.4.67) and (4.4.68) give the unique solution of (4.2.12), together with the estimates (4.3.12) and (4.3.14).

4.5 Proof of Theorem 2

In order to conclude Theorem 4, it is sufficient to prove that $f_{p_{xx}} \in C^0([0, T]; L^2(0, 1))$. Derive the system of $f_{p_{xx}}$ and apply L^2 well-posedness for linear system.

From (4.2.10) and take derivative with respect to x in (4.2.10), we have

$$\begin{cases} \partial_t f_{p_x}(t, x) + \alpha_p(t, x) \partial_x f_{p_x}(t, x) = -\alpha_{p_x} f_{p_x}(t, x), & (t, x) \in Q \\ f_{p_x}(0, x) = f_{p_x}^0(x), & x \in (0, 1) \\ f_{p_x}(t, 0) = \frac{-l(t)}{\zeta N(t)} \cdot \frac{F'_{in}(t)\theta(N(t)) - F_{in}(t)\theta'(N(t))N'(t)}{\theta^2(N(t))}, & t \in (0, T) \end{cases} \quad (4.5.1)$$

Similarly to the proof of Theorem 3, when $t \in [0, \delta]$, with δ defined by (4.4.11), we have

$$f_{p_x}(t, x) = \begin{cases} \frac{-l(\hat{t})}{\zeta N(\hat{t})} \cdot \frac{F'_{in}(\hat{t})\theta(N(\hat{t})) - F_{in}(\hat{t})\theta'(N(\hat{t}))N'(\hat{t})}{\theta^2(N(\hat{t}))} \cdot e^{\int_{\hat{t}}^t \frac{F(l(s), N(s), f_p(s, 1))}{l(s)} ds}, & 0 \leq x \leq \xi(t), \\ f_{p_x}^0(\hat{x}) \cdot e^{\int_0^t \frac{F(l(s), N(s), f_p(s, 1))}{l(s)} ds}, & \xi(t) \leq x \leq 1, \end{cases} \quad (4.5.2)$$

where \hat{t} and \hat{x} are defined by (5.2.14) and (4.4.24).

Since H^2 can be embedded in $W^{1, \infty}$, in order to prove Theorem 4, we only have to prove $f_{p_{xx}}(t, \cdot) \in L^2(0, 1)$ for any given $t \in [0, \delta]$. From (4.5.2), we have

$$\begin{aligned} & \int_0^1 |f_{p_{xx}}(t, x)|^2 dx \\ & \leq 2 \int_0^1 \left| \frac{d}{d\hat{t}} \left(\frac{l(\hat{t})}{\zeta N(\hat{t})} \cdot \frac{d}{d\hat{t}} \left(\frac{F_{in}(\hat{t})}{\theta(N(\hat{t}))} \right) \cdot e^{\int_{\hat{t}}^t \frac{F(l(s), N(s), f_p(s, 1))}{l(s)} ds} \right) \frac{\partial \hat{t}}{\partial x} \right|^2 dx \end{aligned} \quad (4.5.3)$$

$$+ 2 \int_0^1 \left| \frac{d}{d\hat{x}} \left(f_{p_x}^0(\hat{x}) \cdot e^{\int_0^t \frac{F(l(s), N(s), f_p(s, 1))}{l(s)} ds} \right) \frac{\partial \hat{x}}{\partial x} \right|^2 dx. \quad (4.5.4)$$

Concerning (4.5.4), by (4.4.28), we have

$$\begin{aligned} & 2 \int_0^1 \left| \frac{d}{d\hat{x}} \left(f_{p_x}^0(\hat{x}) \cdot e^{\int_0^t \frac{F(l(s), N(s), f_p(s, 1))}{l(s)} ds} \right) \frac{\partial \hat{x}}{\partial x} \right|^2 dx \\ & = 2e^4 \int_0^t \frac{F(l(s), N(s), f_p(s, 1))}{l(s)} ds \int_0^1 |f_{p_{xx}}^0(\hat{x})|^2 dx \\ & = 2e^3 \int_0^t \frac{F(l(s), N(s), f_p(s, 1))}{l(s)} ds \int_0^1 |f_{p_{xx}}^0(\hat{x})|^2 d\hat{x} \\ & \leq 2e^{\frac{3\delta \|F\|_{W^{1, \infty}}}{l_{e-\varepsilon}}} \|f_p^0(t, \cdot)\|_{H^2(0, 1)}^2. \end{aligned} \quad (4.5.5)$$

Concerning (4.5.3), by (4.4.26), we get

$$\begin{aligned}
& 2 \int_0^1 \left| \frac{d}{d\hat{t}} \left(\frac{l(\hat{t})}{\zeta N(\hat{t})} \cdot \frac{d}{d\hat{t}} \left(\frac{F_{in}(\hat{t})}{\theta(N(\hat{t}))} \right) \cdot e^{\int_{\hat{t}}^t \frac{F(l(s), N(s), f_p(s, 1))}{l(s)} ds} \right) \frac{\partial \hat{t}}{\partial x} \right|^2 dx \\
& \leq \frac{2(l_e + \varepsilon)}{\zeta(N_e - \varepsilon)} \int_0^\delta \left| \frac{d}{d\hat{t}} \left(\frac{l(\hat{t})}{\zeta N(\hat{t})} \cdot \frac{d}{d\hat{t}} \left(\frac{F_{in}(\hat{t})}{\theta(N(\hat{t}))} \right) \cdot e^{\int_{\hat{t}}^t \frac{F(l(s), N(s), f_p(s, 1))}{l(s)} ds} \right) \right|^2 d\hat{t} \\
& = \frac{6(l_e + \varepsilon)}{\zeta(N_e - \varepsilon)} \left\{ \int_0^\delta \left| \frac{d}{d\hat{t}} \left(\frac{l(\hat{t})}{\zeta N(\hat{t})} \right) \cdot \frac{d}{d\hat{t}} \left(\frac{F_{in}(\hat{t})}{\theta(N(\hat{t}))} \right) \cdot e^{\int_{\hat{t}}^t \frac{F(l(s), N(s), f_p(s, 1))}{l(s)} ds} \right|^2 d\hat{t} \right. \\
& \quad + \int_0^\delta \left| \frac{l(\hat{t})}{\zeta N(\hat{t})} \cdot \frac{d^2}{d\hat{t}^2} \left(\frac{F_{in}(\hat{t})}{\theta(N(\hat{t}))} \right) \cdot e^{\int_{\hat{t}}^t \frac{F(l(s), N(s), f_p(s, 1))}{l(s)} ds} \right|^2 d\hat{t} \\
& \quad \left. + \int_0^\delta \left| \frac{l(\hat{t})}{\zeta N(\hat{t})} \cdot \frac{d}{d\hat{t}} \left(\frac{F_{in}(\hat{t})}{\theta(N(\hat{t}))} \right) \cdot e^{\int_{\hat{t}}^t \frac{F(l(s), N(s), f_p(s, 1))}{l(s)} ds} \cdot \frac{F(l(\hat{t}), N(\hat{t}), f_p(\hat{t}, 1))}{l(\hat{t})} \right|^2 d\hat{t} \right\} \\
& \leq \frac{6(l_e + \varepsilon)}{\zeta(N_e - \varepsilon)} \left\{ \frac{2(\|l\|_{W^{1,\infty}}^2 N_1^2 + (l_e + \varepsilon)^2 \|N\|_{W^{1,\infty}}^2)}{\zeta^2 N_0^4} \cdot e^{\frac{2\delta \|F\|_{W^{1,\infty}}}{l_e - \varepsilon}} \cdot \left\| \frac{F_{in}(\cdot)}{\theta(N(\cdot))} \right\|_{H^2(0,T)}^2 \right. \\
& \quad + \frac{(l_e + \varepsilon)^2}{\zeta^2 N_0^2} \cdot e^{\frac{2\delta \|F\|_{W^{1,\infty}}}{l_e - \varepsilon}} \cdot \left\| \frac{F_{in}(\cdot)}{\theta(N(\cdot))} \right\|_{H^2(0,T)}^2 \\
& \quad \left. + \frac{(l_e + \varepsilon)^2}{\zeta^2 N_0^2} \cdot \frac{\|F\|_{W^{1,\infty}}^2}{(l_e - \varepsilon)^2} \cdot e^{\frac{2\delta \|F\|_{W^{1,\infty}}}{l_e - \varepsilon}} \cdot \left\| \frac{F_{in}(\cdot)}{\theta(N(\cdot))} \right\|_{H^2(0,T)}^2 \right\} \\
& = \frac{6(l_e + \varepsilon)}{\zeta^3 N_0^3} \cdot e^{\frac{2\delta \|F\|_{W^{1,\infty}}}{l_e - \varepsilon}} \cdot \left\| \frac{F_{in}(\cdot)}{\theta(N(\cdot))} \right\|_{H^2(0,T)}^2 \left\{ \frac{2(\|l\|_{W^{1,\infty}}^2 N_1^2 + (l_e + \varepsilon)^2 \|N\|_{W^{1,\infty}}^2)}{N_0^2} \right. \\
& \quad \left. + (l_e + \varepsilon)^2 \left(1 + \frac{\|F\|_{W^{1,\infty}}^2}{(l_e - \varepsilon)^2} \right) \right\}. \tag{4.5.6}
\end{aligned}$$

Combining (4.5.3), (4.5.4), (4.5.5) and (4.5.6), we get $f_{p_{xx}}(t, \cdot) \in L^2(0, 1)$ for any given $t \in [0, \delta]$. The proof is complete. \square

4.6 Conclusion

In this chapter we perform an mathematical analysis of coupled transport equations which are defined in complementary time varying domains. The goal of the analysis is to prove the well-posedness of this class of system. The *Partially Filled Zone* equations are characterized by a time-varying velocity which is a function of the screw speed $N(t)$. In the *Fully Filled Zone* the convection velocity is strongly related to the interface properties by its dependence on die net flow rate $F_d(t)$. We approach this problem by performing a change of coordinates which consists to express the system in a fixed domain $(0, 1)$. This transformation generates fictive convective terms in the transport operator. By contraction mapping principle (Banach fixed point theorem), we prove the existence and uniqueness of $l(t)$ and $f_p(t; 1)$ for t small. With the existence of $l(t)$ and $f_p(t; 1)$, we then construct a local solution to Cauchy problem. By an iterative method we extend the results to the existence and the uniqueness of semi-global solution. The solution we obtained in *Theorem 3* and *Theorem 4* is called semi-global solution since it exists on any preassigned time interval $[0; T]$ if the initial and boundary data has some kind of smallness (depending on T). We point out that the assumption of constant viscosity

allows to release the strong coupling relation between the equation of e mass, moisture and energy balances. The coupled system which is composed by the transport equation of the filling ratio and the interface motion equation is in a sense a free boundary problem which can be treated independently. Here the free boundary dynamic is a function of the difference of pressure $\Delta P(t)$ and it evolves independently from the energy and moisture balances. Ours future works in the context of well-posedness and moving interface problems will deal with this extrusion process model with distributed viscosity and pressure continuity relation at the interface.

4.7 Acknowledgements

This work is done in collaboration with:

- Peipei SHANG, Department of Mathematics, Tongji University, Shanghai 200092, China,
- Zhiqiang WANG, School of Mathematical Sciences, Fudan University, Shanghai 200433, China.

The authors would like to thank Professor Jean-Michel Coron (Laboratoire Jacques-Louis Lions Université Pierre et Marie Curie 4, place Jussieu 75005 Paris France) for his helpful comments and constant support.

Chapter 5

Mass transport equation with moving interface and its control as an input delay system

5.1 Introduction

In this part we address the problem of the stabilization of the position of the moving interface given by the equation (3.3.7) thanks to the inlet flow rate acting on the boundary of the transport equation of the *Partially Filled Zone* (3.5.11). The control input does not appears directly in (3.3.7) but it appears with a delay depending on the position of the moving interface through the filling ratio $f_p(l(t), t)$. So we propose to tackle the problem as a time input delay system control problem.

So far the control oriented models of extruders are issued from some black box linear model identification around some operating conditions. Following the objectives of the control and the choice of the manipulated variables these models can be time delay linear MIMO or SISO models [105, 108, 145, 118, 58]. These time delays are due to time delays associated with the off line measurements of key product properties, non physical time delays due to approximation of nonlinear dynamics and in some case due to the transport of the matter in the extruder [105]. These time delays are always assumed to be constant. In some sense the basic nature of the extruders: the two-zone model is never exploited. We leave the reader refer to the introduction of **Chapter 3** to have more details about the control strategy used for these extrusion processes.

Time delay systems are not commonly used in chemical engineering even if the dynamic models of many chemical engineering processes involve significant time delays due to transportation lag such as the example treated in [39] of two chemical reactors represented as continuous stirred tank reactors with recycle loop. Others examples can be found in [12, 151, 152, 31]. For spatially distributed parameter systems, some authors treats the regulation problem of

convection governed dynamical processes described by linear first order partial differential equations by using the method of characteristics(MC) in order to transform the PDEs into a set of time delayed ordinary differential equations [65, 125, 4, 3].

Research on time delay systems initially focused on open-loop stable linear systems with a single manipulated input delay which are described by transfer function models, in which the presence of the time delay prevents the use of large controller gains. To overcome the destabilizing effect of the high gain, Smith [128] proposed in 1957 a control structure, known as the Smith predictor that permits to improve the control performance; it completely eliminates the time delay from the characteristic equation of the closed-loop system, allowing the use of larger controller gains.

Various controllers have been developed to address time-delay induced performance and stability issues as described in the survey paper [121]. Delay systems can be controlled in different manners using methods based on an algebraic Riccati approach (where stability conditions are expressed by the solvability of a Riccati equation or by the feasibility of a linear matrix inequality) [97, 153], sliding mode controllers [53, 64, 63, 154, 129, 74, 101] or variants of the Smith predictor [128, 96, 15, 55, 72, 19].

For the problem under consideration we will have to deal with the class of the input delay systems more precisely the class of state dependent input delay systems. The approach chosen for the synthesis of the control is based on the works proposed in [19, 20] for state dependent input delay systems using a predictor.

5.1.1 Organization of the chapter

This chapter is organized as follow: in section 5.2 the system formed by the transport PDE coupled with the ODE of the moving boundary is transformed into a state dependent input delay system. In section 5.3 we propose a rapid overview of the predictor based controllers for input delay systems. The design of the controller is described in section 5.4. Simulation results are proposed in section 5.5. Finally concluding remarks are established in section 5.6.

5.1.2 Contribution

This chapter is dedicated to the control of 1D hyperbolic partial differential equation with moving interface as a delay system. The model derives from the mass balance of the extrusion process that describes the strong coupling between the mass transport equation and an ordinary differential equation which represents the interface motion. Solving the transport equation of filling ratio by the method of characteristics , we obtain an state-dependent-input-delay control problem. The stabilization of the system around an equilibrium is done by using a state predictor.

5.2 From transport equation to delay system for the extrusion process

The main idea in this section is to define a delay system from the model given by equations (3.5.11) and (3.3.7). Our aim is to solve the hyperbolic partial differential equation by the method of characteristics and to express the solution as a function of the boundary inflow data. The delay represents the propagation time of the matter from the boundary $\{x = 0\}$ to the interface $\{x = l(t)\}$ due to the screw speed. The solution is injected in the equation (5.2.2) in order to obtain a delay system. This computation leads to a nonlinear scalar state dependent input system depending on the interface position $l(t)$.

5.2.1 Mass conservation equations in an extrusion process

In *Chapter 3* we have presented the model of the extrusion process considering an homogeneous melt which is convected from the feed to the die by screw rotation.

The modelling of the extruder makes appear two geometric zones in which the matter flows at different velocities. These two zones are separated by an moving interface whose dynamics is given by an ordinary differential equation expressing the mass balance in the *Fully Filled Zone*.

In this section we recall the mass transport model of homogeneous material in the PFZ given by equation (3.3.7) as well as the total mass balance in the FFZ gives rise to the moving interface dynamics (3.5.11).

The PFZ is defined in $[0, l(t)[$ and the FFZ in $]l(t), L]$ (where L represents the extruder length and $l(t)$ the interface position).

- Considering the filling ratio $f_p(x, t)$ as the distributed variable, the PFZ mass balance leads to a transport equation whose velocity is determined by the screw speed $N(t)$ and the equivalent pitch ξ of the screw. Under the flow continuity assumption at $\{x = 0\}$, one can express the boundary filling ratio in terms of the PFZ convective velocity $\xi N(t)$, the available volume V_{eff} , the material feed rate $F_{in}(t)$ and the mass density ρ_0 .

$$\begin{cases} \frac{\partial f_p}{\partial t}(x, t) = -\xi N(t) \frac{\partial f_p}{\partial x}(x, t) & x \in [0, l(t)[\\ f_p(0, t) = f_p^{in}(t) = \frac{F_{in}(t)}{\rho_0 \xi N(t) V_{eff}} \end{cases} \quad (5.2.1)$$

- In the FFZ, the velocity of the convection is determined by the net flow at the die $F_d(t)$. The FFZ mass balance is associated to the motion of the moving interface $l(t)$ between there two zones:

$$\begin{cases} \frac{dl(t)}{dt} = \frac{F_d(t) - \rho_0 N(t) V_{eff} f_p(l(t), t)}{\rho_0 S_{eff} (1 - f_p(l(t), t))} \\ l(0) = l^0 \quad 0 < l^0 < L, \end{cases} \quad (5.2.2)$$

where L is the extruder length. $F_d(t)$, the net flow at the die is a function of the geometric characteristics of the die K_d , the constant viscosity η and the pressure build-up in this zone $P(x, t)$.

$$\begin{cases} F_d(t) = \frac{K_d}{\eta} \Delta P(t) \\ \Delta P(t) = (P(L, t) - P_0), \end{cases} \quad (5.2.3)$$

where P_0 is the air pressure.

5.2.2 Recalling the formulation of coupling relations at $l(t)$

As it is described in *Chapter 3* the coupling relation between the two zones ($PFZ - l(t) - FFZ$) can be formulated in two ways:

1. The first one is a flux coupling relation (3.5.14) and derives from the continuity of the momentum flux and allows to express the die pressure $P(L, t)$ as a function of $N(t)$, $l(t)$, and $f_p(l(t), t)$:

$$\Delta P(t) = \frac{-[1 + \frac{K_d}{B\rho_0}(L - l(t))] + \sqrt{\Delta}}{\frac{2K_d^2}{\eta^2 \rho_0 S_{eff}^2}} \quad (5.2.4)$$

with

$$\Delta = [1 + \frac{K_d}{B\rho_0}(L - l(t))]^2 + \Omega_3(f_p(l(t), t), N(t), l(t))$$

and

$$\begin{aligned} \Omega_3 = & \left(\frac{2K_d}{\eta S_{eff}} \right)^2 \left(\frac{\eta V_{eff} N(t)}{B\rho_0} (L - l(t)) \right. \\ & \left. + (\xi^2 N^2(t) + \frac{P_0}{\rho_0}) f_p(l(t), t) - \frac{P_0}{\rho_0} \right) \end{aligned} \quad (5.2.5)$$

2. the second one is a state coupling relation and derives from the continuity of the pressure at the interface $l(t)$ ($P(l^-, t) = P(l^+, t) = P_0$), then:

$$\Delta P(t) = \frac{\eta V_{eff} N(t) \rho_0 (L - l(t))}{(B\rho_0 + K_d(L - l(t)))} \quad (5.2.6)$$

Recall that the main assumption of this modelling point of view is the existence of two zones PFZ and FFZ to make appear the interface dynamics. This property is preserved if and only if $\Delta P(t)$ is strictly positive. It means that the output flow at the die $F_d(t)$ must be a positive quantity. This constraint implies by the following inequalities:

- For continuous momentum flux at $l(t)$

$$\Omega_3(f_p(l(t), t), N(t), l(t)) > 0 \quad (5.2.7)$$

Then a critical value of the filling ratio at the interface coupling is defined as $f_{pc}(l(t), t)$. Its expression is recalled here (3.5.18):

$$f_{pc}(l(t), t) > \frac{P_0 - \frac{\eta V_{eff} N(t)}{B} (L - l(t))}{\rho_0 \xi^2 N^2(t) + P_0} \quad (5.2.8)$$

For a given function $N(t)$, one can define the set $(f_p(l(t), t), l(t))$ which satisfies the constraint (5.2.8).

- For continuous pressure at $l(t)$ there is no constraint because the positivity condition on $\Delta P(L, t)$ is always satisfied ($L > l(t)$).

5.2.3 Transport equation solution

Consider the first order linear transport equation (5.2.1) in the two variables t and x with the boundary condition $f_p(0, t)$.

The total derivative with respect to some variable τ can be written as:

$$\frac{df_p(x(\tau), t)}{d\tau} = \frac{dt}{d\tau} \frac{\partial f_p(x(\tau), t)}{\partial t} + \frac{dx(\tau)}{d\tau} \frac{\partial f_p(x(\tau), t)}{\partial x}$$

Defining the solution along the characteristic curves, we have:

$$\begin{cases} \frac{dt}{d\tau} = 1 \\ \frac{dx(\tau)}{d\tau} = \xi N(t) \\ \frac{df_p(x(\tau), t)}{d\tau} = 0 \end{cases} \quad (5.2.9)$$

The last equation is deduced from equation (5.2.1) and $f_p(x(\tau), t)$ is a constant function along the characteristics.

Since $N(t)$ is an unknown function of t , the system (5.2.9) cannot be explicitly solved. Integrating the characteristics equations

$$\begin{pmatrix} x_1 & x_2 & x_3 \end{pmatrix} = \begin{pmatrix} t & x & f_p \end{pmatrix} \in \mathbb{R}^3$$

we obtain:

$$\begin{cases} x_1(\tau, s) = \tau + s \\ x_2(\tau, s) = \xi \int_s^{\tau+s} N(\tau') d\tau' \\ x_3(s) = f_p(s) \end{cases} \quad (5.2.10)$$

Where s is the constant of integration. Let us introduce $\bar{N}(t)$ as the primitive function of $N(t)$. It is obvious that:

$$\bar{N}(s) = \bar{N}(\tau + s) - \frac{x_2}{\xi} \quad (5.2.11)$$

Using equation (5.2.10) the following equality is deduced:

$$s = \bar{N}^{-1}\left(\bar{N}(t) - \frac{x}{\xi}\right) \quad (5.2.12)$$

Any function which is constant along the characteristic curves can be expressed as:

$$f_p(x, t) = f_p\left(\bar{N}^{-1}\left(\bar{N}(t) - \frac{x}{\xi}\right)\right) \quad (5.2.13)$$

To find the solution that satisfies the prescribed boundary conditions (5.2.1), we substitute the general solution formula and obtain:

$$f_p(x, t) = f_p^{in}\left(\bar{N}^{-1}\left(\bar{N}(t) - \frac{x}{\xi}\right)\right) \quad (5.2.14)$$

Recall that we assume the flow continuity at $\{x = 0\}$. Thus, the input filling ratio $f_p^{in}(t)$ which is the boundary condition can be deduced from the feed rate $F_{in}(t)$, we obtain:

$$f_p^{in}\left(\bar{N}^{-1}\left(\bar{N}(t) - \frac{x}{\xi}\right)\right) = \frac{F_{in}\left(\bar{N}^{-1}\left(\bar{N}(t) - \frac{x}{\xi}\right)\right)}{\rho_0 N(t) V_{eff}}, \quad (5.2.15)$$

Where ρ_0 is the mass density and V_{eff} the effective volume.

5.2.4 State dependent input delay system for the extruder model

In the following we assume that the screw speed is constant $N(t) = N_0$. The control problem consists to stabilize the interface position by a feedback on the "abstract" input variable f_p^{in} which depends on the feed rate (5.2.15). We find:

$$\begin{cases} f_p(x, t) = f_p^{in}\left(t - \frac{x}{N_0 \xi}\right) \\ f_p(l(t), t) = f_p^{in}\left(t - \frac{l(t)}{N_0 \xi}\right), \end{cases} \quad (5.2.16)$$

and this simplification results to the following system:

$$\begin{cases} \frac{dl(t)}{dt} = \frac{F_d(t) - \rho_0 N_0 V_{eff} f_p^{in}\left(t - \frac{l(t)}{N_0 \xi}\right)}{\rho_0 S_{eff} \left[1 - f_p^{in}\left(t - \frac{l(t)}{N_0 \xi}\right)\right]} \\ F_d(t) = \frac{K_d}{\eta} \Delta P(t) \end{cases} \quad (5.2.17)$$

Now, it becomes clear that equation (5.2.17) defines a nonlinear state dependent input delay system which can be written in the abstract form:

$$\begin{cases} \frac{dl(t)}{dt} = f(l(t), U(t - D(l(t)))) \\ U(t) = f_p^{in}(t) \end{cases} \quad (5.2.18)$$

Where f is the nonlinear function and $D(l(t))$ the delay function depending in the state variable and acting on the input function $U(t)$. As it will be presented in section 5.3.3,

[19, 20] solve the regional stabilization of this class of problem using a predictor with an horizon depending on the future value of the state. The stability around the equilibrium is ensured for small variations of the initial conditions of the state and the input when the delay is large. The section 5.3 is dedicated to the general review of predictor-based controllers in the cases of constant input delay, varying input delay and finally state dependent input delay.

5.3 Generality on predictor-based controllers

5.3.1 Predictor-based controllers for constant input delay systems

As already mentioned the predictor-based controllers were first introduced for linear system by Smith [128] in the frequency domain and later in the state space representation by [96, 15]. These latter references use the terms finite spectrum assignment (FSA) and model reduction respectively to represent the modified Smith predictor. These extensions offer more possibilities on stability issues since they work for unstable systems contrary to the Smith predictor.

We present first the philosophy of such modified Smith predictors.

We consider a linear system with constant input time-delay D as (5.3.1):

$$\dot{X}(t) = AX(t) + BU(t - D) \quad X \in \mathbb{R}^n \quad U \in \mathbb{R}^m \quad (5.3.1)$$

The important point here is that the knowledge of an initial data as $X(t_0)$ and the future inputs U is not sufficient to compute the future dynamics of the state $X(t)$. One should complete the system by defining the input $U(t)$ over the history window $[t_0 - D, t_0]$. Supposing that this system (5.3.1) is controllable and introducing $K \in \mathbb{R}^{m \times n}$ as vector gain which stabilizes the free-delay system $\dot{X}(t) = AX(t) + BU(t)$ (by static state feedback), one can build the predictor which guaranteed the stability of the delayed system. A modification of the classical Smith predictor scheme allows to compensate the delay D by introducing control law which makes the system free of delay. This control law is defined by the following equation:

$$U(t) = KX(t + D) \quad X \in \mathbb{R}^n \quad X \in \mathbb{R}^m \quad (5.3.2)$$

This alternative feedback allows to transform the delayed system (5.3.1) to an free-delay system after a dead-time D as it is represented here:

$$\dot{X}(t) = (A + BK)X(t) \quad (5.3.3)$$

This equivalence is achieved if one can predict the value of the state at time $(t + D)$. This prediction is obtained by integrating (5.3.1) from an initial condition given by the current state vector $X(t)$:

$$X(t + D) = e^{AD} X(t) - \int_{t-D}^t e^{A(t-\tau)} BU(\tau) d\tau \quad \forall t > t_0 \quad (5.3.4)$$

It follows that the corresponding feedback law is given by the relation 5.3.4:

$$U(t) = K \left[e^{AD} X(t) - \int_{t-D}^t e^{A(t-\tau)} BU(\tau) d\tau \right] \quad \forall t > t_0 \quad (5.3.5)$$

Knowing the input along the delay interval $[t - D; t]$, it becomes easy to compute the integral term $\int_{t-D}^t e^{A(t-\tau)} BU(\tau) d\tau$ and to design this infinite dimensional feedback law (5.3.5).

The numerical approximation of the integral term should be done carefully to guarantee the stability when the controller is implemented [103].

So the feedback law (5.3.5) for the system (5.3.1) determines the so called FSA method since the spectrum of the closed loop system coincides with the spectrum of the matrix $A + BK$.

Considering the predicted state determined by equation (5.3.4):

$$\mathcal{P}(t) = X(t + D) \quad (5.3.6)$$

One easily deduces the predictor that obeys to an free-delay system with its associated feedback as:

$$\begin{cases} \dot{\mathcal{P}}(t) = A\mathcal{P}(t) + BU(t) \\ U(t) = K\mathcal{P}(t) \end{cases} \quad (5.3.7)$$

This framework corresponds to the reduction model approach.

The predictor (5.3.6) can be extended to nonlinear systems. We present here the result as proposed in [82, 84]. We consider systems of the form:

$$\dot{X}(t) = f(X(t), U(t - D)) \quad (5.3.8)$$

In [84] the author defined the predictor for nonlinear forward-complete systems, namely, systems such that have bounded solutions and a suitable continuous gain function for any bounded input function $U(t)$.

The construction of the feedback predictor-based control law for nonlinear system with constant input delay follows the same method as previously. The controlled free-delay nonlinear system (5.3.9) is supposed to be globally asymptotically stable by a feedback law given by equation (5.3.10):

$$\dot{X}(t) = f(X(t), U(t)) \quad (5.3.9)$$

$$U(t) = \kappa(X(t)) \quad (5.3.10)$$

The delay compensation is then guaranteed by the predictor-based control law:

$$\begin{cases} U(t) = \kappa(\mathcal{P}(t)) \\ \mathcal{P}(t) = X(t) + \int_{t-D}^t f(\mathcal{P}(\tau), U(\tau))d\tau \end{cases} \quad (5.3.11)$$

This control law is implicit but it is computable.

5.3.2 Predictor design for time-varying delay

The study of time-varying delay system is performed for state dependent delay and few results are proposed for the input delay cases [30]. [109] proposes a parameter-adaptive design in very particular cases of scalar system which a known time varying input delay. In [110], a general result based on an explicit state-feedback control law for linear time-invariant (LTI) plants with time-varying input delays was presented. But no analysis of stability or feasibility of controller are performed. In the context of Network Controlled Systems (NCS), [150, 149, 148] propose the control design of a particular case of linear system with time varying input delay. The authors consider an internal delay dynamics representing the transmission channel model and implement a predictor-based controller.

There exist few papers that deal with the compensation of time-varying input delay in nonlinear systems [77, 83, 59]. In [59], the control design approach is based on state prediction computation and the overall method is illustrated on an example of water flow control in open-channel systems.

The key idea in this case is that the state prediction is calculated over a time-varying window starting with the current state as an initial condition and taking into account the future values of the delay.

As in [110, 83] we consider the following linear system:

$$\dot{X}(t) = AX(t) + BU(\phi(t)) \quad X \in \mathbb{R}^n \quad (5.3.12)$$

U is the input and $\phi(t)$ a continuous function which contains the delay. The predictor based controller is build under the following assumptions:

- $\phi(t)$ is a differentiable function that satisfies $\dot{\phi}(t)$ is strictly upper-bounded.

with these assumptions that guarantee the causality of the system (5.3.12) and the invertibility of $\phi(t)$, the predictor-based controller is generated by introducing the closed loop system :

$$\begin{cases} \dot{X}(t) = AX(t) + BU(\phi(t)) \\ U(\phi(t)) = KX(t) \quad \forall \phi(t) \geq 0 \end{cases} \quad (5.3.13)$$

Consequently, the system (5.3.12) is rewritten as:

$$\dot{X}(t) = (A + BK)X(t) \quad \forall \phi(t) \geq 0 \quad (5.3.14)$$

where the gain vector K is chosen to ensure the convergence of the closed loop system. The control law can be written using the inverse of $\phi(t)$ as:

$$U(t) = KX(\phi^{-1}(t)) \quad \forall t \geq 0 \quad (5.3.15)$$

Using integration formula on equation (5.3.12) we obtain for $\phi(t) \leq \theta \leq t$:

$$X(\phi^{-1}(t)) = e^{A(\phi^{-1}(t)-t)}X(t) + \int_t^{\phi^{-1}(t)} e^{A(\phi^{-1}(t)-\tau)}BU(\phi(\tau))d\tau \quad (5.3.16)$$

or equivalently by introducing the change of coordinates $\mu = \phi(\tau)$:

$$X(\phi^{-1}(t)) = e^{A(\phi^{-1}(t)-t)}X(t) + \int_{\phi(t)}^t e^{A(\phi^{-1}(t)-\phi^{-1}(\mu))}B\frac{U(\mu)}{\phi'[\phi^{-1}(\mu)]}d\mu \quad (5.3.17)$$

Replacing (5.3.17) in the control law (5.3.15), it follows that :

$$U(t) = K \left[e^{A(\phi^{-1}(t)-t)}X(t) + \int_{\phi(t)}^t e^{A(\phi^{-1}(t)-\phi^{-1}(\mu))}B\frac{U(\mu)}{\phi'[\phi^{-1}(\mu)]}d\mu \right] \quad (5.3.18)$$

Equation (5.3.18) is the predictor feedback of the time-varying input delay (5.3.12) with the predicted state given by equation (5.3.17): $P(t) = X(\phi^{-1}(t))$.

Remark 12. In can be noted that the exponential stability of the feedback system with the predictor controller proposed in [110] is proven in [83]. The proof lays on the construction of a Lyapunov functional using a backstepping transformation with time varying kernels, and transforming the actuator state into a transport partial differential equation with a convection speed coefficient that varies with both space and time.

Prediction of the state of a time varying delay system is very complicated. It necessitates future values of the delay for the horizon $[t, \phi^{-1}(t)]$ that may be not available. Some methodology to compute this horizon is proposed in [18] when the delay evolution is known.

5.3.3 Predictor design for state-dependent input delay system

The first results on the stabilization of a state-dependent input delay linear and nonlinear systems are proposed in [19, 20]. These papers are an extension of the works on time varying delay systems (see section 5.3.2).

The predictor-based compensator is designed for a particular class of nonlinear systems which are, in the absence of the input delay, either forward complete and globally or locally stabilizable (by a possible time-varying control law). Again the controller uses predictions of future values of the state on appropriate prediction horizons that depend on the current values of the state. Only a regional stability result, is obtained even for the case of forward-complete systems. Also, an estimate of the region of attraction for a control scheme based on the construction of a strict, time-varying Lyapunov functional is determined.

The global result is achieved for forward-complete systems under a restrictive Lyapunov-like condition, which has to be verified. This feasibility condition \mathcal{F}_c (5.3.31), is that the delay rate must be bounded by unity irrespective of the values of the state and input. This condition corresponds to the upper bounded condition established for time varying input delay system. In this context, the control signal never reaches the plant if the delay rate is larger than one.

We present the predictor for the state dependent input delay nonlinear system [19, 20].

Consider the system which is governed by the following nonlinear equation:

$$\dot{X}(t) = f(X(t), U(t - D(X(t)))) \text{ with } f(0, 0) = 0 \quad (5.3.19)$$

where $X \in \mathbb{R}^n$; $U : [t_0 - D(X(t_0)), \infty[\rightarrow \mathbb{R}^n$; $t > t_0 > 0$ $D \in C^1(\mathbb{R}^n; \mathbb{R}^+)$.

$f : (\mathbb{R}^n; \mathbb{R}^+) \rightarrow \mathbb{R}^n$ is assumed to be locally Lipschitz and the following holds:

$$|f(X(t), \omega)| \leq \alpha_1(|X| + |\omega|) \quad (5.3.20)$$

Where α_1 is a class \mathcal{K}_∞ function*.

The state predictor is given by:

$$\mathcal{P}(t) = X(t + D(\mathcal{P}(t))) \quad (5.3.21)$$

Indeed the predictor $\mathcal{P}(t)$ is associated to the value of the state at the time when the applied control reaches the system. This time is itself depending on the state at this time, so $\mathcal{P}(t)$. The existence of this implicit relation makes the problem completely different from the case of system with independent time varying delay function as it is exposed previously.

The key of the resolution in [19, 20], is based on the transformations of the time variable $t \rightarrow t + D(\mathcal{P}(t))$ and $t \rightarrow t - D(X(t))$. The predictor-based controller is given by the following relation:

$$U(t) = \kappa(\sigma(t), \mathcal{P}(t)) \quad (5.3.22)$$

where for all $t - D(X(t)) < \tau < t$ and $t > t_0$:

$$\mathcal{P}(\tau) = X(t) + \int_{t-D(X(t))}^{\tau} \frac{f(\mathcal{P}(\mu), U(\mu))}{1 - \nabla D(\mathcal{P}(\mu))f(\mathcal{P}(\mu), U(\mu))} d\mu \quad (5.3.23)$$

with the prediction time

$$\sigma(\mu) = \mu + D(\mathcal{P}(\mu)) \quad (5.3.24)$$

The initial predictor $\mathcal{P}(\tau)$ is given by (5.3.23) for $t = t_0$ and $\tau \in [t_0 - D(X(t_0)); t_0]$. Analyzing the initial predictor for $\tau = t_0 - D(X(t_0))$, one deduce that:

$$\mathcal{P}(t_0 - D(X(t_0))) = X(t_0) \quad (5.3.25)$$

*a continuous function $\alpha : [0, a) \rightarrow [0, \infty)$ is said to belong to class \mathcal{K}_∞ if $a = \infty$ and $\alpha(r) \rightarrow \infty$ as $r \rightarrow \infty$

This condition means that at the initial time the predictor fits perfectly with the initial state argument.

The fact that $\mathcal{P}(t)$ as given in (5.3.23) is the $\sigma(t) - t = D(\mathcal{P}(t))$ time units ahead predictor of $X(t)$ can be seen performing the following coordinates change:

$$\begin{cases} \phi(t) = t - D(X(t)) \\ \phi^{-1}(\tau) = \sigma(\tau) \quad \forall \tau \in [t - D(X(t)), t] \end{cases} \quad (5.3.26)$$

Equation (5.3.25) is rewritten as:

$$\mathcal{P}(\phi(t_0)) = X(t_0) \quad (5.3.27)$$

Applying ϕ^{-1} to the equation above one obtains:

$$\mathcal{P}(t_0) = X(\sigma(t_0)) \quad (5.3.28)$$

Then for $t > t_0$, the following equality holds:

$$\mathcal{P}(t) = X(\sigma(t)) \quad (5.3.29)$$

Considering the change of coordinates (5.3.26), it is obvious that $\sigma(t) = t + D(X(\sigma(t)))$ and differentiating this equality it follows that:

$$\dot{\sigma}(\tau) = \frac{1}{1 - \nabla D(\mathcal{P}(\tau))f(\mathcal{P}(\tau), U(\tau))} \quad \forall \tau \in [t - D(X(t)), t] \quad (5.3.30)$$

It is now clear that the gradient-of-delay term in the denominator of (5.3.23) is the result of a change in the time variable, which allows the predictor to be defined using an integral from the known delayed time $\phi(t) = t - D(X(t))$ until present time, rather than an integral from the present time until the unknown prediction time $\sigma(t) = t + D(\mathcal{P}(t))$ as it is mentioned previously.

The denominator of the predictor equation (5.3.23) should be positive and this condition stands as the feasibility condition:

$$\mathcal{F}_c : \nabla D(\mathcal{P}(\tau))f(\mathcal{P}(\tau), U(\tau)) < c \quad c \in (0, 1] \quad (5.3.31)$$

Because of this feasibility condition the stabilizing results are not global in general.

- In [19, 20], the local stability of the nonlinear state dependent-input delay system (5.3.19) is guaranteed under assumptions of global stabilizability and forward completeness of the free-delay system $\dot{X} = f(X, \omega)$.

Recall that the forward completeness assumption means that for every initial condition and every locally bounded input signal, the solution of the system $\dot{X} = f(X, \omega)$ is defined for all $t \geq t_0$. Mathematically, this means that there exists a smooth positive define function $R(X)$ and K_∞ functions α_2, α_3 and α_4 such that:

$$\alpha_2(|X|) < R(X) < \alpha_3(|X|) \quad (5.3.32)$$

$$\frac{\partial R(X)}{\partial X} f(X, \omega) < R(X) + \alpha_4(|\omega|) \quad (5.3.33)$$

- For nonlinear state dependent-input delay systems (5.3.19) which are more restrictive in the sense that the free-delay system is only locally stable, the problem is more complicated [19, 20].

The regional stability of the delay system (5.3.19) is achieved if the control reaches the system while the state is within the region of attraction of the delay-free closed-loop system and the solution remains at any time within the controller's feasibility region, so that the control signal is never retarded to earlier values, and the delay remains compensated for all subsequent times. This requirement corresponds to set of initial conditions from which all of the solutions belong to this the region of attraction.

It is important to note that in both cases the feasibility condition (5.3.31) must be checked.

Remark 13. For the linear state dependent input delay system the same analysis can be performed. Let us consider the plant:

$$\dot{X}(t) = AX(t) + BU(t - D(X(t))) \quad X \in \mathbb{R}^n \quad (5.3.34)$$

As soon as the pair (A, B) is stabilizable the free delay system $\dot{X}(t) = AX(t) + BU(t)$ satisfies all the required condition to synthesize the controller for the linear state dependent input delay system. The controller for the time delay system is given by

$$\begin{aligned} U(t) &= K\mathcal{P}(t) \\ \mathcal{P}(\tau) &= X(t) + \int_{t-D(X(t))}^{\tau} \frac{A\mathcal{P}(\mu) + BU(\mu)}{1 - \nabla D(\mathcal{P}(\mu))(A\mathcal{P}(\mu) + BU(\mu))} d\mu \end{aligned} \quad (5.3.35)$$

for all $t - D(X(t)) < \tau < t$:

The proposed predictor-based controller is perfectly adapted to linear systems, treating them as a special case of the design for nonlinear systems, for which the exponential stability is proved.

5.4 Stabilization of the position of the interface

In this section we shall show that a linear feedback stabilizes indeed the dynamics of the interface position considered as the nonlinear control system (5.2.17) with state-dependent delay on the input. The main feature of our problem in this context arises from the physical constraint:

- the input function corresponds to a filling ratio which takes value in $[0, 1[$;
- the denominator term of (5.2.17) has an singularity in the term $\left[1 - f_p^{in}\left(t - \frac{l(t)}{N_0\xi}\right)\right]$.

This problem of singularity is not considered in [19, 20]. It is clear that the free-delay system which is related to equation (5.2.17) is only locally stable. For the stability issue one should choose carefully the initial condition to guarantee that the delay system stays in the attraction region when the control reaches the system. This basin of attraction must be defined precisely for a stabilization problem around an equilibrium. The net flow at the die is a function of the gradient of pressure $\Delta P(L, t)$ and the interface dynamics depends strongly on this parameter. Consequently, the interface dynamics varies according to the coupling relation that is imposed at the interface. Then, the study of the reachable equilibria appears as an important aspect of the stability analysis.

In order to formulate the control problem, we start by an analysis of the static models associated to the two interface relations consisting of momentum flux continuity or pressure continuity.

5.4.1 Static models associated with the interface relations

The static model of the position of the interface strongly depends on the considered interface relations which are presented below.

1. Firstly, assuming the interface relations (5.2.4) stating the continuity of momentum flux at the interface, the equilibrium (f_{pe}, l_e) is defined by

$$\begin{cases} F_{de} - \rho_0 N_0 V_{eff} f_{pe} = 0 \\ l_e = L - \frac{B P_0}{(\eta S_{eff} \xi N_e)} + \frac{B \rho_0}{K_d} \frac{f_{pe}}{(1-f_{pe})} - \frac{B \rho \xi N_0 f_{pe}}{(\eta S_{eff})} \end{cases} \quad (5.4.1)$$

In order to satisfy the positivity of the die net flow F_{de} , at the boundary the critical value of filling ratio at the equilibrium must satisfy:

$$f_{pce} > \frac{1}{(\xi^2 N_e^2 + \frac{P_0}{\rho_0})} \left(\frac{P_0}{\rho_0} - \frac{\eta V_{eff} N_e}{B \rho_0} (L - l_e) \right) \quad (5.4.2)$$

The graph of equilibria (f_{pe}, l_e) is then shown on the figure (Fig. 5.4.1).

With this interface relation the physically reachable interface position lies in the interval $[0, 1.2]$ meters for a extruder length of $L = 2m$.

- at $l = 0m$: this case corresponds to a full of matter extruder. The inlet filling ration is $f_{pe} = 0.68$. Above this critical inlet flow rate the extruder has only the FFZ zone.
- at $l = 1.2m$ the inlet flow rate is close to zero.

2. Secondly, assuming the interface relation (5.2.6) stating the continuity of pressure at the interface, the equilibrium (f_{pe}, l_e) is defined by :

$$\begin{cases} F_{de} - \rho_0 N_0 V_{eff} f_{pe} = 0 \\ l_e = L - \frac{B \rho_0 f_{pe}}{K_d (1-f_{pe})} \end{cases} \quad (5.4.3)$$

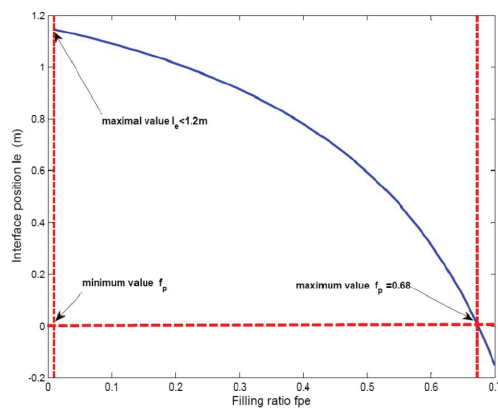


Figure 5.4.1: Static model with continuity of momentum flux at the interface

And the positivity constraint of the die net flow F_{de} implies:

$$L > l_e \quad (5.4.4)$$

The graph of equilibria (f_{pe}, l_e) is then shown on the figure 5.4.2.

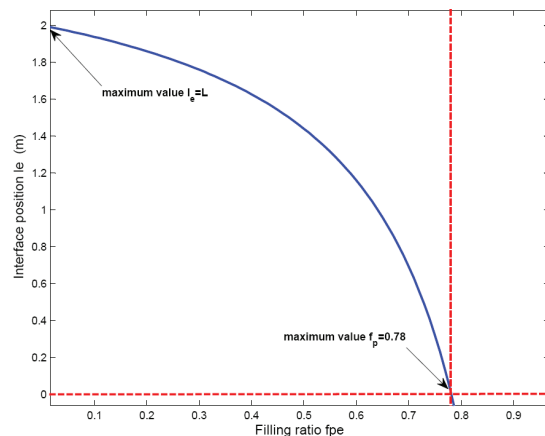


Figure 5.4.2: Static model with continuity of pressure at the interface

Comparing the figures (Fig. 5.4.1) and (Fig. 5.4.2), it may be observed that with the assumption of continuity of pressure, the static model covers a larger domain $(f_{pe}, l_e) \in [0, 0.78] \times [0, L]$ (the total length of the extruder is 2 meters) than with the assumption of continuity of the momentum flux. In this second case, the validity of the equilibrium model is restricted to $(f_{pe}, l_e) \in [0, 0.67] \times [0, 1.2]$. This conclusion was predictable because the constraint related to the pressure continuity relation states that the interface position is located in the interval $]0, L[$. This aspect guarantees the existence of *Partially and Fully Filled Zones* and is considered as a modelling assumption.

5.4.2 Feedback stabilization of the position of the interface

Due to the fact that the pressure continuity relation cover a larger domain than momentum flux coupling condition, we restrict the study to the case with the assumption of continuity of pressure. Then, in the following stability analysis, the gradient of pressure is given by equation (5.2.6).

5.4.2.1 Feedback stabilization of the nonlinear without delay

As in [19, 20], we study the stabilization of the free-delay system of equation (5.2.17) around the equilibrium. To satisfied the property which consists to define the stabilization problem at the origin ($F(0,0) = 0$) we rewrite the system by including the equilibrium point as follows:

$$\frac{dl(t)}{dt} = \frac{F_d(t) - F_{de} - \rho_0 N_0 V_{eff} (f_p^{in}(t) - f_{pe})}{\rho_0 S_{eff} (1 - f_p^{in}(t))} \quad (5.4.5)$$

with a linear abstract control on the incremental system : $\delta f_p^{in} = -K \delta l$.

We mention that the control is implementable if the real input and output variables are considered . As is stated previously the control is directly deduced from the feed rate $F_i n(t)$ by the linear relation:

$$f_p^{in}(t) = \frac{F_{in}(t)}{\rho_0 N_0 V_{eff}}. \quad (5.4.6)$$

Secondly, there is a dependence between δl and $\delta P(L, t)$ which can be measure by a pressure jauge. The relation between $\delta l(t)$ and $\delta P(L, t)$ arise from the linearized model of pressure gradient equation assuming the pressure continuity at the interface:

$$\begin{cases} \Delta P(t) = PL, t) - P_0 \\ P(L, t) = P_0 + \frac{\eta V_{eff} N_0 \rho_0 (L-l(t))}{(B\rho_0 + K_d(L-l(t)))} \end{cases} \quad (5.4.7)$$

and:

$$\delta P(L, t) = C \delta l, \quad (5.4.8)$$

Where C is an constant depending on physical parameters of the system.

The linearized model of the system (5.4.5) around the equilibrium of the open loop system without delay (5.4.5) is given by:

$$\frac{d(\delta l)}{dt} = \alpha_l \delta l + \alpha_f \delta f_p^{in} \quad (5.4.9)$$

with:

$$\alpha_l = -\frac{(\xi N_0 K_d B \rho_0)}{(B\rho_0 + K_d(L - l_e))^2 (1 - f_{pe})} \quad (5.4.10)$$

and:

$$\alpha_f = -\frac{\xi N_0}{(1 - f_{pe})} \quad (5.4.11)$$

It is clear that the stability of the linearized system is achieved if:

$$\begin{cases} K < K_{max} \\ K_{max} = \frac{\alpha_l}{\alpha_f} = \frac{K_d B \rho_0}{(B \rho_0 + K_d (L - l_e))^2} \end{cases} \quad (5.4.12)$$

By implementing the gain K to the nonlinear system, the equation (5.4.5) becomes:

$$\begin{cases} \frac{d\delta l(t)}{dt} = -\varphi_k(\delta l(t)) \\ -\varphi_k(\delta l(t)) = \frac{F_d(\delta l(t)) - F_{de} + \rho_0 N_0 V_{eff} K \delta l(t)}{\rho_0 S_{eff} (1 - f_{pe} + K \delta l(t))} \end{cases} \quad (5.4.13)$$

The stability depends on the sign of $\varphi_k(\delta l(t))$. The physical properties of the process introduce a constraint on the denominator of equation (5.4.13):

$$\begin{cases} 0 < (1 - f_{pe} + K \delta l(t)) < 1 \\ -\frac{1 - f_{pe}}{K} < \delta l(t) < \frac{f_{pe}}{K} \end{cases} \quad (5.4.14)$$

Due to the positivity of the denominator of equation (5.4.13), the positivity of $\varphi_k(\delta l(t))$ is achieved if $\forall \delta l(t) \neq 0$:

$$\delta l(t) (F_d(\delta l(t)) - F_{de} + \rho_0 N_0 V_{eff} K \delta l(t)) < 0 \quad (5.4.15)$$

The above expression will vary depending on the selected hypothesis to define the interface coupling relation. In the case treated in this section, we obtain the following results:

$$\begin{cases} \varphi_k(\delta l(t)) > 0 \\ \Leftrightarrow \frac{K_d^2}{\eta} + K \left(C_e - \frac{K_d}{\eta} \delta l(t) \right) C_e < 0 \\ C_e = \left(B \rho_0 + \frac{K_d}{\eta} (L - l_e) \right) \end{cases} \quad (5.4.16)$$

Which is equivalent to:

$$\delta l(t) > \frac{K_d}{K C_e} - \frac{\eta C_e}{K_d} \quad (5.4.17)$$

Finally combining equations (5.4.14) and (5.4.17), we can determine the basin of attraction under the assumption of continuous pressure at the interface. The obtained relation proves that the stability region is modulated by the feedback gain K :

$$\sup \left\{ -\frac{1 - f_{pe}}{K}; \frac{K_d}{K C_e^2} - \frac{\eta C_e}{K_d} \right\} < \delta l(t) < \frac{f_{pe}}{K} \quad (5.4.18)$$

5.4.2.2 Control of the system with input delay

Now we recall the delay system which relates the coupling of the *PDE* and the boundary equation.

$$\frac{dl(t)}{dt} = \frac{F_d(t) - F_{de} - \rho_0 N_0 V_{eff} \left(f_p^{in} \left(t - \frac{l(t)}{N_0 \xi} \right) - f_{pe} \right)}{\rho_0 S_{eff} \left(1 - f_p^{in} \left(t - \frac{l(t)}{N_0 \xi} \right) \right)} \quad (5.4.19)$$

We design a predictor controller which is developed in section 5.3.3 and physical parameters are chosen to satisfy both assumptions as forward completeness and the delay function $D(l(t))$ is also C^1 . The feasibility condition \mathcal{F}_c which is defined in (5.3.31) is also verified. The control law is the linear feedback given in the above section by the gain K :

$$\begin{cases} U(t) = \delta f_p(l(t), t) = -K \delta l(t) = -K(\mathcal{P}(t) - l_e) \\ D(l(t)) = \frac{l(t)}{\xi N_0} \end{cases} \quad (5.4.20)$$

Where for all $t - D(l(t)) \leq \tau \leq t$

$$\mathcal{P}(\tau) = l(t) + \int_{t-D(l(t))}^{\tau} \frac{F(\mathcal{P}(\mu), U(\mu)) d\mu}{1 - \nabla D(\mathcal{P}(\mu)) F(\mathcal{P}(\mu), U(\mu))} \quad (5.4.21)$$

The initial predictor $\mathcal{P}(\mu)$ with $\mu \in [-D(l_0), 0]$ is given by (5.4.21) at $t = 0$. Applying this controller to the system ensures the stabilization of the desired equilibrium position l_e .

5.5 Simulation results

The Numerical implementation of the predictor (5.4.21) is performed by approximating the distributed delay by a sum of point-wise delays using a numerical quadrature rule. In this way one ends up with a sequence of control-laws of the form:

$$\begin{aligned} \mathcal{P}(t) &= l(t) + \sum_{i=1}^N h(t) \frac{F(\mathcal{P}_{i-1}, U_{i-1})}{1 - \nabla D(\mathcal{P}_{i-1}) F(\mathcal{P}_{i-1}, U_{i-1})} \\ h(t) &= \frac{D(l(t))}{N} \end{aligned} \quad (5.5.1)$$

For the numerical integration, the values of the right-hand side of (5.5.1) involve earlier values of \mathcal{P} and the values of the input U . As we stated previously, the main difficulty is the practical implementation of the integral term, which needs to be calculated on-line [104]. An overview of stability results on the implementation of distributed delay control laws is given in [100, 102, 56, 134]. [23] mentions that the problems raised by the implementation of a control law including time varying delay is much more complicated. In this case, the discretization leads to a discrete controller with variable dimension. The resulting loop system therefore has a variable number of poles and zeros (for linear system), which makes difficult the study of the correlation between the numerical instabilities and the sampling period or the method of discretization.

We use a semi-discretization scheme based on the finite volume method for the simulation of the transport equation (5.2.1) with the controller. Time integration is performed with ODE45 routine of MATLAB. The figure (Fig. 5.5.1) shows the convergence of the moving interface from an initial position ($l_0 = 1m$) to the equilibrium ($l_e = 1.742m$). It remains some static error that can be corrected by using some integrator ($l(t_1) = 1.760m$, $t_1 = 450s$). One conclude that the system can be stabilized using the state predictor 5.4.21 and the linear gain $K_{max} = 0.8383$.

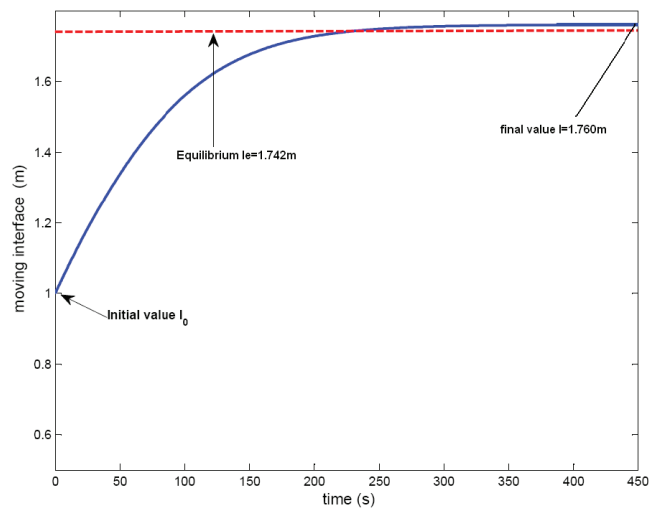


Figure 5.5.1: Moving interface stability

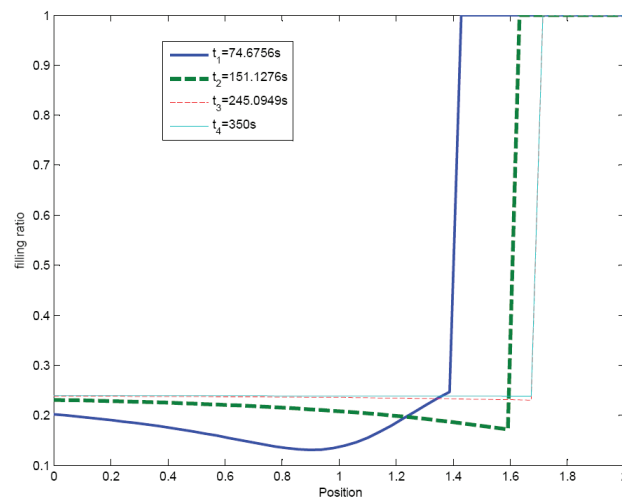


Figure 5.5.2: Filling ratio evolution at different times

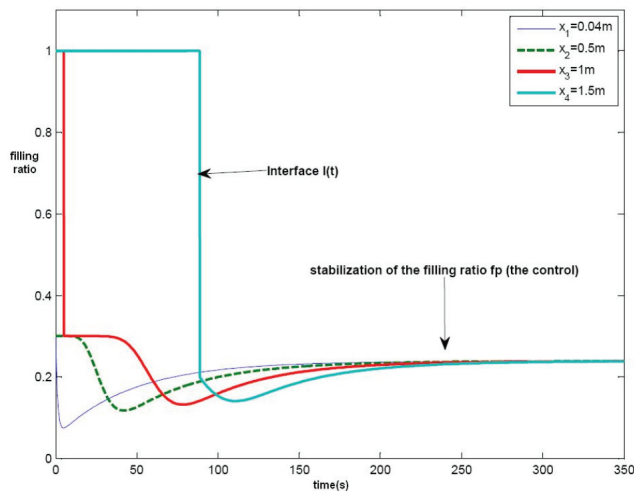


Figure 5.5.3: Filling ratio evolution at different positions

Figure (Fig. 5.5.2) represents the filling ratio dynamics which is the input variable at different times and Figure (Fig. 5.5.3) shows the evolution of the filling ratio at different spatial coordinates. The position of the interface can be read on this figure since it corresponds to filling ratio transition to 1.

Remark 14. An interesting future concerning this application is the robustness analysis of the controller. Recall that the model is based on the strong assumption of constant viscosity which is very restrictive in industrial context. In some sense a perturbation of the delay term may be interpreted as a variation of the viscosity or of some others physical variables. This type of extension will allow to consider more realistic extrusion process with application in industry. We suggest to follow the recent work of [21] to pursue this study on robustness.

5.6 Conclusion

The main idea in our approach relies on the development of a bi-zone model separated by a mobile interface $l(t)$. The model describes the mass balance in the *Partially and Fully Filled Zones* of an extruder as a transport equation coupled with an ordinary differential equation. For such systems we show that the coupling conditions are very important since they determine the reachable set of equilibrium. We illustrated this aspect by considering two coupling relations: The first one is derived from the continuity of pressure and the second one from the continuity of momentum flux.

The coupled mass transport and interface equations are turned in a state-dependent input delay system using the explicit solutions which are obtained by the method of characteristic. Here, the main objective is the stabilization of the moving interface around a given equilibrium. This control problem is equivalent to the regulation of net flow at the die $F_d(t)$ if the continuity

of pressure at the interface $l(t)$ is assumed. Using the control proposed in [19, 20] we show that the desired equilibrium can be reached with reasonable static error.

Ours analysis must be extended for the control of the energy balance equations which describes heat transport phenomena of the extrusion process as in [48]. The associated transport equations are described by (5.6.1,5.6.2) and the source term $\Omega_{p,f}$ groups the heat produced by viscous dissipation that is proportional to $N^2(t)$ and the heat exchange with the barrel (proportional to $(T_b - T_{p,f})$). The temperature $T_p(x, t)$ describes the temperature profile in the *Partially Filled Zone* and $T_f(x, t)$ is related to the *Fully Filled Zone*. The moving interface stability results in the convergence of the velocity associated to the transport equation of the *Fully Filled Zone* which is a function of $F_d(t)$. The influence of the interface stability on the the temperature behavior is shown in Figure (Fig. 5.6.1) and Figure 5.6.2).

$$\left\{ \begin{array}{l} \text{For } x \in [0; l(t)[\\ \frac{\partial}{\partial t} T_p(x, t) = -\xi N_0 \frac{\partial}{\partial x} T_p(x, t) + \Omega_p(T_p, T_b) \\ \text{For } x \in]l(t); L] \\ \frac{\partial}{\partial t} T_f(x, t) = -\frac{F_d(t)\xi}{\rho_0 V_{eff} C} \frac{\partial}{\partial x} T_f(x, t) + \Omega_f(T_f, T_b) \end{array} \right. \quad (5.6.1)$$

$$\Omega_{p,f} = \left\{ \begin{array}{l} \frac{\gamma \eta N_0^2}{f(x,t) \rho_0 V_{eff} C} + \frac{S_e \alpha}{\rho_0 V_{eff} C} (T_b - T_p) \\ \frac{\gamma \eta N_0^2}{f(x,t) \rho_0 V_{eff} C} + \frac{S_e \alpha}{\rho_0 V_{eff} C} (T_b - T_f) \end{array} \right. \quad (5.6.2)$$

The simulations presented in Figure (Fig. 5.6.1) and (Fig. 5.6.2) are performed assuming the continuity of temperature at the interface $l(t)$:

$$T_p(l^-, t) = T_f(l^+, t)$$

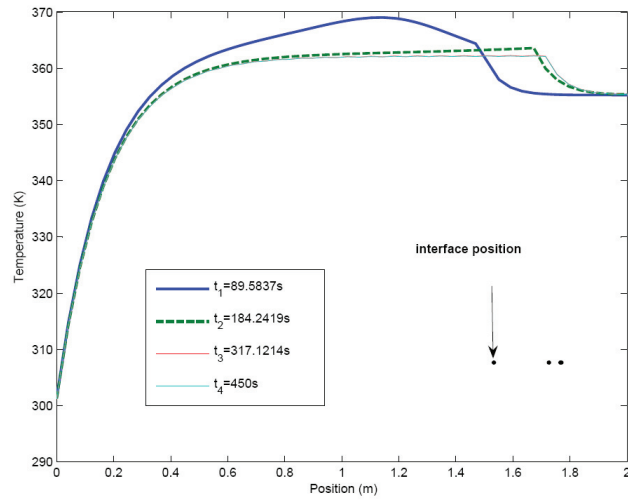


Figure 5.6.1: Temperature dynamics at different times

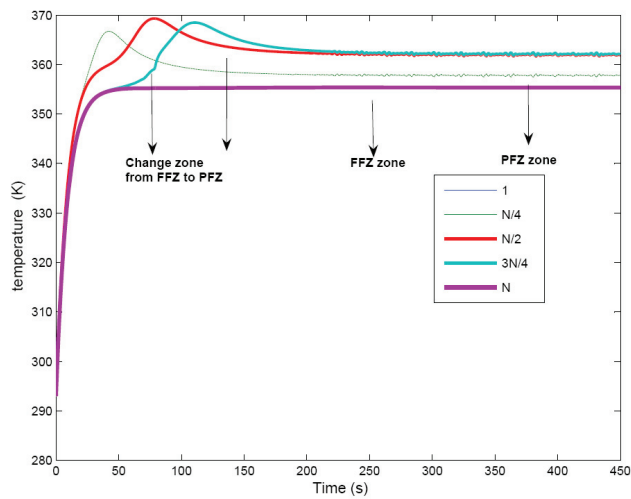


Figure 5.6.2: Temperature dynamics at different positions

Chapter 6

Port Hamiltonian formulation of a system of two conservation laws with a moving interface

6.1 Introduction

It has been shown that a large class of physical distributed parameter systems with boundary external variables, admit a port Hamiltonian formulation and they are called *boundary port Hamiltonian systems* [136, 98, 92]. This structure has led to various methods of analysis concerning the existence of solutions, their well-posedness and control in the linear case [93, 87, 141, 155, 142, 73, 113, 94].

In this chapter we shall investigate whether the port-Hamiltonian formulation may be extended to systems of conservation laws coupled by a moving interface. Such systems occur in various cases when the system is heterogeneous in the considered spatial domain, leading to several phases. The most simple example (which we shall also consider here) consists in two fluids which are separated by some moving wall. This wall separates two phases, the two fluids which might have different properties and induces discontinuities of some variables at the interface. These discontinuities are part of the model of the interface defined by a set of interface relations. The wall separating the two fluid may permit, or not, a mass flow or a pressure discontinuity for instance. The interfaces may also separate bubbles in a fluid in different chemical processes or define the boundary of polymer nanoparticles in a fluid. This interface might also separate the phase in evaporation processes. It might also arise from a constraint on some variables such as volume and lead to a change of causality and order in the spatial domain as for the extrusion process model.

More precisely we are inspired by a classical approach developed for fixed interfaces, consisting in augmenting the system of conservation laws of the physical model with color functions [61, 60, 10, 28]. In first instance we shall show that this system of conservation laws

may be formulated as port-Hamiltonian system with a pair of port variables associated to the interface. In second instance we shall generalize the previous approach to moving interfaces and show that it may again be formulated as a port-Hamiltonian system by adding a second pair of port variables corresponding to the motion of the interface. In this model the velocity of the interface appears like an input and the interface relations defining the dynamics of the displacement of the interface are then defined as an external port-based model. In the whole chapter the spatial domain is an interval of the real line and we shall only consider systems of two conservation laws.

The sketch of this chapter is the following. In a first part we consider two Hamiltonian systems consisting of two conservation laws coupled by a fixed interface. We first recall the definition of Stokes-Dirac structures and the boundary port-Hamiltonian formulation of a system of two conservation laws with flux variables deriving from a Hamiltonian. Then, we recall the extended system obtained by introducing color functions, associated with the characteristic functions of the spatial domains defined by the interface. We then define a Dirac structure and the port Hamiltonian formulation of the systems of conservation laws coupled by a fixed interface. In the second part we consider a moving interface and generalize the formulation of the coupled system of conservation laws before formulating it in the port-Hamiltonian framework. Finally we introduce the interface relations defining the dynamics of the interface as a two-port element and illustrate this on the simple example of two gases coupled by a piston.

6.1.1 Organization of the chapter

This chapter is organized as follows.

In section 5.2.1 we introduce the notion of a p-system in the port-Hamiltonian framework and present the construction of the associated Dirac structure by adding boundary flow and effort. In section 5.2.2 we study the interconnection of two p-systems through a fixed interface and also discuss the transmission condition at the interface in order to define a Dirac structure arising from the composition of the two complementary domains associated to two p-systems of conservation laws. In section 5.2.3 a new formulation is proposed by augmenting the system with color functions which correspond to characteristic functions of those complementary domains. These color functions are useful to extend the definition of the effort and flow variables in the total domain by introducing a modulated differential operator. The total Hamiltonian functional is also defined as an extension of the two Hamiltonian functionals by these color functions. Introducing external interface effort and flow variable the associated Dirac structure is constructed.

In section 5.3 we discuss the moving interface problem in the extended formulation of coupled systems using color functions and modulated differential operator. The main idea is to represent the interface dynamic as an external input variable. We suggest a general structure of

interface models based on the continuity of one effort variable. Then the coupling conditions at the moving interface guaranteed the existence of a Dirac structure. Finally we illustrate this by an example of two isentropic gases (modelled by a systems of two boundary port Hamiltonian systems) coupled at their interface by a piston in motion.

6.1.2 Contributions

In this chapter we consider the port-Hamiltonian formulation of a system of two conservation laws defined on two complementary intervals of some interval of the real line and coupled by a moving interface. We recall first how two port Hamiltonian systems coupled by an interface may be expressed as a port Hamiltonian system augmented with two variables being the characteristic functions of the two spatial domains. Then we consider the case of a moving interface and show that it may be expressed as the preceding port Hamiltonian system augmented with an input, being the velocity of the interface and define a conjugated output variable. We then give some structure to the interface relations defining the dynamics of the displacement of the interface and end with the simple example of two gases coupled by a moving piston.

6.2 Two port Hamiltonian systems coupled by an interface

6.2.1 Port Hamiltonian system of two conservation laws

Let us recall briefly the port Hamiltonian formulation of a system of two conservation laws according to [136, 98, 92] which represents a model of vibrating strings or Lagrangian gas dynamics (the p-system).

We consider systems of two conservation laws:

$$\partial_t x + \partial_z \mathcal{N}(x) = 0 \quad (6.2.1)$$

defined on the spatial domain $Z = [a, b]$, with time $t \in \mathbb{R}^+$ and with the 2-dimensional state vector $x(z, t) = \begin{pmatrix} x_1(z, t) \\ x_2(z, t) \end{pmatrix}$. The flux variable is defined by

$$\mathcal{N}(x) = \begin{pmatrix} 0 & -1 \\ -1 & 0 \end{pmatrix} \begin{pmatrix} \delta_{x_1} \mathcal{H} \\ \delta_{x_2} \mathcal{H} \end{pmatrix} \quad (6.2.2)$$

with respect to the Hamiltonian functional $\mathcal{H}(x) = \int_a^b H(x) dz$ with Hamiltonian density function $H(x)$ (where $\delta_x \mathcal{H}$ denotes the variational derivative of \mathcal{H} with respect to x). Then the system of conservation laws may be rewritten as the Hamiltonian system

$$\partial_t x = \mathcal{J} \delta_x \mathcal{H} \quad (6.2.3)$$

generated by the Hamiltonian functional $\mathcal{H}(x)$ and defined with respect to the differential operator

$$\mathcal{J} = \begin{pmatrix} 0 & -\partial_z \\ \partial_z^* & 0 \end{pmatrix} \quad (6.2.4)$$

where ∂_z^* is the formal adjoint of the operator ∂_z . Indeed if the flux variables (6.2.2) satisfy the boundary conditions given by $\delta_{x_1}\mathcal{H}(a) = \delta_{x_1}\mathcal{H}(b) = \delta_{x_2}\mathcal{H}(a) = \delta_{x_2}\mathcal{H}(b) = 0$, then $\partial_z^* = -\partial_z$ and the equation (6.2.3) is precisely (6.2.1) (6.2.2). Under the same conditions, the operator \mathcal{J} is skew-symmetric. Furthermore as it a matrix differential operator with constant coefficients, it satisfies the Jacobi identities and is a Hamiltonian operator, defining a Poisson bracket on the functionals of the state variables [112].

However for control purposes, it should be assumed that this is not satisfied in order to allow for energy exchange of the system with its environment. Therefore the Hamiltonian system is augmented with the boundary port variables

$$\begin{pmatrix} f_\partial \\ e_\partial \end{pmatrix} = \begin{pmatrix} \delta_{x_2}\mathcal{H} \\ \delta_{x_1}\mathcal{H} \end{pmatrix} \Big|_{a,b} = \begin{pmatrix} 0 & 1 \\ 1 & 0 \end{pmatrix} \begin{pmatrix} \delta_{x_1}\mathcal{H} \\ \delta_{x_2}\mathcal{H} \end{pmatrix} \Big|_{a,b} \quad (6.2.5)$$

and is thereby extended to a boundary port-Hamiltonian system [136, 98, 92]. This port-Hamiltonian system is defined with respect to a Dirac structure which extend the Hamiltonian operator (6.2.4).

Let us recall the definition of a Dirac structure which will be extensively used in this chapter.

Definition 5. [42] Consider two real vector spaces, \mathcal{F} the *space of flow variables* and \mathcal{E} the *space of effort variables*, together with a pairing, that is, a bilinear operation

$$\begin{aligned} \mathcal{F} \times \mathcal{E} &: \rightarrow \mathbb{R} \\ (f, e) &\mapsto \langle e, f \rangle \end{aligned} \quad (6.2.6)$$

which induces the symmetric bilinear form \ll, \gg on the bond space $\mathcal{B} = \mathcal{F} \times \mathcal{E}$ defined as

$$\ll (f_1, e_1), (f_2, e_2) \gg := \langle e_1, f_2 \rangle + \langle e_2, f_1 \rangle, \quad (f_i, e_i) \in \mathcal{F} \times \mathcal{E} \quad (6.2.7)$$

A *Dirac structure* is a linear subspace $D \subset \mathcal{F} \times \mathcal{E}$ which is isotropic and co-isotropic that is satisfies $D = D^\perp$, with \perp denoting the orthogonal complement with respect to the bilinear form \ll, \gg .

Particular Dirac structures, called Stokes-Dirac structures, are associated with Hamiltonian differential operators [136, 92, 87]; here we recall the particular case of the Stokes-Dirac structure associated with the Hamiltonian operator \mathcal{J} defined in (6.2.4).

Proposition 6. *The linear subspace of the bond space $\mathcal{B} = \mathcal{F} \times \mathcal{E}$, product space of the space of flow variables \mathcal{F} and effort variables \mathcal{E} where $\mathcal{F} = \mathcal{E} = L^2((a, b), \mathbb{R}^2) \times \mathbb{R}^2$ defined by*

$$\mathcal{D} = \left\{ \left(\begin{pmatrix} f_1 \\ f_2 \\ f_\partial \end{pmatrix}, \begin{pmatrix} e_1 \\ e_2 \\ e_\partial \end{pmatrix} \right) \in \mathcal{F} \times \mathcal{E} \mid \begin{pmatrix} e_1 \\ e_2 \end{pmatrix} \in H^1((a, b), \mathbb{R}^2)^2, \begin{pmatrix} f_1 \\ f_2 \end{pmatrix} = \mathcal{J} \begin{pmatrix} e_1 \\ e_2 \end{pmatrix} \right. \\ \left. \text{and } \begin{pmatrix} f_\partial \\ e_\partial \end{pmatrix} = \begin{pmatrix} 0 & 1 \\ 1 & 0 \end{pmatrix} \begin{pmatrix} e_1 \\ e_2 \end{pmatrix} \Big|_{a,b} \right\} \quad (6.2.8)$$

is a Dirac structure and is called Stokes-Dirac structure, with respect to the pairing

$$\left\langle \begin{pmatrix} f_1 \\ f_2 \\ f_\partial \end{pmatrix}, \begin{pmatrix} e_1 \\ e_2 \\ e_\partial \end{pmatrix} \right\rangle = \int_a^b (f_1 e_1 + f_2 e_2) dz + e_\partial^\top \Sigma f_\partial$$

with

$$\Sigma = \text{diag}(-1, 1). \quad (6.2.9)$$

In the same way as Hamiltonian systems are defined with respect to Poisson brackets, port-Hamiltonian systems are defined with respect to Dirac structures [135, 137]. Again we refer with [136, 92, 87] for the general definition of boundary port-Hamiltonian defined respect to a Stokes-Dirac structure and will only recall the definition for the case of a system of two conservation laws.

Proposition 7. *The system consisting of two conservation laws (6.2.3) augmented with the port variables (6.2.5) is equivalent to*

$$\left(\begin{pmatrix} \partial_t x_1 \\ \partial_t x_2 \\ f_\partial \end{pmatrix}, \begin{pmatrix} \delta_{x_1} \mathcal{H} \\ \delta_{x_2} \mathcal{H} \\ e_\partial \end{pmatrix} \right) \in \mathcal{D} \quad (6.2.10)$$

and defines a boundary port-Hamiltonian system.

As a consequence of the properties of the Stokes-Dirac structure [136], the Hamiltonian function obeys the following balance equation

$$\frac{d}{dt} H = -e_\partial^\top \Sigma f_\partial$$

6.2.2 Interconnection of port Hamiltonian systems through an interface

In this section we consider two systems of conservation laws which are defined in the spatial domains $[a, 0[$ and $]0, b]$ respectively. We denote their state variables and Hamiltonian with exponent $-$ and $+$ depending on which half real line they are defined. The two systems

are coupled through interface relations coupling the boundary values of the two systems at $z = 0$, the interface of the two systems. Considering two systems of conservation laws coupled through an interface the most currently considered interface relations are [61, 28, 10] the continuity of the flux variable or the continuity of some other functions of the state variables, called *privileged variables* [27, p. 5].

For boundary port Hamiltonian systems it is natural to express the interface relations using the boundary port variables (6.2.5) which are in fact, in the case of the canonical systems of two conservation laws, actually the flux variables at the boundary. In this case the space of flow and effort variables are defined as the product space of the flow and effort spaces on each domain: $\mathcal{F} = \mathcal{E} = L^2((a, 0), \mathbb{R}^2) \times \mathbb{R}^2 \times L^2((0, b), \mathbb{R}^2) \times \mathbb{R}^2$ and the Dirac structure is defined with respect to the product operator of (6.2.4)

$$\begin{pmatrix} \mathcal{J} & 0_2 \\ 0_2 & \mathcal{J} \end{pmatrix}$$

Considering for instance the interface relations being the balance equation $\delta_{x_1^+} \mathcal{H}^+ + \delta_{x_1^-} \mathcal{H}^- = 0$ and the continuity equation $\delta_{x_2^+} \mathcal{H}^+ = \delta_{x_2^-} \mathcal{H}^-$, and writing them in vector notation, one obtains the linear relation between the conjugated power variables

$$\begin{pmatrix} \delta_{x_1^+} \mathcal{H}^+ \\ \delta_{x_2^+} \mathcal{H}^+ \end{pmatrix} \Big|_{(0^+)} = \begin{pmatrix} 0 & 1 \\ -1 & 0 \end{pmatrix} \begin{pmatrix} \delta_{x_1^-} \mathcal{H}^- \\ \delta_{x_2^-} \mathcal{H}^- \end{pmatrix} \Big|_{(0^-)} \quad (6.2.11)$$

they may immediately be interpreted as defining a Dirac structure on the boundary port variables at the interface. Then, by composition of Dirac structures, the two boundary port Hamiltonian systems can be composed to a single boundary port Hamiltonian system with boundary port variables being $\delta_{x^-} \mathcal{H}^- (a)$ and $\delta_{x^+} \mathcal{H}^+ (b)$, according to (6.2.5) [136].

In the sequel of the paper, we shall consider the following interface relations where the pair of interface port variables (f_I, e_I) is introduced

$$f_I = \delta_{x_2^+} \mathcal{H}^+ = \delta_{x_2^-} \mathcal{H}^- \quad (6.2.12)$$

$$0 = \delta_{x_1^+} \mathcal{H}^+ + \delta_{x_1^-} \mathcal{H}^- + e_I \quad (6.2.13)$$

The equation (6.2.12) is again a continuity equation and the equation (6.2.13) is a balance equation with an external term e_I . This are commonly considered interface relations [61, 28, 10] consisting of the continuity equation of one of the flux variable (then called *privileged variable*) and the introduction of a source term at the interface, in the balance equation of the other flux variable [27]. Denoting $e_i^+ = \delta_{x_i^+} \mathcal{H}^+$ and $e_i^- = \delta_{x_i^-} \mathcal{H}^-$ with $i = 1, 2$, the interface relations (6.2.12) (6.2.13) define the linear relations between the conjugated power variables

$$\begin{pmatrix} e_2^- \\ e_1^+ \\ f_I \end{pmatrix} \Big|_{(0^+)} = \begin{pmatrix} 0 & 1 & 0 \\ -1 & 0 & -1 \\ 0 & 1 & 0 \end{pmatrix} \begin{pmatrix} e_1^- \\ e_2^+ \\ e_I \end{pmatrix} \Big|_{(0^-)} \quad (6.2.14)$$

with respect to a nonlinear matrix and therefore define a Dirac structure.

The interface relations may of course be much more general using nonlinear functions of the flux variables at the interface, port variables coupled to a dynamical system: if the interface relations define a Dirac structure coupled to a dissipative port Hamiltonian systems then by composition of Dirac structures, a dissipative port Hamiltonian system is obtained on the product space of the state space of the subsystems [34] as for instance in [113, 94].

However in the sequel we shall depart from this procedure of composition of boundary port Hamiltonian systems. Indeed, as a consequence of considering moving interfaces, time-varying spatial domains have to be considered. These do not appear explicitly as *variables* in the definition of boundary port Hamiltonian systems. This is the reason why, in the remaining of the paper, we shall use additional state variables, the characteristic functions of the time-varying spatial domains of each subsystem.

6.2.3 Augmenting the port Hamiltonian systems with color functions

6.2.3.1 Prolongation of the variables on the domain $[a, b]$

There is an alternative approach [61, 28, 10] where instead of considering the product spaces of the variables defined in the different spatial domains, the state variables of the coupled systems are defined on the composed spatial domain, the interval $[a, b]$. The interface at $z = 0$ becomes then an interior point of the spatial domain. However some external variables may still be associated with the interface. Following [1, 29, 6] we shall introduce additional state variables called *color functions* which are actually the characteristic functions of the domains of the two systems

$$c_0(z, t) = \begin{cases} 1 & z \in [a, 0[\\ 0 & z \in [0, b] \end{cases} \quad \text{and} \quad \bar{c}_0(z, t) = \begin{cases} 1 & z \in]0, b] \\ 0 & z \in [a, 0] \end{cases} \quad (6.2.15)$$

Hence the state variables of the coupled system may be expressed as the sum of prolongations of the variables of each subsystem to the total spatial domain $Z = [a, b]$ by

$$x(z, t) = x^-(z, t) + x^+(z, t) \quad (6.2.16)$$

$$x^-(z, t) = c_0(z, t)x(z, t) \quad x^+(z, t) = \bar{c}_0(z, t)x(z, t) \quad (6.2.17)$$

The flux variable of the two conservation laws, becomes

$$\mathcal{N}(x, c_0, \bar{c}_0) = c_0 \mathcal{N}^-(x) + \bar{c}_0 \mathcal{N}^+(x) \quad (6.2.18)$$

The global flux can be written as

$$c_0 \mathcal{N}(x, c_0, \bar{c}_0) = c_0 \mathcal{N}^-(x) \quad (6.2.19)$$

$$\bar{c}_0 \mathcal{N}(x, c_0, \bar{c}_0) = \bar{c}_0 \mathcal{N}^+(x), \quad (6.2.20)$$

where it should be noticed that $\mathcal{N}^-(x)$ and $\mathcal{N}^+(x)$ in (6.2.18), (6.2.19), (6.2.20), are different flux functions. Now the system is given by the conservation laws defined on the total spatial domain

6.2.3.2 Conservation laws and interface relations as a single system of balance equations

We shall now consider the two systems of Hamiltonian conservation laws coupled by the interface relations defined in (6.2.12) and (6.2.13). As a consequence of these relations, considering the definition of the flux variables (6.2.2), it appears that the flux variable \mathcal{N}_1 satisfies a continuity equation at the interface whereas the flux variable \mathcal{N}_2 satisfies a balance equation at the interface.

In the first instance, let us consider the conservation law of the state variable x_1 which may be written (on the whole domain $[a, b]$)

$$\begin{aligned} \partial_t x_1 &= -\partial_z (c_0 \mathcal{N}_1^-(x) + \bar{c}_0 \mathcal{N}_1^+(x)) \\ &= -\partial_z (c_0 \mathcal{N}_1(x, c_0, \bar{c}_0) + \bar{c}_0 \mathcal{N}_1(x, c_0, \bar{c}_0)) \\ &= -\underbrace{[\partial_z c_0 + \partial_z \bar{c}_0]}_{\mathbf{d}_0} \mathcal{N}_1(x, c_0, \bar{c}_0) \end{aligned} \quad (6.2.21)$$

where the operator

$$\mathbf{d}_0 = -[\partial_z c_0 + \partial_z \bar{c}_0] \quad (6.2.22)$$

acts as the differential operator $-\partial_z$ on each sub-domain (according to the system (6.2.3) (6.2.4)).

Indeed (6.2.21) corresponds to the local formulation of the conservation laws on arbitrary domain $[a', b']$ with either on an interval $[a', b']$ on the negative real line ($a \leq a' \leq b' < 0$)

$$\frac{d}{dt} \int_{a'}^{b'} x_1(z, t) = -\mathcal{N}_1^-(a', t) + \mathcal{N}_1^-(b', t)$$

or on an interval $[a', b']$ on the positive real line ($0 < a' < b' \leq b$)

$$\frac{d}{dt} \int_{a'}^{b'} x_1(z, t) = -\mathcal{N}_1^+(a', t) + \mathcal{N}_1^+(b', t)$$

Now let us consider the formulation of the conservation law of x_1 on an arbitrary interval $[a', b']$ containing the interface (with $a \leq a' < 0 < b' \leq b$). The assumption the continuity of the flux variable \mathcal{N}_1 , implies the following consequence on the conservation law of the

variable x_1

$$\begin{aligned}
\frac{d}{dt} \int_{a'}^{b'} x_1(z, t) dz &= \frac{d}{dt} \int_{a'}^0 x_1(z, t) dz + \frac{d}{dt} \int_0^{b'} x_1(z, t) dz \\
&= \int_{a'}^{b'} \mathbf{d}_0 \mathcal{N}_1(x, c_0, \bar{c}_0) dz \\
&= \int_{a'}^{b'} -[\partial_z c_0 \cdot + \partial_z \bar{c}_0 \cdot] \mathcal{N}_1(x, c_0, \bar{c}_0) dz \\
&= -\mathcal{N}_1^-(a', t) + \mathcal{N}_1^-(0^-, t) - \mathcal{N}_1^+(0^-, t) + \mathcal{N}_1^+(b', t) \quad (6.2.23) \\
&= -\mathcal{N}_1^-(a', t) + \mathcal{N}_1^+(b', t) \\
&= -\mathcal{N}_1(a', t) + \mathcal{N}_1(b', t) \\
&= -e_2(a', t) + e_2(b', t)
\end{aligned}$$

In the second instance, let us consider the conservation law of the state variable x_2 and remind that , at the interface, the associated flux variable \mathcal{N}_2 is supposed to satisfy the balance equation (6.2.13) with the source term $e_I \delta(z)$ (a Dirac distribution), localized at the interface. But firstly we have to calculate the dual operator, denoted by \mathbf{d}_0^* , to the operator \mathbf{d}_0 defined in (6.2.22), in order to be able to express the power pairing. Therefore consider two effort variables e_1 and e_2 and compute

$$\begin{aligned}
\int_a^b e_1 (\mathbf{d}_0 e_2) dz &= - \int_a^b (e_1 [\partial_z c_0 \cdot + \partial_z \bar{c}_0 \cdot] e_2) dz \\
&= - \int_a^b (e_1 [\partial_z (c_0 e_2) + \partial_z (\bar{c}_0 e_2)]) dz \\
&= - [(c_0 + \bar{c}_0) e_1 e_2]_a^b + \int_a^b (c_0 e_2 + \bar{c}_0 e_2) (\partial_z e_1) dz \\
&= - [(c_0 + \bar{c}_0) e_1 e_2]_a^b \\
&\quad + \int_a^b e_2 [\partial_z c_0 \cdot + \partial_z \bar{c}_0 \cdot] e_1 dz - \int_a^b e_2 [(\partial_z c_0) + (\partial_z \bar{c}_0)] e_1 dz
\end{aligned}$$

Hence the dual operator is defined by

$$\begin{aligned}
\mathbf{d}_0^* &= [\partial_z c_0 \cdot + \partial_z \bar{c}_0 \cdot] - [(\partial_z c_0) + (\partial_z \bar{c}_0)] \\
&= -\mathbf{d}_0 + [(\partial_z c_0) + (\partial_z \bar{c}_0)] \quad (6.2.24)
\end{aligned}$$

Using this dual operator the conservation law of the variable x_2 becomes

$$\partial_t x_2 = -\mathbf{d}_0^* \mathcal{N}_2 - e_I \delta(z) \quad (6.2.25)$$

where $\delta(z)$ denote the Dirac mass. Indeed, using similar calculation as in the preceding paragraph, one shows that (6.2.25) corresponds to the local formulation of the conservation laws on arbitrary interval $[a', b']$ on the negative real line ($a \leq a' \leq b' < 0$) or on the positive real line ($0 < a' < b' \leq b$). On these intervals the operator $-\mathbf{d}_0^*$ acts as the differential operator $-\partial_z^*$ according to the Hamiltonian system (6.2.3) (6.2.4).

On an arbitrary interval $[a', b']$ containing the interface (with $a \leq a' < 0 < b' \leq b$), the

balance equation on the variable x_2 is

$$\begin{aligned}
\frac{d}{dt} \int_{a'}^{b'} x_2(z, t) &= \int_{a'}^{b'} \{-\mathbf{d}_0^* \mathcal{N}_2(x, c_0, \bar{c}_0) - e_I(t) \delta(z)\} dz \\
&= \int_{a'}^{b'} \{(\mathbf{d}_0 - [(\partial_z c_0) - (\partial_z \bar{c}_0)]) \mathcal{N}_2(x, c_0, \bar{c}_0) - e_I(t) \delta(z)\} dz \\
&= \int_{a'}^{b'} \mathbf{d}_0 \mathcal{N}_2(x, c_0, \bar{c}_0) dz \\
&\quad + \int_{a'}^{b'} \{[(\partial_z c_0) - (\partial_z \bar{c}_0)] \mathcal{N}_2(x, c_0, \bar{c}_0) - e_I(t) \delta(z)\} dz \\
&= -\mathcal{N}_2^-(a', t) + \mathcal{N}_2^-(0^-, t) - \mathcal{N}_2^+(0^-, t) + \mathcal{N}_2^+(b', t) \\
&\quad - \mathcal{N}_2^-(0^-, t) + \mathcal{N}_2^+(0^-, t) - \int_{a'}^{b'} e_I(t) \delta(z) dz \\
&= -\mathcal{N}_2^-(a', t) + \mathcal{N}_2^+(b', t) + e_I(t) \\
&= -e_1(a', t) + e_1(b', t) - e_I(t)
\end{aligned} \tag{6.2.26}$$

On this balance equation, it appears clearly that the flux variables at the interface $\mathcal{N}_2^-(0^-, t)$ and $\mathcal{N}_2^+(0^-, t)$ are eliminated according to the balance equation (6.2.13).

6.2.3.3 Hamiltonian system extended with color functions

In the preceding paragraph we have formulated the dynamical equations of the system with an interface, as the system of balance equations (6.2.21) and (6.2.25) using the dual differential operators (6.2.22) and (6.2.24) which depend on the characteristic functions of the two domains separated by the interface. Following [61][28][10], we shall introduce explicitly these functions as variables of the system; they are then called *color functions* and will be denoted by $c(z, t)$ and $\bar{c}(z, t)$. Noticing that the spatial domains separated by the *fixed* interface are *constant*, hence also their characteristic functions c_0 and \bar{c}_0 defined in (6.2.15), it is clear that they satisfy the trivial conservation laws

$$\partial_t c = \partial_t \bar{c} = 0 \tag{6.2.27}$$

with initial conditions being precisely c_0 and \bar{c}_0 and compatible boundary conditions.

In the sequel we shall define an extended Hamiltonian system composed of the two balance equations (6.2.21) and (6.2.25) with closure equations (6.2.2) indexed by $+$ and $-$ for each spatial subdomain and augmented with the trivial conservation laws (6.2.27). Therefore define the Hamiltonian functional $\mathcal{H}(x, c, \bar{c}) = \int_a^b H(x, c, \bar{c}) dz$ with density

$$H(x, c, \bar{c}) = c H^-(x) + \bar{c} H^+(x) \tag{6.2.28}$$

Denoting the *extended state variable* by

$$\tilde{x} = (x^T, c, \bar{c})^T \tag{6.2.29}$$

one computes the variational derivatives

$$\delta_{\tilde{x}} \mathcal{H}(\tilde{x}) = \begin{pmatrix} \delta_x \mathcal{H}(x, c, \bar{c}) \\ \delta_c \mathcal{H}(x, c, \bar{c}) \\ \delta_{\bar{c}} \mathcal{H}(x, c, \bar{c}) \end{pmatrix} = \begin{pmatrix} c \delta_x \mathcal{H}^-(x) + \bar{c} \delta_x \mathcal{H}^+(x) \\ \mathcal{H}^-(x) \\ \mathcal{H}^+(x) \end{pmatrix} \tag{6.2.30}$$

Note that the first row corresponds precisely to the definition of the flux variable (6.2.18) for the particular solution c_0 and \bar{c}_0

$$\delta_x \mathcal{H}(x, c, \bar{c}) = c \delta_x \mathcal{H}^-(x) + \bar{c} \delta_x \mathcal{H}^+(x) = c \mathcal{N}^-(x) + \bar{c} \mathcal{N}^+(x) = \mathcal{N}(x, c, \bar{c})$$

This allows to augment the Hamiltonian system (6.2.3) with the trivial conservation laws of the color functions (6.2.27) obtaining the Hamiltonian system:

$$\partial_t \tilde{x} = \mathcal{J}_a \delta_{\tilde{x}} \mathcal{H}(\tilde{x}) + I e_I \quad (6.2.31)$$

$$I^T = \begin{pmatrix} 0 & -1 & 0 & 0 \end{pmatrix} \quad (6.2.32)$$

with respect to the operator

$$\mathcal{J}_a = \begin{pmatrix} 0 & \mathbf{d} & 0_2 \\ -\mathbf{d}^* & 0 & 0_2 \\ 0_2 & 0_2 & 0_2 \end{pmatrix} \quad (6.2.33)$$

where operator \mathbf{d} is the nonlinear differential operator, modulated by $c(z, t)$ and $\bar{c}(z, t)$ defined by

$$\mathbf{d} = -[\partial_z c + \partial \bar{c}] \quad (6.2.34)$$

and its formal dual

$$\mathbf{d}^* = -\mathbf{d} + [(\partial_z c) - (\partial_z \bar{c})] \quad (6.2.35)$$

Furthermore the two operators satisfies, for any two effort variables e_1 and e_2 which do not vanish at the boundary

$$\int_a^b e_1 (\mathbf{d} e_2) dz = \int_a^b e_2 (\mathbf{d}^* e_1) dz - [(c + \bar{c}) e_1 e_2]_a^b \quad (6.2.36)$$

6.2.3.4 Extension to a Boundary Port Hamiltonian system arising from a skew-adjoint operator

In order to take account of the energy exchange at the boundary $\{a, b\}$ and defining a conjugated flow variable f_I to the interface source term e_I at the interface, the Hamiltonian system (6.2.31) will now be extended to a port Hamiltonian systems with boundary and distributed ports. In the begin, the operator \mathcal{J}_a defined in (6.2.33) and the input map at the interface defined by (6.2.32) are extended to a Stokes-Dirac structure using a similar procedure as in [136].

Proposition 8. *The set of relations \mathcal{D}_I associated with a system of two conservation laws defined on the variables $\begin{pmatrix} x_1 \\ x_2 \end{pmatrix}$ defined on a spatial domain $[a, b] \ni z$ with an interface*

at the point $z = 0$ which imposes the continuity of the effort variable e_2 and allows for the discontinuity of the effort variable e_1 is defined by

$$\mathcal{D}_I = \left\{ \left(\begin{pmatrix} \tilde{f} \\ f_I \\ f_\partial \end{pmatrix}, \begin{pmatrix} \tilde{e} \\ e_I \\ e_\partial \end{pmatrix} \right) \in \mathcal{F} \times \mathcal{E} / \right. \\ \left. \begin{pmatrix} \tilde{f} \\ f_I \end{pmatrix} = \begin{pmatrix} \mathcal{J}_a & I \\ -I^T & 0 \end{pmatrix} \begin{pmatrix} \tilde{e} \\ e_I \end{pmatrix} \right. \\ \left. \text{and } \begin{pmatrix} f_\partial \\ e_\partial \end{pmatrix} = \begin{pmatrix} 0 & 1 \\ (c + \bar{c}) & 0 \end{pmatrix} \begin{pmatrix} e_1 \\ e_2 \end{pmatrix} \Big|_{a,b} \right\} \quad (6.2.37)$$

with the flow variable $\tilde{f} = (f_1, f_2, f_c, f_{\bar{c}})^T$ and the effort variable $\tilde{e} = (e_1, e_2, e_c, e_{\bar{c}})^T$ associated with the extended state (6.2.29), the differential operator \mathcal{J}_a defined in (6.2.33), the operators \mathbf{d} , resp. \mathbf{d}^* defined in (6.2.34), resp. (6.2.35), the column vector I defined in (6.2.32), and bond space $\mathcal{B} = \mathcal{F} \times \mathcal{E}$ with $\mathcal{F} = L^2((a, b), \mathbb{R})^5 \times \mathbb{R}^2$ and $\mathcal{E} = \text{dom } \mathbf{d}^* \times \text{dom } \mathbf{d} \times L^2((a, b), \mathbb{R})^3 \times \mathbb{R}^2$ endowed with the pairing

$$\left\langle \begin{pmatrix} \tilde{f} \\ f_I \\ f_\partial \end{pmatrix}, \begin{pmatrix} \tilde{e} \\ e_I \\ e_\partial \end{pmatrix} \right\rangle = \int_a^b \tilde{e}^T \tilde{f} dz + e_\partial^T \Sigma f_\partial + \int_a^b e_I^T f_I dz \quad (6.2.38)$$

with $e_\partial^T \Sigma f_\partial = e_\partial(a) f_\partial(a) - e_\partial(b) f_\partial(b)$, defines a Dirac structure.

One may notice immediately that the pair of port variables (e_I, f_I) at the interface are *distributed* variables. Let us prove that the set (6.3.12) is indeed a Dirac structure. Note that we shall use the following notation

$$\bar{f} = \begin{pmatrix} \tilde{f} \\ f_I \\ f_\partial \end{pmatrix}; \quad \bar{e} = \begin{pmatrix} \tilde{e} \\ e_I \\ e_\partial \end{pmatrix} \quad (6.2.39)$$

Proof. Let us first show the isotropy condition $\mathcal{D}_I \subset \mathcal{D}_I^\perp$:

$$\langle (\bar{f}^1, \bar{e}^1), (\bar{f}^2, \bar{e}^2) \rangle = 0 \quad \forall (\bar{f}^1, \bar{e}^1), (\bar{f}^2, \bar{e}^2) \in \mathcal{D}_I \quad (6.2.40)$$

with respect to the bilinear product associated with the pairing (6.2.38) and denoted in the

sequel by \mathcal{P}

$$\begin{aligned}
\mathcal{P} &= \langle\langle (\bar{f}^1, \bar{e}^1), (\bar{f}^2, \bar{e}^2) \rangle\rangle \\
&= \langle \bar{f}^1, \bar{e}^2 \rangle + \langle \bar{f}^2, \bar{e}^1 \rangle \\
&= \int_a^b \tilde{e}^{2T} \tilde{f}^1 dz + \int_a^b \tilde{e}^{1T} \tilde{f}^2 dz + \int_a^b e_I^{1T} f_I^2 dz + \int_a^b e_I^{2T} f_I^1 dz \\
&\quad + e_\partial^{1T} \Sigma f_\partial^2 + e_\partial^{2T} \Sigma f_\partial^1
\end{aligned} \tag{6.2.41}$$

Using the constitutive relations of the set \mathcal{D}_I , the power product becomes

$$\begin{aligned}
\mathcal{P} &= \int_a^b (e_1^2 \mathbf{d}e_2^1 + e_2^2 [(-\mathbf{d}^*) e_1^1 - e_I^1]) dz \\
&\quad + \int_a^b (e_1^1 \mathbf{d}e_2^2 + e_2^1 [(-\mathbf{d}^*) e_1^2 - e_I^2]) dz \\
&\quad + \int_a^b e_I^1 e_2^2 dz + \int_a^b e_I^2 e_2^1 dz + [(c + \bar{c}) e_1^1 e_2^2]_a^b + [(c + \bar{c}) e_1^2 e_2^1]_a^b
\end{aligned}$$

and after noticing that the terms in the interface variables e_I^1 and e_I^2 cancel, may be reorganized as follows

$$\begin{aligned}
\mathcal{P} &= \int_a^b (e_1^2 \mathbf{d}e_2^1 + e_2^1 (-\mathbf{d}^*) e_1^2) dz + [(c + \bar{c}) e_1^1 e_2^2]_a^b \\
&\quad + \int_a^b (e_2^2 (-\mathbf{d}^*) e_1^1 + e_1^1 \mathbf{d}e_2^2) dz + [(c + \bar{c}) e_1^2 e_2^1]_a^b \\
&= \int_a^b (e_1^2 \mathbf{d}e_2^1 + e_2^1 (-\mathbf{d}^*) e_1^2) dz + \int_a^b (e_2^2 (-\mathbf{d}^*) e_1^1 + e_1^1 \mathbf{d}e_2^2) dz
\end{aligned}$$

and using the identity (6.2.36), one obtains that $\mathcal{P} = 0$ which proves the isotropy condition.

Let us now prove the co-isotropy condition $\mathcal{D}_I^\perp \subset \mathcal{D}_I$. This amounts to prove that if $(\bar{f}^2, \bar{e}^2) \in \mathcal{B}$ satisfies $\forall (\bar{f}^1, \bar{e}^1) \in \mathcal{D}_I; \langle\langle (\bar{f}^1, \bar{e}^1), (\bar{f}^2, \bar{e}^2) \rangle\rangle = 0$ then $(\bar{f}^2, \bar{e}^2) \in \mathcal{D}_I$. Therefore let us compute the bilinear product (6.2.41), assuming that $(\bar{f}^1, \bar{e}^1) \in \mathcal{D}_I$. One computes

$$\begin{aligned}
\mathcal{P} &= \int_a^b \left(\tilde{e}^{2T} (\mathcal{J}_a \tilde{e}^1) + \tilde{e}^{1T} \tilde{f}^2 \right) dz + \int_a^b e_I^1 f_I^2 dz + \int_a^b e_I^2 e_2^1 dz \\
&\quad + ((c + \bar{c}) e_1^1)_{|_{a,b}}^T \Sigma f_\partial^2 + e_\partial^{2T} \Sigma (e_2^1)_{|_{a,b}}
\end{aligned} \tag{6.2.42}$$

Remind that, from the definition of \mathcal{D}_I , the variables \tilde{e}^1 and e_I^1 may be chosen freely.

Firstly, let us choose $e_1^1 = 0$, $e_2^1 = 0$, $e_I^1 = 0$ and $e_c^1 = 0$. The the bilinear product reduces to: $\mathcal{P} = \int_a^b e_c^1 f_c^2 dz$ and the condition that it vanishes for any e_c^1 , implies the relation: $f_c^2 = 0$. By symmetry one obtains $f_c^2 = 0$.

Secondly, let us choose $e_2^1 = 0$, $e_I^1 = 0$ and $e_1^1(a) = e_2^1(b) = 0$, then, using the definition of f_2 of the constitutive relations of \mathcal{D}_I and (6.2.36) with zero boundary conditions, the bilinear

product becomes

$$\begin{aligned}\mathcal{P} &= \int_a^b (e_2^2 (-\mathbf{d}^* e_1^1) + e_1^1 f_1^2) dz \\ &= \int_a^b e_1^1 (-\mathbf{d} e_2^2 + f_1^2) dz\end{aligned}\quad (6.2.43)$$

The condition that \mathcal{P} vanishes for any e_1^1 hence implies that : $f_1^2 = \mathbf{d} e_2^2$.

Thirdly, let us choose $e_1^1 = 0$, $e_I^1 = 0$ and $e_1^1(a) = e_2^1(b) = 0$, then, using the definition of f_1 of the constitutive relations of \mathcal{D}_I and (6.2.36) with zero boundary conditions, the bilinear product becomes

$$\begin{aligned}\mathcal{P} &= \int_a^b (e_1^2 (\mathbf{d} e_2^1) + e_2^1 f_2^2 + e_2^1 e_I^2) dz \\ &= \int_a^b e_2^1 (\mathbf{d}^* e_1^2 + f_2^2 + e_I^2) dz\end{aligned}\quad (6.2.44)$$

The condition that \mathcal{P} vanishes for any e_2^1 hence implies that : $f_2^2 = -\mathbf{d}^* e_1^2 - e_I^2$.

Fourthly, let us choose $\tilde{e}_1^1 = 0$, $\tilde{e}_2^1 = 0$, then, using the definition of f_I of the constitutive relations of \mathcal{D}_I , the bilinear product becomes

$$\begin{aligned}\mathcal{P} &= \int_a^b (-e_I^1 e_2^2 + f_I^2 e_I^1) dz \\ &= \int_a^b e_I^1 (-e_2^2 + f_I^2) dz\end{aligned}\quad (6.2.45)$$

The condition that \mathcal{P} vanishes for any e_I^1 hence implies that : $f_I^2 = e_2^2$.

Fifth, let us choose $e_I^1 = 0$, then, using the constitutive relations of \mathcal{D}_I , the previously established relations on f_1^2 , f_2^2 and f_I^2 , the relation (6.2.36), the bilinear product becomes

$$\begin{aligned}\mathcal{P} &= \int_a^b (e_1^2 \mathbf{d} e_2^1 + e_2^2 (-\mathbf{d}^*) e_1^1) dz + \int_a^b (e_1^1 \mathbf{d} e_2^2 + e_2^1 (-\mathbf{d}^*) e_1^2) dz \\ &\quad + ((c + \bar{c}) e_1^1) |_{a,b} {}^T \Sigma f_\partial^2 + e_\partial^{2T} \Sigma (e_2^1) |_{a,b} \\ &= -[(c + \bar{c}) e_1^1 e_2^2]_a^b - [(c + \bar{c}) e_1^2 e_2^1]_a^b \\ &\quad + ((c + \bar{c}) e_1^1) |_{a,b} {}^T \Sigma f_\partial^2 + e_\partial^{2T} \Sigma (e_2^1) |_{a,b}\end{aligned}$$

The condition that \mathcal{P} vanishes for any $e_1^1(a)$ and $e_2^1(b)$ hence implies the boundary port variables and $\begin{pmatrix} f_\partial^2 \\ e_\partial^2 \end{pmatrix} = \begin{pmatrix} 0 & 1 \\ (c + \bar{c}) & 0 \end{pmatrix} \begin{pmatrix} e_1^1 \\ e_2^1 \end{pmatrix} |_{a,b}$ \square

Comparing the constitutive relations of the Dirac structure \mathcal{D}_I defined in (6.3.12) with the augmented Hamiltonian system (6.2.31), one may easily see that it may be endowed with a port Hamiltonian structure.

Corollary 9. *The augmented Hamiltonian systems (6.2.31) with the conjugated flow variable $f_I = e_2$ may be defined as a boundary port-Hamiltonian system with respect to the Dirac*

$$\text{structure } \mathcal{D}_I \text{ by : } \left(\left(\begin{array}{c} \partial_t \tilde{x} \\ f_I \\ f_\partial \end{array} \right), \left(\begin{array}{c} \delta_{\tilde{x}} H(\tilde{x}) \\ e_I \\ e_\partial \end{array} \right) \right) \in \mathcal{D}_I,$$

where the state vector \tilde{x} , defined in (6.2.29), is the vector of conserved quantities of the conservation laws augmented by the color functions of each spatial subdomain, the Hamiltonian $H(\tilde{x})$, defined in (6.2.28), is the sum of the Hamiltonian of each spatial subdomain, the pair of port variables (f_I, e_I) are associated with the interface and the pair of port variables (f_∂, e_∂) are associated with the boundary of the spatial domain $[a, b]$.

As a consequence of the port-Hamiltonian structure, the augmented Hamiltonian system (6.2.31) with the conjugated flow variable $f_I = e_2$, satisfies the following power balance equation:

$$\frac{d}{dt} H(x) = e_\partial^T \Sigma f_\partial + \int_a^b e_I^T f_I dz \quad (6.2.46)$$

Furthermore, if the Hamiltonians $H^-(x)$ and $H^+(x)$ are bounded from below, the augmented system has passivity properties. Indeed, although the Hamiltonian of the augmented system (6.2.31) is linear in the two color functions, they are invariants of the system hence, restricted to the invariant submanifold of invariance, it is indeed bounded from below.

Observe that, as we consider general color functions which are not Heaviside functions, *the interface is now only defined by the continuity and discontinuity assumption on the two effort variables.* The port variables (f_I, e_I) are *distributed* variables on the complete domain (a, b) and hence are not the restriction at the point interface of the effort variables as for instance in (6.2.11). If the color functions are restricted to Heaviside functions then the power inflow at the interface appearing in the power balance equation (6.2.46) depends only on the values of the effort variables at the interface

$$\int_a^b e_I^T f_I dz = -e_1(0^-) e_2(0^+) + e_1(0^-) e_2(0^+)$$

involving the same variables as in (6.2.14).

6.3 Port Hamiltonian systems coupled through a moving interface

In this section we shall consider the problem of two systems of two conservation laws which are coupled through a *moving* interface. We shall denote by $l(t)$ the time-varying position of the interface in the interval $[a, b]$ and its velocity by $\dot{l}(t) = \frac{dl}{dt}$. In first instance we shall show how the formulation as a port-Hamiltonian systems of corollary 9 may be extended to a moving interface. To this end we shall consider the velocity $\dot{l}(t)$ of displacement of the interface as an input. After formulating the conservation laws in the case of a moving

interface, we show that they lead to a Port Hamiltonian system obtained by completing the system of corollary 9 with an input relation and a conjugated port variable to $\dot{l}(t)$. Secondly, we shall define a class of models associated with interface relations. We conclude with the simple example of two gases in interaction through a piston.

6.3.1 Balance equations with moving interface

For a time-varying position $l(t)$ of the interface the spatial domains of the two subsystems are the intervals $[a, l(t)[$ and $]l(t), b]$. The two color functions, the characteristic functions of the domains, depend now on the position of the interface :

$$c_{l(t)}(z, t) = \begin{cases} 1 & z \in [a, l(t)[\\ 0 & z \in [l(t), b] \end{cases} \quad (6.3.1)$$

and

$$\bar{c}_{l(t)}(z, t) = \begin{cases} 1 & z \in]l(t), b] \\ 0 & z \in [a, l(t)] \end{cases} \quad (6.3.2)$$

It may be noted immediately that these color functions, depending on the position of the interface $l(t)$, also are the solutions of some conservation laws, namely the transport equations depending on the velocity $\dot{l}(t)$ of the interface

$$\partial_t c(z, t) = -\dot{l}(t) \partial_z c(z, t) \quad \text{and} \quad \partial_t \bar{c}(z, t) = -\dot{l}(t) \partial_z \bar{c}(z, t) \quad (6.3.3)$$

with initial conditions

$$c(z, 0) = c_{l(0)}(z, t) \quad \text{and} \quad \bar{c}(z, 0) = \bar{c}_{l(0)}(z, t) \quad (6.3.4)$$

and associated boundary conditions.

The state variables, the flux variables and the energy function may be defined according to the definitions (6.2.16), (6.2.18) and (6.2.28). Now due to the moving interface, the balance equations on interval $[a', b']$ with $a \leq a' < l(t) < b' \leq b$ containing the interface, will include an additional term, depending on the velocity $\dot{l}(t)$ of the interface.

Assuming again the continuity of the effort e_2 at the interface at $l(t)$ (or equivalently of the flux variable \mathcal{N}_1), the conservation law associated to the variable x_1 becomes

$$\begin{aligned} \frac{d}{dt} \int_{a'}^{b'} x_1(z, t) dz &= \frac{d}{dt} \int_{a'}^{l(t)} x_1(z, t) dz + \frac{d}{dt} \int_{l(t)}^{b'} x_1(z, t) dz \\ &= \int_{a'}^{l(t)} \partial_t x_1(z, t) dz + \int_{l(t)}^{b'} \partial_t x_1(z, t) dz \\ &\quad + \dot{l}(t) [x_1^-(l(t), t) - x_1^+(l(t), t)] \\ &= \int_{a'}^{b'} \mathbf{d}_0 \mathcal{N}_1(x, c_l, \bar{c}_l) dz + \dot{l}(t) [x_1^-(l(t), t) - x_1^+(l(t), t)] \\ &= -\mathcal{N}_1(a', t) + \mathcal{N}_1(b', t) + \dot{l}(t) [x_1^-(l(t), t) - x_1^+(l(t), t)] \\ &= -e_2(a', t) + e_2(b', t) + \dot{l}(t) [x_1^-(l(t), t) - x_1^+(l(t), t)] \end{aligned} \quad (6.3.5)$$

and its local formulation becomes

$$\partial_t x_1 = \mathbf{d}_0 \mathcal{N}_1(x, c_l, \bar{c}_l) + \dot{l}(t) [c x_1 \partial_z c + \bar{c} x_1 \partial_z \bar{c}] \quad (6.3.6)$$

Allowing again a discontinuity of the effort variable e_1 (or equivalently of the flux variable \mathcal{N}_2), the conservation law associated to the variable x_2 becomes, in a similar way as above

$$\begin{aligned}
\frac{d}{dt} \int_{a'}^{b'} x_2(z, t) &= \int_{a'}^{b'} \{-\mathbf{d}_0^* \mathcal{N}_2(x, c_l, \bar{c}_l) - e_I\} dz + \dot{l}(t) [x_2^-(l(t), t) - x_2^+(l(t), t)] \\
&= \int_{a'}^{b'} \{\mathbf{d}_0 - [(\partial_z c_l) - (\partial_z \bar{c}_l)]\} \mathcal{N}_2(x, c_l, \bar{c}_l) - e_I\} dz \\
&\quad + \dot{l}(t) [x_2^-(l(t), t) - x_2^+(l(t), t)] \\
&= -\mathcal{N}_2^-(a', t) + \mathcal{N}_2^+(b', t) + e_I(l(t)) + \dot{l}(t) [x_2^-(l(t), t) - x_2^+(l(t), t)] \\
&= -e_2(a', t) + e_2(b', t) - e_I(l(t)) + \dot{l}(t) [x_2^-(l(t), t) - x_2^+(l(t), t)]
\end{aligned} \tag{6.3.7}$$

and its local formulation becomes

$$\partial_t x_2 = -\mathbf{d}_0^* \mathcal{N}_2(x, c_l, \bar{c}_l) - e_I + \dot{l}(t) [c x_2 \partial_z c + \bar{c} x_2 \partial_z \bar{c}] \tag{6.3.8}$$

6.3.2 Port Hamiltonian Formulation

The four balance equations (6.3.3), (6.3.6) and (6.3.8) may be recognized as the augmented Hamiltonian formulation (6.2.31) of the system of two conservation laws with fixed interface which is completed with an additive term proportional to the velocity. They may be written in state space form

$$\partial_t \begin{pmatrix} x \\ c \\ \bar{c} \end{pmatrix} = \mathcal{J}_a \begin{pmatrix} \delta_x \mathcal{H}(x, c, \bar{c}) \\ \delta_c \mathcal{H}(x, c, \bar{c}) \\ \delta_{\bar{c}} \mathcal{H}(x, c, \bar{c}) \end{pmatrix} + I e_I + \dot{l}(t) \begin{pmatrix} c x & \bar{c} x \\ -1 & 0 \\ 0 & -1 \end{pmatrix} \partial_z \begin{pmatrix} c \\ \bar{c} \end{pmatrix} \tag{6.3.9}$$

with I defined in (6.2.32).

This defines an input map associated with the input $\dot{l}(t)$, velocity of the interface, as follows

$$G(x, c, \bar{c}) = \begin{pmatrix} c x & \bar{c} x \\ -1 & 0 \\ 0 & -1 \end{pmatrix} \partial_z \begin{pmatrix} c \\ \bar{c} \end{pmatrix} \tag{6.3.10}$$

One may define then the *conjugated output* e_l by

$$e_l = \int_a^b \delta_{\tilde{x}} \mathcal{H}(\tilde{x})^T G(x, c, \bar{c}) dz$$

which may also be defined as the pairing

$$e_l = \langle G(Tx, c, \bar{c}) |, \delta_{\tilde{x}} \mathcal{H}(\tilde{x}) \rangle = \int_a^b \delta_{\tilde{x}} \mathcal{H}(\tilde{x})^T G(x, c, \bar{c}) dz \tag{6.3.11}$$

This leads to a Dirac structure associated with systems of conservation laws with a moving interface as follows.

Proposition 10. *The set of relations \mathcal{D}_M associated with a system of two conservation laws defined with the variables $\begin{pmatrix} x_1 \\ x_2 \end{pmatrix}$ on the spatial domain $[a, b] \ni z$ and an interface moving with velocity \dot{l} which imposes the continuity of the effort variable e_2 and allows for the discontinuity of the effort variable e_1 is defined by*

$$\mathcal{D}_M = \left\{ \left(\begin{pmatrix} \tilde{f} \\ f_I \\ e_l \\ f_\partial \end{pmatrix}, \begin{pmatrix} \tilde{e} \\ e_I \\ i \\ e_\partial \end{pmatrix} \right) \in \mathcal{F} \times \mathcal{E} / \right.$$

$$\left. \begin{pmatrix} \tilde{f} \\ f_I \\ -e_l \end{pmatrix} = \begin{pmatrix} \mathcal{J}_a & I & G(x, c, \bar{c}) \\ -I^T & 0 & 0 \\ -\langle G^T(x, c, \bar{c}) | & 0 & 0 \end{pmatrix} \begin{pmatrix} \tilde{e} \\ e_I \\ i \end{pmatrix} \right. \quad (6.3.12)$$

$$\left. \text{and } \begin{pmatrix} f_\partial \\ e_\partial \end{pmatrix} = \begin{pmatrix} 0 & 1 \\ (c + \bar{c}) & 0 \end{pmatrix} \begin{pmatrix} e_1 \\ e_2 \end{pmatrix}_{a,b} \right\}$$

with the flow variable $\tilde{f} = (f_1, f_2, f_c, f_{\bar{c}})^T$ and the effort variable $\tilde{e} = (e_1, e_2, e_c, e_{\bar{c}})^T$ associated with the extended state (6.2.29), the differential operator \mathcal{J}_a defined in (6.2.33), the operators \mathbf{d} , resp. \mathbf{d}^* defined in (6.2.34), resp. (6.2.35), the column vector I defined in (6.2.32), the input map G defined in (6.3.10) and its adjoint $\langle G^T |$ in (6.3.11) and bond space $\mathcal{B} = \mathcal{F} \times \mathcal{E}$ with $\mathcal{F} = L^2((a, b), \mathbb{R})^5 \times \mathbb{R} \times \mathbb{R}^9$ and $\mathcal{E} = \text{dom } \mathbf{d}^* \times \text{dom } \mathbf{d} \times L^2((a, b), \mathbb{R})^3 \times \mathbb{R} \times \mathbb{R}^9$ endowed with the pairing

$$\left\langle \begin{pmatrix} \tilde{f} \\ f_I \\ e_l \\ f_\partial \end{pmatrix}, \begin{pmatrix} \tilde{e} \\ e_I \\ i \\ e_\partial \end{pmatrix} \right\rangle = \int_a^b \tilde{e}^T \tilde{f} dz + \int_a^b e_I^T f_I dz + e_\partial^T \Sigma f_\partial - e_l i \quad (6.3.13)$$

with $e_\partial^T \Sigma f_\partial = e_\partial(a) f_\partial(a) - e_\partial(b) f_\partial(b)$, defines a Dirac structure.

Proof. Let us first show the isotropy condition $\mathcal{D}_M \subset \mathcal{D}_M^\perp$.

Denote

$$\hat{f} = \begin{pmatrix} \tilde{f} \\ f_I \\ e_l \\ f_\partial \end{pmatrix}$$

and the pairing (6.3.13) by $\langle \hat{e}, \hat{f} \rangle$. Then the isotropy condition is written

$$\langle \langle (\hat{f}^1, \hat{e}^1), (\hat{f}^2, \hat{e}^2) \rangle \rangle = \langle \hat{e}^1, \hat{f}^2 \rangle + \langle \hat{e}^2, \hat{f}^1 \rangle = 0 \quad \forall ((\hat{f}^1, \hat{e}^1), (\hat{f}^2, \hat{e}^2)) \in \mathcal{D}_M$$

with respect to the bilinear product associated with the pairing (6.3.13) or in an equivalent way

$$\langle \hat{e}, \hat{f} \rangle = 0 \quad \forall (\hat{f}, \hat{e}) \in \mathcal{D}_M$$

Let us hence compute the pairing

$$\begin{aligned}
\langle \hat{e}, \hat{f} \rangle &= \int_a^b \tilde{e}^T \tilde{f} dz + \int_a^b e_I^T f_I dz + e_\partial^T \Sigma f_\partial - e_l \dot{l} \\
&= \int_a^b \tilde{e}^T (\mathcal{J}_a \tilde{e} + I e_I + G \dot{l}) dz + \int_a^b e_I^T (-I^T \tilde{e}) dz + e_\partial^T \Sigma f_\partial \\
&\quad - \left(\int_a^b \tilde{e}^T G dz \right) \dot{l} \\
&= \left(\int_a^b e_I^T I^T \tilde{e} dz + \int_a^b e_I^T (-I^T \tilde{e}) dz \right) + \left(\int_a^b \tilde{e}^T \mathcal{J}_a \tilde{e} dz + e_\partial^T \Sigma f_\partial \right) \\
&\quad + \int_a^b \tilde{e}^T G \dot{l} dz - \left(\int_a^b \tilde{e}^T G dz \right) \dot{l} \\
&= 0
\end{aligned} \tag{6.3.14}$$

using the definition of the boundary port-variables f_∂ and e_∂ .

Let us now prove the co-isotropy condition $\mathcal{D}_M^\perp \subset \mathcal{D}_M$. This amounts to proving that if $(\hat{f}^2, \hat{e}^2) \in \mathcal{B}$ satisfies $\forall (\hat{f}^1, \hat{e}^1) \in \mathcal{D}_M; \langle (\hat{f}^1, \hat{e}^1), (\hat{f}^2, \hat{e}^2) \rangle = 0$ then $(\hat{f}^2, \hat{e}^2) \in \mathcal{D}_M$. Therefore let us compute the bilinear product (6.3.14), assuming that $(\hat{f}^1, \hat{e}^1) \in \mathcal{D}_M$.

$$\begin{aligned}
\mathcal{P}_e &= \int_a^b \left(\tilde{e}^{2T} (\mathcal{J}_a \tilde{e}^1 + I e_I^1 + G \dot{l}^1) + \tilde{e}^{1T} \tilde{f}^2 \right) dz \\
&\quad + \int_a^b e_I^1 f_I^2 dz + \int_a^b e_I^2 e_2^1 dz
\end{aligned} \tag{6.3.15}$$

$$+ ((c + \bar{c}) e_1^1) \Big|_{a,b}^T \Sigma f_\partial^2 + e_\partial^{2T} \Sigma (e_2^1) \Big|_{a,b} \tag{6.3.16}$$

$$+ \int_a^b [(\partial_z c) e_c^1 + (\partial_z \bar{c}) e_{\bar{c}}^1] f_c^2 dz + \int_a^b e_c^2 (-\dot{l}^1) dz \tag{6.3.17}$$

$$- \left(\int_a^b G^T(x, c, \bar{c}) \tilde{e}^1 dz \right) \dot{l}^2 - e_l^2 \dot{l}^1 \tag{6.3.18}$$

Remind that, from the definition of \mathcal{D}_M , the variables \tilde{e}^1 , e_I^1 and \dot{l}^1 may be chosen freely. **In a first instance, choose $\dot{l}^1 = 0$.** Then the power product becomes

$$\begin{aligned}
\mathcal{P}_e &= \int_a^b \left(\tilde{e}^{2T} (\mathcal{J}_a \tilde{e}^1 + I e_I^1) + \tilde{e}^{1T} \tilde{f}^2 \right) dz \\
&\quad + \int_a^b e_I^1 f_I^2 dz + \int_a^b e_I^2 e_2^1 dz
\end{aligned} \tag{6.3.19}$$

$$+ ((c + \bar{c}) e_1^1) \Big|_{a,b}^T \Sigma f_\partial^2 + e_\partial^{2T} \Sigma (e_2^1) \Big|_{a,b} \tag{6.3.20}$$

$$+ \int_a^b [(\partial_z c) e_c^1 + (\partial_z \bar{c}) e_{\bar{c}}^1] f_c^2 dz \tag{6.3.21}$$

$$- \left(\int_a^b G^T(x, c, \bar{c}) \tilde{e}^1 dz \right) \dot{l}^2 \tag{6.3.22}$$

Then, firstly, let us choose $e_1^1 = 0$, $e_2^1 = 0$, $e_I^1 = 0$ and $e_c^1 = 0$. Then, the bilinear product reduces to:

$$\mathcal{P}_e = \int_a^b e_c^1 f_c^2 dz - \left(\int_a^b -\partial_z c e_c^1 dz \right) i^2 = \int_a^b (f_c^2 + i^2 \partial_z c) e_c^1 dz$$

and the condition that it vanishes for any e_c^1 , implies the relation:

$$f_c^2 + i^2 \partial_z c = 0.$$

By symmetry one obtains $f_c^2 + i^2 \partial_z \bar{c} = 0$.

Secondly, let us choose $e_2^1 = 0$, $e_I^1 = 0$ and $e_1^1(a) = e_2^1(b) = 0$, then, using the preceding equalities, the definition of f_2 of the constitutive relations of \mathcal{D}_M and (6.2.36) with zero boundary conditions, the bilinear product becomes

$$\begin{aligned} \mathcal{P}_e &= \int_a^b (e_2^2 (-\mathbf{d}^* e_1^1) + e_1^1 f_1^2) dz - \left(\int_a^b (c x_1 \partial_z c + \bar{c} x_1 \partial_z \bar{c}) e_1^1 dz \right) i^2 \\ &= \int_a^b e_1^1 (-\mathbf{d} e_2^2 + f_1^2 - (c x_1 \partial_z c + \bar{c} x_1 \partial_z \bar{c})) dz \end{aligned} \quad (6.3.23)$$

The condition that \mathcal{P}_e vanishes for any e_1^1 hence implies that :

$$f_1^2 = \mathbf{d} e_2^2 + (c x_1 \partial_z c + \bar{c} x_1 \partial_z \bar{c}).$$

Thirdly, let us choose $e_1^1 = 0$, $e_I^1 = 0$ and $e_1^1(a) = e_2^1(b) = 0$, then, using the preceding derived equalities and the definition of f_1 of the constitutive relations of \mathcal{D}_M and (6.2.36) with zero boundary conditions, the bilinear product becomes

$$\begin{aligned} \mathcal{P}_e &= \int_a^b (e_1^2 (\mathbf{d} e_2^1) + e_2^1 f_2^2 + e_2^1 e_I^2) dz - \left(\int_a^b (c x_2 \partial_z c + \bar{c} x_2 \partial_z \bar{c}) e_2^1 dz \right) i^2 \\ &= \int_a^b e_2^1 (\mathbf{d}^* e_1^2 + f_2^2 + e_I^2 - (c x_2 \partial_z c + \bar{c} x_2 \partial_z \bar{c})) dz \end{aligned} \quad (6.3.24)$$

The condition that \mathcal{P}_e vanishes for any e_2^1 hence implies that :

$$f_2^2 = -\mathbf{d}^* e_1^2 - e_I^2 + (c x_2 \partial_z c + \bar{c} x_2 \partial_z \bar{c}) i^2.$$

Fourthly, let us choose $\bar{e}_1^1 = 0$, $\bar{e}_2^1 = 0$, then, using the definition of f_I of the constitutive relations of \mathcal{D}_M , the bilinear product becomes

$$\begin{aligned} \mathcal{P}_e &= \int_a^b (-e_I^1 e_2^2 + f_I^2 e_I^1) dz \\ &= \int_a^b e_I^1 (-e_2^2 + f_I^2) dz \end{aligned} \quad (6.3.25)$$

The condition that \mathcal{P}_e vanishes for any e_I^1 hence implies that: $f_I^2 = e_2^2$.

Fifth, let us choose $e_I^1 = 0$, then, using the constitutive relations of \mathcal{D}_I , the previously established relations on f_1^2 , f_2^2 and f_I^2 , the relation (6.2.36), the bilinear product becomes

$$\begin{aligned} \mathcal{P} &= \int_a^b (e_1^2 \mathbf{d} e_2^1 + e_2^2 (-\mathbf{d}^*) e_1^1) dz + \int_a^b (e_1^1 \mathbf{d} e_2^2 + e_2^1 (-\mathbf{d}^*) e_1^2) dz \\ &\quad + ((c + \bar{c}) e_1^1) \Big|_{a,b} {}^T \Sigma f_\partial^2 + e_\partial^2 {}^T \Sigma (e_2^1) \Big|_{a,b} \\ &= -[(c + \bar{c}) e_1^1 e_2^2]_a^b - [(c + \bar{c}) e_1^2 e_2^1]_a^b \\ &\quad + ((c + \bar{c}) e_1^1) \Big|_{a,b} {}^T \Sigma f_\partial^2 + e_\partial^2 {}^T \Sigma (e_2^1) \Big|_{a,b} \end{aligned}$$

The condition that \mathcal{P}_e vanishes for any $e_1^1(a)$ and $e_2^1(b)$ hence implies

$$\begin{pmatrix} f_{\partial}^2 \\ e_{\partial}^2 \end{pmatrix} = \begin{pmatrix} 0 & 1 \\ (c + \bar{c}) & 0 \end{pmatrix} \begin{pmatrix} e_1^2 \\ e_2^2 \end{pmatrix}_{a,b}.$$

In a second instance, choose $\dot{l}^1 \neq 0$. Then, using the previously derived equalities, the power product becomes

$$\begin{aligned} \mathcal{P}_e &= \int_a^b \left(\tilde{e}^{2T} G \dot{l}^1 \right) dz + \left(-e_l^2 \dot{l}^1 \right) \\ &= \left(\int_a^b \tilde{e}^{2T} G dz - e_l^2 \right) \dot{l}^1 \end{aligned} \quad (6.3.26)$$

The condition that \mathcal{P}_e vanishes for any \dot{l}^1 hence implies $e_l^2 = \int_a^b G^T \tilde{e}^2 dz$.

□

Note that with the choice of the two additional port variables associated with the color functions, the power balance on the effort and flow variables associated with the color functions do not contribute to the total power balance (corresponding, for physical systems, to the energy balance equation).

The port-Hamiltonian formulation of the system of two conservation laws with a moving interface with velocity \dot{l} may be formulated as a port-Hamiltonian system.

Corollary 11. *The augmented Hamiltonian systems (6.3.9) with the conjugated interface flow variable $f_I = e_2$ and conjugated variable e_l to the interface velocity, defined in (6.3.11), may be defined as a boundary port-Hamiltonian system with respect to the Dirac structure \mathcal{D}_M by*

$$\left(\begin{pmatrix} \partial_t \tilde{x} \\ f_I \\ e_l \\ f_{\partial} \end{pmatrix}, \begin{pmatrix} \delta_{\tilde{x}} \mathcal{H} \\ e_I \\ \dot{l} \\ e_{\partial} \end{pmatrix} \right) \in \mathcal{D}_M \quad (6.3.27)$$

where the state vector \tilde{x} , defined in (6.2.29), is the vector of conserved quantities of the conservation laws augmented by the color functions of each spatial subdomain, the Hamiltonian $H(\tilde{x})$, defined in (6.2.28), is the sum of the Hamiltonian of each spatial subdomain, the pair of port variables (f_I, e_I) are associated with the flux variables at the interface, the pair of port variables (l, e_l) are associated with the displacement of the interface and the pair of port variables $(f_{\partial}, e_{\partial})$ are associated with the boundary of the spatial domain $[a, b]$. The pairs of port variables $(f_{\partial}^c, e_{\partial}^c)$ balance the power product associated with the transport equations of the color functions.

Computing the balance equation for the Hamiltonian we find

$$\frac{d}{dt} H(x) = e_{\partial} \Sigma f_{\partial} + \int_a^b e_I^T f_I dz + \dot{l} e_l \quad (6.3.28)$$

It may be observed that, when restricting to the particular solution of the color functions (6.3.2) obtained with initial conditions (6.3.4), one can relate these port variables to interfacial effort and flux variables in a similar way as for a fixed interface. In this case the balance equation of the Hamiltonian is given by

$$\begin{aligned} \frac{d\mathcal{H}}{dt} &= e_\partial \Sigma f_\partial \\ &\quad + e_1(l^-) e_2(l^+) - e_1(l^-) e_2(l^+) - \dot{l} e_l \end{aligned}$$

with output conjugated to the velocity of the interface being the *discontinuity of energy density at the interface*

$$e_l = (-\mathcal{H}^-(l) + \mathcal{H}^+(l))$$

6.3.3 Model of the interface's displacement

In the preceding section we have defined the dynamic model of a system of two conservation laws coupled by a moving interface with velocity \dot{l} considered as an input variable and the interface relations (6.2.12) and (6.2.13). The port Hamiltonian model with the moving interface, admit as port variables, the port variables (f_I, e_I) associated with the flux variables at the interface and the port variables (\dot{l}, e_l) associated with the displacement of the interface. In this section we shall discuss possible closure relations which could be imposed of these two pairs of port variables at the interface and illustrate it on a very simple example: two gases with a piston at the interface.

In a first instance one should observe that the dynamics of displacement of the interface is necessarily finite-dimensional while the port variables (f_I, e_I) are distributed. Coming back to the motivating example of a thin interface, that is located at some point $l(t)$ which was the departure for the definition of the model in the section 6.3.1, the port variables (f_I, e_I) may be related to a finite-dimensional pair of variables $(\phi_I, \epsilon_I) \in \mathbb{R}^2$ with the following adjoint relations

$$\begin{pmatrix} \phi_I \\ e_I \end{pmatrix} = \begin{pmatrix} \int_a^b \delta(z-l) f_I dz \\ \epsilon_I \delta(z-l) \end{pmatrix} \quad (6.3.29)$$

which preserves the power product : $\phi_I \epsilon_I = \int_a^b e_I f_I dz$.

It should be noted that one could also define a thick interface by choosing another kernel than $\delta(z-l)$, with positive values and finite support.

In a second instance, one has complete the interface relation with the dynamics of the position of the interface $l(t)$ for instance in terms of a port Hamiltonian system with state variables including $l(t)$ and the port variables (ϕ_I, ϵ_I) and (\dot{l}, e_l) . In this case by interconnection of port Hamiltonian systems through a Dirac structure one may conclude that the complete system is again port Hamiltonian and use its properties for the proof of well-posedness and passivity-based control design.

Example 12. Let us conclude this paragraph with *the example of two isentropic gases* (modelled by a systems of two boundary port Hamiltonian systems [136]) *coupled at their interface*

by some piston in motion. The port Hamiltonian model of the gases is given precisely by the proposition 7 with state variables being the specific volume $x_1(t, z) = \mathbf{v}(t, z)$, the velocity $x_2(t, z) = v(t, z)$, Hamiltonian is the sum of the internal energy density $\mathcal{U}(\mathbf{v})$ and the kinetic energy density : $\mathcal{H}(\mathbf{v}, v) = \mathcal{U}(\mathbf{v}) + \frac{v^2}{2}$. The variational derivative of the Hamiltonian is then

$$\begin{pmatrix} \delta_{\mathbf{v}} H \\ \delta_v H \end{pmatrix} = \begin{pmatrix} e_1 \\ e_2 \end{pmatrix} = \begin{pmatrix} -p(\mathbf{v}) \\ v \end{pmatrix}$$

where $p(\mathbf{v}) = -\delta_{\mathbf{v}} \mathcal{U}(\mathbf{v})$ is the pressure. The interface relation (6.2.12) corresponds to the continuity of the effort variable $e_2 = v$ at the interface, which is the usual hypothesis that there is no cavitation at the piston and that the velocities of the fluids on both sides of the piston are equal to the velocity of the piston. And the interface relation (6.2.13) corresponds to the balance of forces exerted on the piston by the pressures $e_1 = -p(\mathbf{v})$ of the gases from both gases and the external force f_I .

The system of the two gases with a moving interface is then formulated by the corollary 11 with the color functions being the characteristic functions of each subdomain. As the piston is considered as a thin interface, we use the relation (6.3.29). In order to complete the interface relations we shall assume that the piston has no mass but is subject to friction with coefficient ν and an linear elastic force with stiffness k . In this case the dynamics of the piston is defined as a simple integrator

$$\frac{dl}{dt} = \phi_I = v$$

and the conjugated effort variable is the sum of all forces applying on the piston

$$\epsilon_i = -k l - \nu \phi_I$$

It may be interpreted as a finite-dimensional port Hamiltonian system with state variable l , structure matrix being zero, Hamiltonian function $\frac{1}{2} k l^2$ port-variables (ϕ_I, ϵ_I) and dissipative term. Finally the model has to be coupled with the pair of port variables (\dot{l}, e_l) . One relation is trivial

$$\dot{l} = \phi_I = v$$

The second one is less trivial and involves the effort variable e_l which is, when the color functions are the characteristic functions of both subdomains, the difference of the Hamiltonian density function at the interface: $e_l = (-\mathcal{H}^-(l) + \mathcal{H}^+(l))$. The most simple way of defining some relation is impose the continuity of the Hamiltonian density (which plays then the role of a *privileged variable*) which indeed complete the boundary conditions at the interface

$$e_l = 0$$

As a consequence using the total energy of the conservation laws and the interface model $H_{tot}(\mathbf{v}, v, l) = \int_a^b \left(\mathcal{U}(\mathbf{v}) + \frac{v^2}{2} \right) dz + \frac{1}{2} k l^2$ one obtains the power balance equation

$$\frac{dH_{tot}}{dt} = -\nu v^2 - v^-(a) p^-(\mathbf{v})(a) + v^+(b) p^+(\mathbf{v})(b)$$

6.4 Conclusion

In this chapter we have suggested port Hamiltonian formulation of a system of two conservation laws (on a 1-dimensional spatial domain) coupled by a moving interface. We have firstly augmented the system of conservation laws with two transport equations of the characteristic functions of the subdomains defined by the interface. Then we have derived a the port Hamiltonian formulation of this augmented system with, in addition to the boundary port variables at the boundary of the total domain two pairs of port-variables associated with the interface. The first pair corresponds to a particular choice of interface relation corresponding to a continuity and a balance equation on the flux variables at the interface and the second pair is defined by the velocity of interface and its conjugated variable. Finally we have illustrated this model with the example of two gases coupled by a moving piston.

This is the first step towards considering the coupling through an interface of Hamiltonian systems composed of an arbitrary number of conservation laws. However the most interesting feature of this formulation is that it makes explicit the pairs of conjugated variables needed to express the interface relations when derived from a port Hamiltonian formulation. This might be a powerful insight in the various suggested interface relations in the literature and towards a passivity-based definition and classification of these interface relations.

Finally this port Hamiltonian formulation might open the way to the analysis of the well-posedness of these systems (in the continuation of [87, 155]) as well as their passivity-based control which will be the aim of future work.

Chapter 7

Conclusion

7.1 General conclusion

This thesis is focused on modelling, control, and mathematical analysis of 1D transport equations coupled on two complementary time-varying domains. Along the manuscript, we show how a rigorous description of the interface is a major factor for such class of systems. The lack of physical model to express clearly the interface structure and the coupling conditions can be considered as the main challenge in modelling point of view. These interfaces which appear in many problems as the extrusion process and the Stefan problems are sources of real difficulties due to the discontinuity of the variables and the interface motion in many physical systems. This discontinuity is expressed in the extrusion modelling by a change of causality between the filling ratio in the *Partially Filled Zone* and the gradient of pressure which is the associated conjugate variable in the *Fully Filled Zone*. Many studies of mathematical interest are performed concerning the fixed interface in the context of existence and regularity of solutions and well-balanced numerical computation as it is discussed along this thesis.

In Chapter 3 the modelling of an extrusion process has been studied. The proposed model is based on mass and energy balance of an homogeneous material which is heated and transported along the extruder. The rheological behavior of the transported material is related essentially to the viscosity which strongly depends on dynamic variables as the material temperature and moisture content. The distributed viscosity prevents an explicit formulation of interface relations and represents in that sense a very interesting problem for control and mathematical analysis.

In our study we consider a simplified model with constant viscosity. Then, the interface coupling conditions can be explicitly formulated by assuming the continuity of variables as pressure or momentum flux. By numerical computations based on the finite volume method, we simulate the evolution of pressure, die net flow, filling ratio and temperature along the extruder. The tracking of the interface is achieved using an extension of the variables in the whole coupled complementary time-varying domains by means of color functions as charac-

teristic functions of the two moving intervals.

In Chapter 4 a mathematical analysis of the extrusion process model has been performed. It has been shown that the Cauchy problem admits a unique solution if initial and boundary data are closed to the equilibrium. Our strategy is based on the transformation of moving domains in fixed one using changes of coordinates. Contraction mapping principle (Banach fixed point argument) allows to define the conditions such that the uniqueness and existence of solution are guaranteed. We first prove the existence of solution for small time and extend ours analysis to semi-global time by iterations.

In Chapter 5, we deal with the control of the extrusion process. We only consider the homogeneous mass balance equation as an independent system. One should point out that the system can be decoupled only if the viscosity is constant. Indeed, for the process the dynamics of moisture content which is continuous at the interface does not affect the design of the desired properties of the material at the die and the temperature also evolves independently. The evolution of the moisture is in this case determined by an input value (boundary condition) which is transported along the extruder with a delay depending on the velocity of the transport in the partially and *Fully Filled Zone*. The filling ratio transport equation and the interface dynamics are combined to obtain a delay system framework by solving the partial differential equation using the method of characteristics. Assuming that the rotation speed of the screw is constant and defining the feed rate as an input variable we obtain a state-dependent input delay system and construct an predictor based controller to stabilize the interface around a given equilibrium. Consequently, we stabilize the net flow at the die. Comparing the interface coupling relations, we show that the admissible set of equilibrium for filling ratio and interface position is more large if we consider continuity of pressure. We conclude that the momentum flux continuity represents a restrictive coupling relation and we perform the control analysis by considering pressure continuity at the interface. The stabilization of the interface leads to the stability of the temperature as it is shown by simulations.

In Chapter 6 we consider coupled port-Hamiltonian systems through a mobile interface. The motivation of the study in this context is to classify the interface relations for coupled port-Hamiltonian systems in complementary time varying domains. By augmenting the system with the colors functions, we define a global port-Hamiltonian system on the total domain. The transport operator is then given by a differential operator which is modulated by the distributed color functions. We show that the extended system is also a Dirac structure by adding two pairs of port-variables which are associated to interface. The first pair corresponds to the discontinuity assumption on one of the flux variables (the other one being continuous) and the second pair being the velocity of interface and its conjugated variable. The velocity of the color functions transport equations corresponds in this case to the interface velocity. It is important to note that the efforts and flux variables which are associated to the color functions dynamics do not appear in the power balance equation.

7.2 Future research

Coupled partial differential equations through mobile interface is an emergent subject in control theory. In that perspective, this thesis stands as an exploration which suggests many open problems. In the context of extrusion process modelling, the problem which is related to distributed viscosity is a major interest for various applications. One should also mention that a more complex geometry of screw profile may lead to a succession of partially and fully filled zones which makes arise several mobile interfaces. Another challenge is to deal with reactive extrusion which consisted to a mixture of different materials which different densities. Well-posedness issues of such system for distributed viscosity can be explored in future works. The extension of the predictor based controller by introducing a time-varying screw speed is a real challenge, for the delay system control. One should mention that the extension of the controller to the temperature design should be performed to guarantee the stability of the whole system. By studying moving interface problem in port-Hamiltonian framework, we make explicit the pairs of conjugated variables needed to express the interface relations. This might be a powerful insight in the various suggested interface relations in the literature and towards a passivity-based definition and classification of these interface relations.

Chapter 8

Nomenclature

$B (m^4)$	coefficient of pressure flow
$F_{in} (kg s^{-1})$	Mass flow feed rate
$F_d (kg s^{-1})$	Mass flow rate at the die
$f_p (-)$	Filling ratio
$K_d (m^3)$	Die conductance
$l (m)$	Moving interface
$L (m)$	Length of the screw
$N (rd s^{-1})$	Screw velocity
$P (Pa)$	Pressure
$S_{eff}(m^2)$	Available section
$V_{eff} = \xi S_{eff}(m^3)$	Available volume
$\eta (Pa s^{-1})$	Viscosity of the matter
$\rho_0(kg m^{-3})$	Density
$\xi (m)$	Pitch length
$\zeta (m)$	Pitch length
$S_{ech}(m^2)$	Exchange area between melt barrel
$T_{p,f}(K)$	Melt temperature
$T_b(K)$	Barrel temperature
$\alpha (Jm^{-2}s^{-1}K^{-1})$	Heat exchange coefficient
$\mu(J kg^{-1} K^{-1})$	Viscous heat generation parameter

Bibliography

- [1] R. Abgrall and S. Karni. Computations of compressible multifluids. *J. Comput. Phys.*, 169:594–623, May 2001.
- [2] J.F. Agassant. *La Mise en forme des matières plastiques*. Technique & Documentation, 1996.
- [3] E. Aguilar-Garnica, J.P. Garcia-Sandoval, , and V. Gonzalez-Alvarez. PI controller design for a class of distributed parameter systems. *Chemical Engineering Science*, 66:4009–4019, 2011.
- [4] E. Aguilar-Garnica, V. Gonzalez-Alvarez, and C. Pelayo-Ortiz. Robust continuous velocity control of convective spatially distributed systems. *Chemical Engineering Science*, 63(17):4373–4385, 2008.
- [5] K. Akouz, A. Benhammou, P. O. Malaterre, B. Dahbou, and G. Roux. Predictive control applied to asce canal 2. In *Proceedings of the 1998 IEEE International Conference on Systems, Man, and Cybernetics*, San Diego, California, October 1998.
- [6] A. Ambroso, B. Boutin, F. Coquel, E. Godlewski, and P. G. LeFloch. *Coupling Two Scalar Conservation Laws via Dafermos Self-Similar Regularization*. Springer Berlin Heidelberg, 2008.
- [7] A. Ambroso, C. Chalons, F. Coquel, and T. Galié. Interface model coupling via prescribed local flux balance. In *18th AIAA Computational Fluid Dynamics Conference*, Miami, Florida, June 25-28 2007.
- [8] A. Ambroso, C. Chalons, F. Coquel, E. Godlewski, F. Lagoutière, P.-A. Raviart, and N. Seguin. Extension of interface coupling to general Lagrangian systems. In *Numerical mathematics and advanced applications*, pages 852–860, 2006.
- [9] A. Ambroso, C. Chalons, F. Coquel, E. Godlewski, F. Lagoutière, P.-A. Raviart, and N. Seguin. Coupling of general Lagrangian systems. *Math. Comp.*, 77(262):909–941, 2008.

- [10] A. Ambroso, C. Chalons, F. Coquel, E. Godlewski, F. Lagoutière, P. A. Raviart, and N. Seguin. *A Relaxation Method for the Coupling of Systems of Conservation Laws*. Springer Berlin Heidelberg, 2008.
- [11] A. Ambroso, C. Chalons, F. Coquel, E. Godlewski, F. Lagoutière, P.-A. Raviart, and N. Seguin. Relaxation methods and coupling procedures. *Internat. J. Numer. Methods Fluids*, 56(8):1123–1129, 2008.
- [12] C. Antoniadès and P.D. Christofides. Robust control of nonlinear time-delay systems. *Int. J. Appl. Math. and Comp. Sci.*, 9(4):811–837, 1999.
- [13] A. Armaou and P.D. Christofides. Nonlinear feedback control of parabolic partial differential equation systems with time-dependent spatial domains. *Journal of Mathematical Analysis and Applications*, 239(1):124–157, 1999.
- [14] A. Armaou and P.D. Christofides. Robust control of parabolic pde systems with time-dependent spatial domains. *Automatica*, 37(1):61 – 69, 2001.
- [15] Z. Artstein. Linear systems with delayed controls: A reduction. *IEEE Transactions on Automatic Control*, 27(4):869–879, 1982.
- [16] F. Bachmann and J. Vovelle. Existence and uniqueness of entropy solution of scalar conservation laws with a flux function involving discontinuous coefficients. *Comm. Partial Differential Equations*, 31:371–395, 2008.
- [17] O. Begovich, V. M. Ruiz, G. Besançon, C. I. Aldana, and D. Georges. Predictive control with constraints of a multi-pool irrigation canal prototype. *Latin American Applied Research*, 37:177–185, 2007.
- [18] N. Bekiaris-Liberis, M. Jankovic, and M. Krstic. Compensation of state-dependent input delay for nonlinear systems. In *Proceedings of American Control Conference*, 2012.
- [19] N. Bekiaris-Liberis and M. Krstic. Compensation of time-varying input delay for nonlinear systems. In *19th Mediterranean Conference on Control Automation*, pages 1040–1045, 2011.
- [20] N. Bekiaris-Liberis and M. Krstic. Compensation of state-dependent input delay for nonlinear systems. *IEEE Transactions on Automatic Control*, 58(2):275–289, 2013.
- [21] N.K. Bekiaris-Liberis and M. Krstic. Robustness of nonlinear predictor feedback laws to time- and state-dependent delay perturbations. *Automatica*, 49(4):1576–1590, 2013.
- [22] S. Bianchini and A. Bressan. Vanishing viscosity solutions of nonlinear hyperbolic systems. *Ann. of Math.*, 161(1):223–342, 2005.

- [23] C. Bidard. *Stabilisation des systèmes commandés par réseaux*. PhD thesis, Institut National Polytechnique de Grenoble, Grenoble, France, September 2005. in french.
- [24] M. L. Booy. Geometry of fully wiped twin-screw equipment. *Polymer Engineering & Science*, 18(12):973–984, 1978.
- [25] M. L. Booy. Isothermal flow of viscous liquids in corotating twin screw devices. *Polymer Engineering Science*, 20:1220–1228, 1980.
- [26] K. Bouchemal, F. Couenne, S. Briancon, H. Fessi, and M. Tayakout. Polyamides nanocapsules : Modeling and wall thickness estimation. *AiChE*, 52:2161–2170, 2006.
- [27] B. Boutin. *Etude Mathématique et Numérique des Equations Hyperboliques Non-linéaires: couplage de modèles et chocs non classiques*. PhD thesis, University Pierre et Marie Curie, Paris 6, Paris, France, Nov. 2009.
- [28] B. Boutin, F. Coquel, and E. Godlewski. Dafermos regularization for interface coupling of conservation laws. *Hyperbolic Problems: Theory, Numerics, Applications*, 4:567–575, 2008.
- [29] B. Boutin, F. Coquel, and E. Godlewski. *Dafermos Regularization for Interface Coupling of Conservation Laws*. Springer Berlin Heidelberg, 2008.
- [30] D. Bresch-Pietri, J. Chauvin, and N. Petit. Invoking halanay inequality to conclude on closed-loop stability of processes with input-varying delay. In *proceedings of the 10-th IFAC Workshop on Time Delay Systems TDS*, 2012.
- [31] M. Bués and M. Panfilov. Delay model for a cycling transport through porous medium. *Transport in Porous Media*, 55:215–241, 2004.
- [32] R. Burger and K. H. Karlsen. Conservation laws with discontinuous flux : a short introduction. *J. Eng. Math*, 60:241–247, 2008.
- [33] Suncica Canic, Andro Mikelic, Tae-Beom Kim, and Giovanna Guidoboni. *Existence of a Unique Solution to a Nonlinear Moving-Boundary Problem of Mixed Type Arising in Modelling Blood Flow*, volume 153. Springer US, 2011.
- [34] J. Cervera, A.J. van der Schaft, and A. Baños. Interconnection of port-Hamiltonian systems and composition of Dirac structures. *Automatica*, 43:212–225, 2007.
- [35] M. Chapet and B. Vergnes. Procédés d’extrusion bivis. *Techniques de l’ingénieur Plasturgie : procédés d’extrusion*, 2013.
- [36] Y. S. Choi and Craig Miller. Global existence of solutions to a coupled parabolic-hyperbolic system with moving boundary. In *proceedings of the American Mathematical Society*, volume 139, page 3257–3270, 2011.

- [37] S. Choulak, F. Couenne, Y. Le Gorrec, C. Jallut, P. Cassagnau, and A. Michel. Generic dynamic model for simulation and control of reactive extrusion. *Ind. Eng. Chem. Res.*, 43:7373–7382, 2004.
- [38] S. E. Choulak. *Modélisation et commande d'un procédé d'extrusion reactive*. PhD thesis, Université Claude Bernard Lyon 1, Lyon, France, 2004.
- [39] P.D. Christofides and C. Antoniadis. Feedback control of nonlinear differential difference equation systems. *Chemical Engineering Science*, 54(1):5677–5709, 1999.
- [40] Jean-Michel Coron. *Control and nonlinearity*, volume 136 of *Mathematical Surveys and Monographs*. American Mathematical Society, Providence, RI, 2007.
- [41] Jean-Michel Coron, Matthias Kawski, and Zhiqiang Wang. Analysis of a conservation law modeling a highly re-entrant manufacturing system. *Discrete Contin. Dyn. Syst. Ser. B*, 14(4):1337–1359, 2010.
- [42] T.J. Courant. Dirac manifolds. *Trans. American Math. Soc.* 319, pages 631–661, 1990.
- [43] D. Coutand and S. Shkoller. Well-posedness in smooth function spaces for moving-boundary 1-d compressible euler equations in physical vacuum. *Communications on pure and applied*, 64:328–366, 2011.
- [44] Chen D. and Friedman A. A two-phase free boundary problem with discontinuous velocity: Application to tumor model. *Journal of Mathematical Analysis and Applications*, 1(399):378–393, 2013.
- [45] B.J. Daly. Numerical study of two fluid Rayleigh-Taylor instability. *Physics of Fluids*, 10:297–307, 1967.
- [46] B.J. Daly and A. E. Pratch. Numerical study of density current surges. *Physics of Fluids*, 11:15–30, 1968.
- [47] N. Daraoui, P. Dufour, H. Hammouri, and A. Hottot. Model predictive control during the primary drying stage of lyophilisation. *Control Engineering Practice*, 18(5):483–494, 2010.
- [48] M. Diagne, V. Dos Santos Martins, F. Couenne, and B. Maschke. Well posedness of the model of an extruder in infinite dimension. *50th IEEE Conference on Decision and Control and European Control Conference (CDC-ECC)*, 1926, 2011.
- [49] M. Diagne, V. Dos Santos Martins, F. Couenne, B. Maschke, and C. Jallut. Modélisation et commande d'un système d'équations aux dérivées partielles à frontière mobile : application au procédé d'extrusion. *Journal Européen des Systèmes Automatisés*, 45:665–691, 2011.

- [50] J.-Y. Dieulot, N. Petit, P. Rouchon, and G. Delaplace. An arrangement of ideal zones with shifting boundaries as a way to model mixing processes in unsteady stirring conditions in agitated vessels. *Chemical Engineering Science*, 60(20):5544–5554, 2005.
- [51] W. B. Dunbar, N. Petit, P. Rouchon, and Ph. Martin. Motion planning for a nonlinear stefan problem. *ESAIM: Control, Optimisation and Calculus of Variations*, 9:275–296, 2003.
- [52] N.H. El-Farra, A. Armaou, and P.D. Christofides. Constrained nonlinear control of parabolic PDE systems. In *American Control Conference, 2000. Proceedings of the 2000*, volume 4, pages 2275 –2279, 2000.
- [53] R. El-Khazali. Robust stabilization of uncertain time-delay systems using variable structure output feedback control. In *Proceedings of the American Control Conference*, volume 6, pages 4236–4237, 95.
- [54] J. Elsey, J. Riepenhausen, B. Mckay, G.W. Barton, and M. Willis. Modeling and control of a food extrusion process. *Computers Chemical Engineering*, 21:361–366, 1997.
- [55] S. Evesque, A. Annaswamy, S. Niculescu, and A. Dowling. Adaptive control scheme for uncertain time-delay systems. *Journal of Dynamic Systems, Measurement and Control*, 125(2), 2003.
- [56] A. Fattouh, O. Sename, and J.-M. Dion. Pulse controller design for linear systems with delayed state and control. In *Proceedings of the 1st IFAC Symposium on System Structure and Control, Prague, Czeck Republic*, pages 4668–4672, 2001.
- [57] T. Fukuoka. Numerical analysis of a reactive extrusion process. part ii: simulations and verifications for the twin screw extrusion. *Polym. Eng. Sci.*, 40:2524–2538, 2000.
- [58] S. C. Garge, M. D. Wetzel, and B. A. Ogunnaike. Inference-based scheme for controlling product end-use properties in reactive extrusion processes. *Ind. Eng. Chem. Res*, 49:8021–8034, 2010.
- [59] D. Georges, G. Besançon, Z. Benayache, and E. Witrant. A nonlinear state feedback design for nonlinear systems with input delay. In *Proceedings of the European Control Conference, Kos, Grèce*, 2007.
- [60] E. Godlewski, K.-C. Le Than, and P.A. Raviart. The numerical interface coupling of nonlinear systems of conservation laws: II. the case of systems. *ESAIM: Mathematical Modelling and Numerical Analysis*, 39(4):649–692, 2005.
- [61] E. Godlewski and P.-A. Raviart. The numerical interface coupling of nonlinear hyperbolic systems of conservation laws: I. the scalar case. *Numer. Math.*, 97:81–130, 2004.

- [62] E. Godlewski and N. Seguin. The Riemann problem for a simple model of phase transition. *Commun. Math. Sci*, 4:227–247, 2006.
- [63] F. Gouaisbaut, M. Dambrine, and J.P. Richard. Robust control of delay systems: a sliding mode control design via lmi. *Systems & Control Letters*, 46(4):219–230, 2002.
- [64] F. Gouaisbaut, W. Perruquetti, and J.-P. Richard. A sliding mode control for linear systems with input and state delays. In *Proceedings of the 38th IEEE Conference on Decision and Control*, volume 4, pages 4234–4239, 1999.
- [65] P.K. Gundeputi and J.C Friedly. Velocity control of partial differential equation systems with single characteristic variable. *Chemical Engineering Science*, 53(24):4055–4072, 1998.
- [66] S. Gupta. *The classical Stefan problem. Basic concepts, Modelling and Analysis*. Applied mathematics and Mechanics. North-Holland, 2003.
- [67] T.A. Haley and S.J. Mulvaney. On-line system identification and control design of an extrusion cooking process: Part II. system model predictive and inferential control design. *Food Control*, 11:121–129, 2000.
- [68] T.A. Haley and S.J. Mulvaney. On-line system identification and control design of an extrusion cooking process: Part I. system identification. *Food Control*, 11:103–120, 2000.
- [69] H. Hamane, S. Yokoyama, H. Onogaki, and M. Iwatani. Design of decoupling system for eliminating disturbance on extruder temperature control system. *IEEE Transactions on Automatic Control*, 48, 2003.
- [70] F. Harlow and J. Welch. Numerical calculation of time-dependent viscous incompressible flow of fluid with free surfaces. *Physics of Fluids*, 8:2182–2189, 1965.
- [71] P. Helluy and N. Seguin. Relaxation models of phase transition flows. *M2AN Math. Model. Numer. Anal.*, 40(2):331–352, 2006.
- [72] J. Hua, T. Liang, H. Sun, and Z. Lei. Time-delay compensation control of networked control systems using time-stamp based state prediction. In *International Colloquium on Computing, Communication, Control, and Management*, volume 2, pages 198–202, 2008.
- [73] B. Jacob and H. J. Zwart. *Linear Port-Hamiltonian Systems on Infinite-dimensional Spaces*, volume 223 of *Operator Theory: Advances and Applications*. Springer Basel, 2012.

- [74] E.M. Jafarov. Robust delay-dependent stabilization of uncertain time-delay systems by variable structure control. In *International Workshop on Variable Structure Systems*, pages 250–255, 2008.
- [75] L. P. B. M. Janssen, P. F. Rozendal, and M. Cioffi H. W. Hoogstraten. A dynamic model for multiple steady states in reactive extrusion. *International Polymer Processing*, 16:263–271, 2001.
- [76] L. P. B. M. Janssen, P. F. Rozendal, and M. Cioffi H. W. Hoogstraten. A dynamic model accounting for oscillating behavior in extrusion reaction. *International Polymer Processing*, 18:277–284, 2003.
- [77] I. Karafyllis. Finite-time global stabilization by means of time-varying distributed delay feedback. *SIAM J. Control and Optimization*, 45(1):320–342, 2006.
- [78] K. H. Karlsen, M. Rascle, and E. Tadmor. On the existence and compactness of a two-dimensional resonant system of conservation laws. *Commun. Math. Sci.*, 5(2):253–265, 2007.
- [79] T. Kato. *Perturbation Theory for Linear Operators*. Classics in Mathematics. Springer Verlag, 1995.
- [80] E. K. Kim and J. L. White. Isothermal transient startup for starved flow modular co-rotating twin screw extruder. *Polymer Engineering and Science*, 40:543–553, 2004.
- [81] E. K. Kim and J. L. White. Non-isothermal transient startup for starved flow modular co-rotating twin screw extruder. *International Polymer Processing*, 15:233–241, 2004.
- [82] M. Krstic. On compensating long actuator delays in nonlinear control. *IEEE Transactions on Automatic Control*, 53(7):1684–1688, 2008.
- [83] M. Krstic. Lyapunov stability of linear predictor feedback for time-varying input delay. *IEEE Transactions on Automatic Control*, 55(2):554–559, 2010.
- [84] Miroslav Krstic. *Delay-Adaptive Full-State Predictor Feedback*. Systems & Control: Foundations & Applications. Birkhäuser, Basel, 2009.
- [85] M.K. Kulshreshtha, Claudio A Zaror, and David J Jukes. Simulating the performance of a control system for food extruders using model-based set-point adjustment. *Food Control*, 6:135–141, 1995.
- [86] M.K. Kulshreshtha and C.A. Zaror. An unsteady state model for twin screw extruders. *Tran IChemE, Part C*, 70:21–28, 1992.

- [87] Y. Le Gorrec, H. Zwart, and B.M. Maschke. Dirac structures and boundary control systems associated with skew-symmetric differential operators. *SIAM J. of Control and Optimization*, 44(5):1864–1892, 2005.
- [88] Chin-Hsien Li. Modelling extrusion cooking. *Food and Bioproducts Processing*, 77(1):55–63, 1999.
- [89] Chin-Hsien Li. Modelling extrusion cooking. *Mathematical and Computer Modelling*, 33:553–563, 2001.
- [90] Ta-Tsien Li and Yi Jin. Semi-global C_1 solution to the mixed initial-boundary value problem for quasilinear hyperbolic systems. *Chinese Ann. Math. Ser. B*, 22:325–336, 2001.
- [91] W. Lili, J. Yuxi, S. Sheng, Z. Guofang, Z. Guoqun, and A. Lijia. Numerical simulation of reactive extrusion processes for activated anionic polymerization. *Journal of materials processing technology*, 199:156–63, 2008.
- [92] A. Macchelli and B.M. Maschke. *Modeling and Control of Complex Physical Systems - The Port-Hamiltonian Approach*, chapter Infinite-dimensional Port-Hamiltonian Systems, pages 211–272. Springer, Sept. 2009. ISBN 978-3-642-03195-3.
- [93] A. Macchelli and C. Melchiorri. Modeling and control of the Timoshenko beam. the Distributed Port Hamiltonian approach. *SIAM Journal On Control and Optimization*, 43(2):743–767, 2004.
- [94] A. Macchelli and C. Melchiorri. Control by interconnection of mixed Port Hamiltonian systems. *IEEE Trans. on Automatic Control*, 50(11):1839–1844, 2005.
- [95] P. O. Malaterre, D. C. Rogers, and J. Schuurmans. Multivariable predictive control of irrigation canals. design and evaluation on a 2-pool model. In *Proceedings of the International Workshop on Regulation of Irrigation Canals: State of the Art of Research and Applications*, Marrakech, Morocco, April 1997.
- [96] A. Manitius and A.W. Olbrot. Finite spectrum assignment problem for systems with delays. *IEEE Transactions on Automatic Control*, 24(4):541–552, 1979.
- [97] Wei-Jie Mao and Juan Chu. D-stability for linear continuous-time systems with multiple time delays. *Automatica*, 42:1589–1592, 20086.
- [98] B. Maschke and A.J. van der Schaft. *Advanced Topics in Control Systems Theory. Lecture Notes from FAP 2004*, volume 311 of *Lecture Notes on Control and Information Sciences*, chapter Compositional modelling of distributed-parameter systems, pages 115–154. Springer, 2005.

- [99] M. McAfee and S. Thompson. A novel approach to dynamic modeling of polymer extrusion for improved process control. *Systems and Control Engineering*, 221:617–627, 2007.
- [100] W. Michiels, S. Mondié, D. Roose, and M. Dambrine. The effect of approximating distributed delay control laws on stability. In Silviu-Iulian Niculescu and Keqin Gu, editors, *Advances in Time-Delay Systems*, volume 38 of *Lecture Notes in Computational Science and Engineering*, pages 207–222. Springer Berlin Heidelberg, 2004.
- [101] B. Mirkin, P. O Gutman, and Y. Shtessel. Continuous model reference adaptive control with sliding mode for a class of nonlinear plants with unknown state delay. In *American Control Conference*, pages 574–579, 2009.
- [102] L. Mirkin. On the approximation of distributed-delay control laws. *Syst. Control Lett.*, 51:331–342, 2004.
- [103] S. Mondié and W. Michiels. Finite spectrum assignment of unstable time-delay systems with a safe implementation. *IEEE Transaction on Automatic Control*, 48(12):2207–2212, 2003.
- [104] S. Mondié and W. Michiels. A safe implementation for finite spectrum assignment : robustness analysis. In *Proceedings of the 42nd IEEE Conference on Decision and Control , Hawaii, USA*, pages 4668–4672, 2003.
- [105] R.G. Moreira, A.K. Srivastava, and J.B. Gerrish. Feedforward control model for a twin-screw food extruder. *Food Control*, 6:361–386, July 1990.
- [106] A. Muntean. Well-posedness of a moving-boundary problem with two moving reaction strips. *Nonlinear Analysis: Real World Applications*, 10:2541–2557, 2009.
- [107] R.R. Negenborn and B. De Schutter. A distributed model predictive control approach for the control of irrigation canals. In *Infrastructure Systems and Services: Building Networks for a Brighter Future (INFRA), 2008 First International Conference on*, pages 1–6, November 2008.
- [108] S.A. Nield, H.M. Budman, and C. Tzoganakis. Control of a LPDE reactive extrusion process. *Control Engineering Practice*, 8:911–920, 2000.
- [109] M.T. Nihtila. Adaptive control of a continuous-time system with time-varying input delay. *Systems & Control Letters*, 12(4):357 – 364, 1989.
- [110] M.T. Nihtila. Finite pole assignment for systems with time-varying input delays. In *Proceedings of the 30th IEEE Conference on Decision and Control*, volume 1, pages 927–928, 1991.

- [111] W.F. Noh and P. Woodward. Slic (simple line interface calculation). *Proceedings, Fifth International Conference on Numerical Methods in Fluid Dynamics, Lecture Notes in Physics*, 59:330–340, 1976.
- [112] P.J. Olver. *Applications of Lie Groups to Differential Equations*, volume 107 of *Graduate texts in mathematics*. Springer, New-York, ii edition, 1993. ISBN 0-387-94007-3.
- [113] R. Ortega, M.W. Spong, S. Lee, and K. Nam. On compensation of wave reflexions in transmission lines and applications to the overvoltage problem in AC motor drives. *IEEE Trans. on Automatic Control*, 49(10), 2004.
- [114] S. Osher and J.A. Sethian. Fronts propagating with curvature-dependent speed : algorithms based on Hamilton-Jacobi formulations. *Journal of Computational Physics*, 79:12–49, 1988.
- [115] B.J. Parker and D.L. Youngs. Two and three dimensional eulerian simulation of fluid flow with material interfaces. *Technical report, UK Atomic Weapons Research Establishment (AWRE)*, page 201–225, 1992.
- [116] N. Petit. Control problems for one-dimensional fluids and reactive fluids with moving interfaces. In *Advances in the theory of control, signals and systems with physical modeling*, volume 407 of *Lecture notes in control and information sciences*, pages 323–337, Lausanne, Dec 2010.
- [117] L. Prat, S. N'diaye, L. Rigal, and C. Gourdon. Solid-liquid transport in a modified co-rotating twin-screw extruder-dynamic simulator and experimental validations. *Chemical Engineering and Processing*, 43:881–886, 2004.
- [118] F. Previdi, S. M. Savaresi, and A. Panarotto. Design of a feedback control system for real-time control of flow in a single-screw extruder. *Control Engineering practice*, 14:1111–1121, 2006.
- [119] E. Purlis and V. O. Salvadori. A moving boundary problem in a food material undergoing volume change - simulation of bread baking. *Food Research International*, 43:949–958, 2008.
- [120] R. Raul Borsche, R. M. Colombo, and M. Garavello. On the coupling of systems of hyperbolic conservation laws with ordinary differential equations. *Nonlinearity*, 23, 2010.
- [121] J.P. Richard. Time-delay systems: an overview of some recent advances and open problems. *Automatica*, 39(10):1667–1694, 2003.
- [122] J.R. Robert T. H. Martin and Mark E. Oxley. Moving boundaries in reaction-diffusion systems with absorption. *Nonlinear Analysis. Theory*, 14(2):167–192, 1990.

- [123] V. M. Ruiz and J. Ramirez. Predictive control in irrigation canal operation. In *Proceedings of the 1998 IEEE International Conference on Systems, Man, and Cybernetics*, San Diego, California, October 1998.
- [124] J.S. Saltzman and E.G. Packett. A 3-D adaptive mesh refinement algorithm for multi-material gas dynamics. *Physica D*, 60:84–104, 1992.
- [125] H. Shang, J.F. Forbes, and M. Guay. Feedback control of hyperbolic distributed parameter systems. *Chemical Engineering Science*, 60(4):969–980, 2005.
- [126] Peipei Shang and Zhiqiang Wang. Analysis and control of a scalar conservation law modeling a highly re-entrant manufacturing system. *J. Differential Equations*, 250(2):949–982, 2011.
- [127] Bhajmohan Singh and Steven J. Mulvaney. Modeling and process control of twin-screw cooking food extruder. *Journal of Food Engineering*, 23:403–428, 1994.
- [128] O.J.M. Smith. Closer control of loops with dead time. *Chemical Engineering Progress*, 53(5):217–219, 1957.
- [129] Wenlong Song, Yaqiu Liu, and Liping Sun. Model reference adaptive integral-type sliding mode control design for a class of uncertain systems. In *The Sixth World Congress on Intelligent Control and Automation*, volume 1, pages 2056–2060, 2006.
- [130] Jinglu Tan and James M. Hofer. Self-tuning predictive control of processing temperature for food extrusion. *Journal of process control*, 3:183–189, 1995.
- [131] Leong Ping Tan, Ahmad Lotfi, Eugene Lai, and J.B. Hull. Soft computing applications in dynamic model identification of polymer extrusion process. *Applied Soft Computing*, 4:345–355, 2004.
- [132] T.O.Broadhead, W.I. Patterson, and J. M. Dealy. Closed loop viscosity control of reactive extrusion with an in line rheometer. *Polymer Engineering and Science*, pages 2840–2851, 1996.
- [133] G. Tryggvason, B. Bunner, A. Esmaeli, D. Juric, N. Al-Rawahi, W. Tauber, J. Han, S. Nas, and Y.-J. Jan. A front-tracking method for the computations of multiphase flow. *Journal of Computational Physics*, 169:708–759, 2001.
- [134] V. Van Assche, M. Dambrine, J.-F. Lafay, and J. P Richard. Some problems arising in the implementation of distributed-delay control laws. In *Proceedings of the 38th IEEE Conference on Decision and Control*, volume 5, pages 4668–4672, 1999.
- [135] A.J. van der Schaft and B.M. Maschke. The Hamiltonian formulation of energy conserving physical systems with external ports. *Archiv für Elektronik und Übertragungstechnik*, 49(5/6):362–371, 1995.

- [136] A.J. van der Schaft and B.M. Maschke. Hamiltonian formulation of distributed parameter systems with boundary energy flow. *J. of Geometry and Physics*, 42:166–174, 2002.
- [137] S. Stramigioli V.Duindam, A. Macchelli and H. Bruyninckx eds. *Modeling and Control of Complex Physical Systems - The Port-Hamiltonian Approach*. Springer, Sept. 2009. ISBN 978-3-642-03195-3.
- [138] S. A. Velardi and A. A. Barresi. Development of simplified models for the freeze-drying process and investigation of the optimal operating conditions. *Chemical Engineering Research and Design*, 86:9–22, 2008.
- [139] B. Vergnes and F. Berzin. Modeling of reactive systems in twin-screw extrusion: challenges and applications. *C. R. chimie*, 9:1409–1418, 2006.
- [140] B. Vergnes, V.G. Della, and L. Delamare. Global computer software for polymer flows in corotating twin screw extruders. *Polym. Eng. Sci*, 38:1781–1792, 1998.
- [141] J.A. Villegas. *A Port-Hamiltonian Approach to Distributed Parameter Systems*. PhD thesis, University of Twente, Enschede, The Netherlands, May 2007.
- [142] J.A. Villegas, H. Zwart, Y. Le Gorrec, and B. Maschke. Stability and stabilization of a class of boundary control systems. *IEEE Transaction on Automatic Control*, 54(1):142–147, 2009.
- [143] B. T. Wahlin and A. J. Clemmens. Automatic downstream water-level feedback control of branching canal networks: Simulation results. *Journal of Irrigation and Drainage Engineering*, 132:208–219, 2006.
- [144] L. Wang, S. Smith, and Chessaric C. Continuous-time model predictive control of food extruder. *Control Engineering Practice*, 16:1173–1183, 2008.
- [145] Y. Wang and J. Tan. Dual-target predictive control and application in food extrusion. *Control Engeneering Practice*, 8:1055–1062, 1995.
- [146] Zhiqiang Wang. Exact controllability for nonautonomous first order quasilinear hyperbolic systems. *Chinese Ann. Math. Ser. B*, 27:643–656, 2006.
- [147] S. Welch. Local simulation of two-phase flows including interface tracking with mass transfer. *J. Comput. Phys.*, 17:121–142, 1995.
- [148] E. Witrant, C. Canudas de Wit, and D. Georges. Remote output stabilization under two channels time-varying delays. In *Proc. of the 4th IFAC Workshop on Time Delay Systems, Rocquencourt, France*, 2003.

- [149] E. Witrant, C. Canudas de Wit, D. Georges, and M. Alamir. Remote stabilization via time-varying communication network delays: Application to tcp networks. In *Proc. of the IEEE Conference on Control Applications, Taipei, Taiwan*, 2004.
- [150] E. Witrant, D. Georges, and C. Canudas de Wit. Optimal control design for the stabilization of network controlled systems. In *IEEE American Control Conference, Minneapolis, USA*, 2006.
- [151] Shu Xia, N.H. Hodge, and T.F. Wiesner. Distributed control of plant-wide chemical processes with uncertain time-delays. *Chemical Engineering Science*, 64:2057–2066, 2009.
- [152] Shichao Xu and Jie Bao. Distributed control of plant-wide chemical processes with uncertain time-delays. *Chemical Engineering Science*, 84:512–532, 2012.
- [153] Xin-Gang Yu. An LMI approach to robust H_∞ filtering for uncertain systems with time-varying distributed delays. *Journal of the Franklin Institute*, 345:877–890, 2008.
- [154] Wenjie Zhao and Yuhui Zhao. Integral sliding mode control for a class nonlinear systems. In *International Conference on Neural Networks and Brain*, volume 2, pages 1093–1096, 2005.
- [155] Hans Zwart, Yann Le Gorrec, Bernhard Maschke, and Javier Villegas. Well-posedness and regularity of hyperbolic boundary control systems on a one-dimensional spatial domain . *ESAIM-Control Optimization and Calculus of Variations*, 16(4):1077–1093, Oct.Dec 2010.

